

STATUS OF THESIS

Title of thesis

EFFECT OF CURING ON THE PROPERTIES OF POLYMERIC CONCRETE
--

I SOBIA ANWAR QAZI,

hereby allow my thesis to be placed at the Information Resource Center (IRC) of Universiti Teknologi PETRONAS (UTP) with the following conditions:

1. The thesis becomes the property of UTP
2. The IRC of UTP may make copies of the thesis for academic purposes only.
3. This thesis is classified as

☐ Confidential

☒ Non-confidential

If this thesis is confidential, please state the reason:

The contents of the thesis will remain confidential for _____ years.

Remarks on disclosure:

Endorsed by

Signature of Author
B-303 Basera Towers Block-17
Gulistan-e-Johar Karchi, Pakistan 75290

Signature of Supervisor

Date: _____

Date: _____

UNIVERSITI TEKNOLOGI PETRONAS

EFFECT OF CURING ON THE PROPERTIES OF POLYMERIC CONCRETE

by

SOBIA ANWAR QAZI

The undersigned certify that they have read, and recommend to the Postgraduate Studies Programme for acceptance this thesis for the fulfilment of the requirements for the degree stated.

Signature:

Main Supervisor:

Signature:

Co-Supervisor:

Signature:

Head of Department:

Date:

EFFECT OF CURING ON THE PROPERTIES OF POLYMERIC CONCRETE

by

SOBIA ANWAR QAZI

A Thesis

Submitted to the Postgraduate Studies Programme

as a Requirement for the Degree of

MASTER OF SCIENCE

CIVIL ENGINEERING DEPARTMENT

UNIVERSITI TEKNOLOGI PETRONAS

BANDAR SERI ISKANDAR,

PERAK

AUGUST 2010

DECLARATION OF THESIS

Title of thesis

EFFECT OF CURING ON THE PROPERTIES OF POLYMERIC CONCRETE

I SOBIA ANWAR QAZI,

hereby declare that the thesis is based on my original work except for quotations and citations which have been duly acknowledged. I also declare that it has not been previously or concurrently submitted for any other degree at UTP or other institutions.

Witnessed by

Signature of Author

B-303 Basera Towers Block-17
Gulistan-e-Johar Karchi,
Pakistan 75290

Signature of Supervisor

Date: _____

Date: _____

DEDICATION

This Thesis is Dedicated

To

My Beloved Parents

ACKNOWLEDGEMENTS

First and foremost, I am grateful to Almighty Allah, who bestowed me the opportunity and courage to successfully complete this important research work. This research would have not been possible without the able guidance of my supervisors Assoc. Prof. Ir. Dr. Muhd. Fadhil Nuruddin and Assoc. Prof. Dr. Nasir Shafiq. Special thanks to Assoc. Prof. Dr. Zakaria Man (Chemical Engineering) for his discussion on inorganic polymer chemistry, and Nur liyana bt Mohd Kamal and Siti Asma hani for the translation of abstract to Bahasa Malaysia version.

Secondly, the author would like to acknowledge her family namely her beloved parents Qazi Anwar Ahmed and Kaukab Rakshanda for their never ending love and motivation, siblings Ayesha Anwar Qazi, Mohammad Usman Qazi and Mohammad Imran Qazi for their moral support, her paternal uncle Qazi Irshad and aunty Rohani for their moral support.

Thirdly, the author would like to extend her appreciation to PHD student Andri Kusbianoro for his kind contribution throughout this research study and final year students Siti Asma Hani, Nor hafizah tajudin and Fauzan Jaafar for their kind support during experimental work. The author also likes to acknowledge all the staff in Civil Engineering Department, Universiti Teknologi PETRONAS, for their moral support, concrete lab technicians Mr. Johan Ariff and Muhammad Hafiz b Baharun, Mechanical lab technicians Mr. faisal Ismail, Mr. Shairul Harun and Mr. Khairul Anuar who have given their technical assistance in SEM and XRF analysis and chemical lab Technicians Mohd Jailani B Kassim for his assistance in specific gravity test and Salmiyah Bt Latif for particle size analyser test.

Last but not the least; the author would like to extend special thanks to her fellow postgraduate students especially Sana Moqem, Tayseir Mohammad, Nadia Riaz, Sadaf Qasim, Noor Zainab, Salmia Beddu & Retno Rahardjati for their support.

ABSTRACT

Limestone and clay are the prime raw materials used in the manufacturing of Portland cement and quarrying of them is becoming the source of environmental degradation. Research showed that in near future limestone will be hardly available for cement production. Besides that, carbon footprints due to cement production are causing global warming. In addition to this, waste disposal is also becoming a global issue because of scarcity and expensiveness of landfills. Polymeric concrete utilizes waste materials such as fly ash (FA), rice husk ash and silica fume (SF) together with alkaline solution (NaOH & Na_2SiO_3), to form a green binder to replace cement which is the primary objective of this research. Secondly, this research study focuses on complete elimination of Portland cement for production of concrete that can achieve 28 days cube strength in the range of 40-50 MPa with the emphasis on the curing techniques applicable for in-situ construction namely; hot gunny sack, ambient and external exposure curing. This research study incorporates FA as a base source material and microwave incinerated rice husk ash (MIRHA) or SF. The replacement levels were kept at 3%, 5% and 7% of FA.

In addition to tests for compressive, tensile and flexural strengths, scanning electron microscopy analysis was also performed to study the microstructure of polymeric concrete. Results showed higher compressive and tensile strengths values for external exposure curing as well as better development of microstructure for the same, compared with other types of curing. Flexural strength was also much better as compared to OPC concrete.

Keywords: Polymeric concrete, Fly ash (FA), Microwave incinerated rice husk ash (MIRHA), Silica fume (SF), Scanning electron microscopy (SEM)

ABSTRAK

Batu kapur dan tanah liat adalah bahan utama yang digunakan dalam proses pembuatan simen dan hasil daripada proses mendapatkan bahan tersebut menjadi punca kemusnahan alam sekitar. Beberapa kajian menunjukkan bahawa sumber galian tersebut semakin berkurangan untuk pengeluaran simen. Selain itu, pembebasan jejak kaki karbon daripada proses pengeluaran simen menyumbang kepada pemanasan global. Selain daripada itu, pembuangan sisa juga menjadi isu utama dunia kerana tapak perlupusan semakin berkurangan serta kosnya yang semakin tinggi. Konkrit polimer menggunakan bahan terbuang seperti abu terbang (AT), abu sekam padi (ASP) dan wasap silika (WS) bersama-sama dengan larutan alkali (NaOH & Na_2SiO_3), yang akan menghasilkan bahan pengikat yang mesra alam menggantikan simen adalah objektif utama kajian ini. Objektif kedua, penyelidikan ini menjurus kepada penghapusan lengkap penggunaan simen untuk menghasilkan konkrit yang boleh mencapai kekuatan antara 40-50 MPa pada 28 hari dengan teknik pengawetan yang sesuai di tapak pembinaan yang dinamakan kaedah karung guni panas, pendedahan pada suhu persekitaran dan pendedahan pada suhu luar. Sumber utama dalam penyelidikan adalah AT dan abu sekam padi pembakaran gelombang mikro (ASPPGM) atau WS sebagai bahan pengganti AT. Kadar penggantian AT adalah pada 3%, 5% dan 7%.

Ujian kekuatan mampatan, tegangan dan lenturan dilakukan di samping analisis mikroskop pengimbasan elektron untuk mengkaji struktur mikro konkrit polimer. Hasil eksperimen menunjukkan ujian mampatan dan tegangan untuk sampel di bawah pengawetan menggunakan kaedah pendedahan suhu luar lebih tinggi, begitu juga pengukuhan struktur mikro yang baik berbanding dengan kaedah pengawetan yang lain. Kekuatan lenturan juga adalah lebih tinggi daripada konkrit simen portland biasa (SPB).

Kata kunci: konkrit polymerik, abu terbang (AT), abu sekam padi pembakaran gelombang mikro (ASPPGM), wasap silika (WS), mikroskop pengimbasan elektron.

In compliance with the terms of the Copyright Act 1987 and the IP Policy of the university, the copyright of this thesis has been reassigned by the author to the legal entity of the university,

Institute of Technology PETRONAS Sdn Bhd.

Due acknowledgement shall always be made of the use of any material contained in, or derived from, this thesis.

© Sobia Anwar Qazi, 2010
Institute of Technology PETRONAS Sdn Bhd
All rights reserved.

TABLE OF CONTENTS

STATUS OF THESIS	i
APPROVAL PAGE	v
TITLE PAGE	vi
DECLARATION OF THESIS	iv
DEDICATION	v
ACKNOWLEDGEMENTS	vi
ABSTRACT	vii
ABSTRAK	viii
COPYRIGHT PAGE	ix
TABLE OF CONTENTS	x
LIST OF FIGURES	xiv
LIST OF TABLES	xviii

Chapter

1. INTRODUCTION	1
1.1 BACKGROUND	1
1.2 PROBLEM STATEMENT	3
1.3 OBJECTIVES OF STUDY	4
2. LITERATURE REVIEW	5
2.1 INTRODUCTION	5
2.2 CEMENT AND CONCRETE PRODUCTION	5
2.2.1 Environmental Issues Related to Cement Production	6
2.2.2 Depletion of Resources	7
2.3 WASTE MATERIALS	7
2.3.1 Disposal Effects on Environment	8
2.4 TYPES OF CEMENT REPLACEMENT WASTE MATERIALS	9
2.4.1 Fly Ash	9
2.4.2 Rice Husk Ash	11
2.4.3 Silica Fume	12
2.5 EFFECT OF POZZOLANA ON CONCRETE	13
2.5.1 Fly Ash	14
2.5.2 Rice Husk Ash	14
2.5.3 Silica Fume	15
2.6 GEOPOLYMERS	16

2.6.1	Definition.....	16
2.6.2	Microstructure	17
2.6.3	Geopolymerization	20
2.7	POLYMERIC CONCRETE.....	23
2.8	INGREDIENTS OF POLYMERIC CONCRETE	26
2.8.1	Binder.....	27
2.8.2	Alkaline Activators	27
2.8.2.1	Sodium Hydroxide (NaOH)	28
2.8.2.2	Sodium Silicate (water glass)	28
2.9	MECHANISM OF REACTION	29
2.9.1	Role of Alkali Metals	31
2.9.2	Effect of Curing on Polymeric Concrete	31
3.	METHODOLOGY	33
3.1	MATERIALS SELECTION	33
3.1.1	Fly Ash.....	33
3.1.2	Microwave Incinerated Rice Husk Ash (MIRHA)	33
3.1.3	Silica Fume.....	36
3.1.4	Aggregates.....	37
3.1.5	Sodium Silicate (Na_2SiO_3).....	40
3.1.6	Sodium Hydroxide (NaOH).....	40
3.1.7	Table Sugar	40
3.1.8	Extra Water	41
3.2	SAMPLING AND MIXING OF CONCRETE.....	41
3.3	CONCRETE TESTING	45
3.3.1	Slump Test.....	45
3.3.2	Ultrasonic Pulse Velocity Test	47
3.3.3	Compressive Strength Test	48
3.3.4	Split Cylinder Test	48
3.3.5	Flexural Test	49
3.3.6	Scanning Electron Microscopy Analysis.....	50
4.	RESULTS & DISCUSSIONS	53
4.1	POLYMERIC CONCRETE SAMPLE ANALYSIS	52
4.1.1	Properties of Fresh Polymeric Concrete.....	52
4.1.2	Compressive Strength Test Results.....	56

4.1.2.1	Polymeric Concrete Samples with MIRHA in Hot Gunny Curing.....	58
4.1.2.2	Polymeric Concrete Samples with MIRHA in Ambient Curing.....	59
4.1.2.3	Polymeric Concrete Samples with MIRHA in External Exposure Curing	60
4.1.2.4	Polymeric Concrete Samples with SF in Hot Gunny Curing.....	62
4.1.2.5	Polymeric Concrete Samples with SF in Ambient Curing.....	63
4.1.2.6	Polymeric Concrete Samples with SF in External Exposure Curing	64
4.1.3	Splitting Tensile Strength Test Results.....	65
4.1.3.1	Polymeric Concrete Samples with MIRHA and SF in all Curing Regimes.....	65
4.1.4	Flexural Strength Test Results.....	70
4.1.4.1	Polymeric Concrete Samples with MIRHA and SF in all Curing Regimes.....	70
4.1.5	Ultrasonic Pulse Velocity Test Results	74
4.1.5.1	Polymeric Concrete Samples with MIRHA in Hot Gunny Curing.....	75
4.1.5.2	Polymeric Concrete Samples with MIRHA in Ambient Curing.....	76
4.1.5.3	Polymeric Concrete Samples with MIRHA in External Exposure Curing	77
4.1.5.4	Polymeric Concrete Samples with SF in Hot Gunny Curing.....	78
4.1.5.5	Polymeric Concrete Samples with SF in Ambient Curing.....	79
4.1.5.6	Polymeric Concrete Samples with SF in External Exposure Curing	79
4.1.6	Microstructure Analysis of Polymeric concrete	81
4.1.6.1	SEM Analysis of Control Mix in all Curing Regimes	81
4.1.6.2	SEM Analysis of Polymeric Concrete with MIRHA & SF in Hot gunny Curing	83
4.1.6.3	SEM Analysis of Polymeric Concrete with MIRHA &SF in Ambient Curing.....	85
4.1.6.4	SEM Analysis of Polymeric Concrete with MIRHA & SF in External Exposure Curing	87

5. CONCLUSION & RECOMMENDATION	91
5.1 CONCLUSIONS	89
5.2 RECOMMENDATIONS FOR FUTURE RESEARCH	90
REFERENCES	91
APPENDIX	
A PARTICLE SIZE ANALYSIS OF FLY ASH, MIRHA & SILICA FUME	101
B TECHNICAL SPECIFICATION FOR MICROWAVE INCINERATOR MODEL BENTECH INC-21 ADAPTED FROM BENTECH (BENTECH)	103
C LIST OF PAPERS & PUBLICATIONS	105

LIST OF FIGURES

Figure 1.1: Global CO ₂ production (World cement industry, 2010).....	2
Figure 2.1: The X-ray Diffraction for high calcium fly ash (HFA) and low calcium fly ash (LFA) (Shi & Day, 1995)	10
Figure 2.2: The X-Ray Diffraction of RHA under various temperatures burning (Hwang & Chandra, 1996)	11
Figure 2.3: TEM of a portion of a silica fume sample, showing characteristic linked clusters of spheres (Diamond & Sahu, 2006)	13
Figure 2.4: Chemical structures of polysialates (Davidovits, 2008).....	17
Figure 2.5: SEM images: (a) original fly ash, (b) Fly ash activated with 8 M NaOH for 5 h at 85 °C (Fernández-Jiménez, et al. 2005).....	19
Figure 2.6: SEM images: Fly ash activated with 8 M NaOH for 20 h at 85°C; (a) reaction process of a large sphere, (b) singular details of the reaction of some small spheres (Fernández-Jiménez, <i>et al.</i> 2005).....	19
Figure 2.7: TEM picture of an activated fly ash sample. Activator: 8 M NaOH dissolution. Curing conditions: 7 days at 85°C (Fernández-Jiménez, et al. 2005).....	20
Figure 2.8: Fly ash activated with sodium silicate (Fernández-Jiménez, <i>et al.</i> 2005).	20
Figure 2.9: Polymeric structure of Al–O–Si (Khale & Chaudhary, 2007)	23
Figure 2.10: Conceptual Model for Geopolymerization (Duxson, <i>et al.</i> 2006)	30
Figure 3.1: Automatic microwave incinerator at UTP	34
Figure 3.2: MIRHA after Burning and Sieving.....	35
Figure 3.3: Mechanical Siever	36
Figure 3.4: Coarse Aggregate & Fine Aggregates	37
Figure 3.5: Grading Curve for Coarse Aggregate	39

Figure 3.6: Grading Curve for Fine Aggregate	39
Figure 3.7: Polymeric Concrete after Mixing	42
Figure 3.8: Hot Gunny Curing	43
Figure 3.9: Ambient Curing	43
Figure 3.10: External Exposure Curing.....	43
Figure 3.11: UPV PUNDIT Tester.....	47
Figure 3.12: Digital Compressive Testing Machine	48
Figure 3.13: Split Tensile Strength Test Apparatus	49
Figure 3.14: Flexural Strength Test Assembly.....	50
Figure 3.15: LEO 1430 VP Inca X-Sight Oxford SEM Instrument with Sputter Coater	51
Figure 4.1: FESEM of Fly Ash	54
Figure 4.2: FESEM image of MIRHA.....	54
Figure 4.3: FESEM image of Silica Fume	54
Figure 4.4: Slump test result for FA-Based polymeric concrete with MIRHA	55
Figure 4.5: Slump test result for FA-Based polymeric concrete with SF	55
Figure 4.6: Compressive Strength Development for FA-Based Polymeric Concrete with MIRHA in Hot Gunny Curing	59
Figure 4.7: Compressive Strength Development for FA-Based Polymeric Concrete with MIRHA in Ambient Curing.....	60
Figure 4.8: Compressive Strength Development for FA-Based Polymeric Concrete with MIRHA in External Exposure Curing	61
Figure 4.9: Compressive Strength Development for FA-Based Polymeric Concrete with SF in Hot Gunny Curing	62
Figure 4.10: Compressive Strength Development for FA-Based Polymeric Concrete with SF in Ambient Curing.....	63

Figure 4.11: Compressive Strength Development for FA-Based Polymeric Concrete with SF in External Exposure Curing	65
Figure 4.12: 28-Days Splitting Tensile Strength for FA-Based Polymeric Concrete with MIRHA	68
Figure 4.13: 28-Days Splitting Tensile Strength for FA-Based Polymeric Concrete with SF	68
Figure 4.14: Correlation between Compressive Strength & Tensile Strength of: Polymeric Concrete with MIRHA	69
Figure 4.15: Correlation between Compressive Strength & Tensile Strength of Polymeric Concrete with SF	69
Figure 4.16: 28-Days Flexural Strength for FA-Based Polymeric Concrete with MIRHA	72
Figure 4.17: 28-Days Flexural Strength for FA-Based Polymeric Concrete with SF	72
Figure 4.18: Correlation between Compressive Strength & Flexural Strength of Polymeric Concrete with MIRHA	73
Figure 4.19: Correlation between Compressive Strength & Flexural Strength of Polymeric Concrete with SF	73
Figure 4.20: UPV Test Results for FA-Based Polymeric Concrete with MIRHA in Hot Gunny Curing.....	75
Figure 4.21: Pore Structure Developement.....	76
Figure 4.22: UPV Test Results for FA-Based Polymeric Concrete Replaced by MIRHA with Ambient Curing.....	77
Figure 4.23: UPV Test Results for FA-Based Polymeric Concrete Replaced by MIRHA with External Exposure Curing.....	78
Figure 4.24: UPV Test Results for FA-Based Polymeric Concrete with SF in Hot Gunny Curing	79
Figure 4.25: UPV Test Results for FA-Based Polymeric Concrete with SF in Ambient Curing	80

Figure 4.26: UPV Test Results for FA-Based Polymeric Concrete with SF in External Exposure Curing.....	81
Figure 4.27: SEM images for the Control Polymeric Mixes with a) Hot gunny curing b) Ambient curing and c) External exposure curing.....	82
Figure 4.28: FESEM Image of Polymeric Paste Showing Aluminosilicate gel.....	83
Figure 4.29: SEM images for the FA-based Polymeric Concrete in Hot Gunny Curing with a) 3% MIRHA b) 5% MIRHA and c) 7% MIRHA.....	84
Figure 4.30: SEM images for the FA-based Polymeric Concrete in Hot Gunny Curing with a) 3% SF b) 5% SF and c) 7% SF	84
Figure 4.31: SEM images for the FA-based Polymeric Concrete in Ambient Curing with a) 3% MIRHA b) 5% MIRHA and c) 7% MIRHA.....	86
Figure 4.32: SEM images for the FA-based Polymeric Concrete in Ambient Curing with a) 3% SF b) 5% SF and c) 7% SF	86
Figure 4.33: SEM images for the FA-based Polymeric Concrete in External Exposure Curing with a) 3% MIRHA b) 5% MIRHA and c) 7% MIRHA.....	87
Figure 4.34: SEM images for the FA-based Polymeric Concrete in External Exposure Curing with a) 3% SF b) 5% SF and c) 7% SF	88

LIST OF TABLES

Table 2.1: Average Bulk Composition of a Class F and C Fly Ash (Scheetz, 2004)	10
Table 3.1: Composition of Class F Fly ash using XRF.....	34
Table 3.2: Burning Procedure for 800°C Burning Temperature.....	35
Table 3.3: Composition of MIRHA using XRF.....	36
Table 3.4: Composition of Silica fume using XRF.....	37
Table 3.5: Sieve Analysis Results of Coarse Aggregate.....	38
Table 3.6: Sieve Analysis Results of Fine Aggregate.....	38
Table 3.7: Mix design Proportions.....	44
Table 3.8: Experimental Details of Tests on Concrete Specimen.....	46
Table 4.1: Slump test results for each mix.....	53
Table 4.2: Compressive Strength of FA-Based Polymeric Concrete Replaced by MIRHA.....	56
Table 4.3: Compressive Strength of FA-Based Polymeric Concrete Replaced by SF	57
Table 4.4: Rate of Strength Development of Polymeric Concrete with MIRHA with Respect to 28 Days Strength	57
Table 4.5: Rate of Strength Development of Polymeric Concrete with SF with Respect to 28 Days Strength	58
Table 4.6: Splitting Tensile Strength Test Results of FA-Based Polymeric Concrete with MIRHA	67
Table 4.7: Splitting Tensile Strength Test Results of FA-Based Polymeric Concrete with SF	67
Table 4.8: Flexural Strength of FA-Based Polymeric Concrete with MIRHA.....	70

Table 4.9: Flexural Strength of FA-Based Polymeric Concrete with SF	71
Table 4.10: UPV Test Results of FA-Based Polymeric Concrete with MIRHA	74
Table 4.11: UPV Test Results of FA-Based Polymeric Concrete with SF	74

LIST OF ABBREVIATIONS

etc	Et cetera
FA	Fly Ash
FESEM	Field Emission Scanning Electron Microscopy
i.e.	That is
MASNMR	Magic Angle Spinning Nuclear Magnetic Resonance
MIRHA	Microwave Incinerated Rice Husk Ash
n.d.	No date
OPC	Ordinary Portland Cement
RHA	Rice Husk Ash
SEM	Scanning Electron Microscopy
SF	Silica Fume
TEM	Transmission electron microscopy
XRF	X-Ray Fluorescence

CHAPTER 1

INTRODUCTION

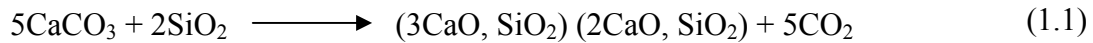
1.1 BACKGROUND

Concrete production is the largest among all man-made materials with an annual global production of about one cubic meter per person on earth (NRC Canada, 2005). Its sophistication lies in the fact that its constituents are universally available. Due to this fact, it has become a distinctive construction material in the world. Concrete is basically a composite mixture containing cement paste and aggregates as its main components. Cement is manufactured by limestone, clay and other mineral, mixed in definite proportions to produce chemical reaction during a burning process at very high temperature. In 2005, cement production made a new record of 2.31 billion metric tons by the increase of 5.5%/yr, that is expected to rise by 4.1% globally to 3.5 billion metric ton in 2013 (World cement industry, 2010).

Nowadays cement industry is at its peak throughout the world and even expected to grow in the coming years. The largest market of cement in the world is China. Besides this other developing countries of Asia, Eastern Europe, Africa, Middle East and Latin America will also nearly be making above average records in cement market gains. Vietnam, Thailand, Malaysia, Ukraine, Turkey and Indonesia will also show significant advances in terms of cement production as predicted (World cement industry, 2010). New technologies are heading towards the construction of high rise buildings; medium and short span bridges, dams etc that is drastically increasing the amount of concrete and production of cement.

The contribution of cement industry to the CO₂ emissions is about 5 % of the global CO₂ emissions (Figure1.1) and one ton of CO₂ is released in the atmosphere from one ton production of Portland cement (Davidovits, 2008). According to Khale

and Chaudhary (2007), cement (OPC) results from calcination of limestone (CaCO_3) and silico-aluminous materials according to the Equation 1.1.



Therefore CO_2 emission from a cement plant is divided into two source categories: combustion and calcination. Combustion contributes 40% and calcinations contributes 60% in the total CO_2 emissions from cement manufacturing process (World cement industry, 2010) (Figure1.1). The emissions from combustion are related to fuel use and the emissions due to calcination are formed when the raw materials (limestone and clay) are heated to over 1500°C and CO_2 is liberated from the decomposed limestone. Emissions of CO_2 from cement production are increasing at a much more rapid rate than all other industrial sources put together. This extends to the need for solutions and new technologies adapted to the economy of the developing countries.

Besides CO_2 emission, quarrying of raw materials (limestone and clay) for the production of cement is becoming the source of environmental degradation. To produce one ton of ordinary portland cement (OPC), 1.6 tons of raw materials are needed and the extraction of raw materials from the earth is 20% faster than the earth replenish it, so raw materials consumed in 12 months will take 14.4 months to be filled back (Naik, 2005).

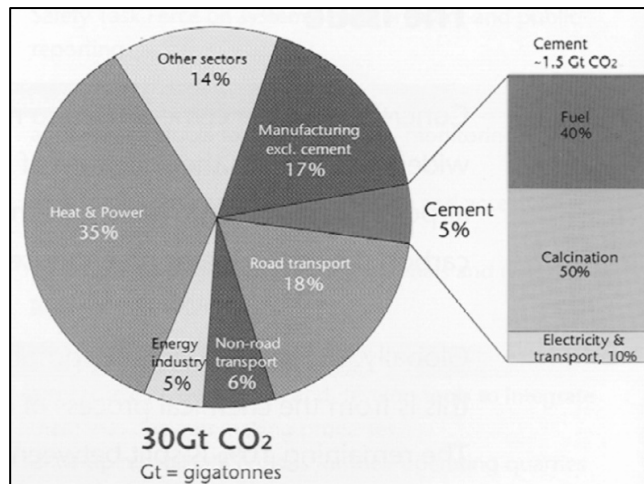


Figure 1.1: Global CO_2 production (World cement industry, 2010)

Many researchers from the world are working on this serious issue and it was found out that one of the solutions is to introduce geopolymer cement through the development of inorganic alumina-silicate polymer (Nuruddin, *et al.* 2009). This cementing property can be obtained by the reaction of industrial by-products such as fly-ash or other mining material and agricultural waste products such as rice husk with the alkaline liquid. Geopolymer cements can reduce 80% to 90% of CO₂ emission as compared to ordinary Portland cement (Davidovits, 2008), which produces 65% of global warming among all green house gases emissions (McCaffrey, 2002), will ultimately lead to the decrease in global warming and depletion of ozone layer.

1.2 PROBLEM STATEMENT

There is a boom in the construction of high rise buildings, medium to long span bridges, dams etc. all over the world from the last few decades. These constructions lead to the utilization of large quantity of concrete which leads to increase in cement production by 5.5% annually. As a consequence CO₂ emission and depletion of raw materials are unavoidable. On the other hand, waste disposal is a global issue and with the passage of time, landfilling is becoming costly as well as a source of water and land pollution on earth. Solution is to get rid of OPC concrete and to introduce polymeric concrete that is a good alternative to address CO₂ emission issues, depletion of raw materials and effective use of waste material. The integrity of geopolymer concrete has to be ascertained and mix design shall be established in this research.

Various studies have shown the use of some percentage of raw materials in concrete but overall less work has been done on polymeric concrete which presents the idea of complete removal of cement from concrete. In place of cement; fly ash, rice husk ash and silica fume can be used that are abundantly available in almost all parts of the world. Until now researchers adopted oven curing or steam curing techniques for polymeric concrete that is only applicable for pre-cast structures while in this research curing regimes used that are those suitable for in-situ construction.

1.3 OBJECTIVES OF STUDY

The objectives of this research study are as follows:

a) Primary Objectives

- To develop a polymeric concrete without cement.
- To establish the most appropriate curing regime for in-situ construction.
- To identify the mechanical properties of polymeric concrete i.e. compression, flexure and tension.

b) Secondary Objectives

- To identify the cementing potential of polymeric concrete through scanning electron microscopy (SEM).
- To establish an optimum polymeric concrete mix containing fly ash, microwave incinerated rice husk ash (MIRHA) and silica fume with 28 days target cube strength of 40-50MPa.

CHAPTER 2

LITERATURE REVIEW

2.1 INTRODUCTION

Waste materials have been introduced into the construction industry to replace cement that proved to be an inimitable shift from past few years. Most abundantly obtained waste materials are fly ash, rice husk and silica fume that are rich in silica and when react with alkaline liquid forms a binder similar to that of cement. Use of these waste materials in concrete to replace cement, will reduce global warming and depletion of ozone layer and on the other hand it will save the space of landfill and raw material depletion on the earth.

2.2 CEMENT AND CONCRETE PRODUCTION

Currently, roughly 3% of the earth's land surface is occupied by urban areas (Global Rural urban mapping project, 2005). It is estimated that by 2025 about 66% of the world's population will live in urban areas on 7% of the land (Dordi, 2010). This means that urbanization will be on a small portion of land and this will need taller buildings and use of high strength concrete in bulk amount. Also good infrastructure would be needed and obviously concrete will be used in their construction because it is cheaper and a globally available material.

The Cement Association of Canada (n.d.) reported that annual global production of concrete is about 5 billion cubic yards and as compared to other building materials like wood, steel etc concrete is used twice than that in construction.

Commodity Research Bureau (2007) reported that global production of hydraulic cement made a new record of 2.31 billion metric tons with a increase of 5.5% /yr. The

world's largest cement producers are China with 45% of world production in 2004, India with 6%, USA with 4% and Japan with 3% of the world's production.

Malhotra (1999) estimated that the production of cement will increase from about 1.5 billion tons in 1995 to 2.2 billion tons in 2010.

2.2.1 Environmental Issues Related to Cement Production

Production of cement is producing CO₂ that gave rise to serious sustainability issue of the 21st century known as global warming. Global warming is due to green house gas emission, mainly CO₂, leading to the continuous increase in the earth's surface temperature since 1950's. World Watch Institute report states that twenty-four years of the last twenty-seven years have been the warmest on record (Mehta, n.d.).

Davidovits (2008) studied that production of one ton of Portland cement emits approximately one ton of CO₂ into the atmosphere.

The contribution of global cement industry to the green house gas emission is around 1.35 billion tons annually that is 7% of total man made greenhouse gas emissions to the earth's atmosphere (Malhotra, 2002) which gives rise to global warming.

Mehta (n.d.) observed the following effects of the global warming:

- A sharp increase in the melting rates of glaciers, polar caps, and ice sheets.
- Rising ocean levels—a potential threat to coastal populations.
- Unusual increase in frequency and intensity of rainstorms, flash floods, cyclones, hurricanes, heat waves, droughts, and wild fires.
- Adverse impact on current sources of agriculture and water.
- Disruption of the earth's carbon cycle due to changes in the botanical species on land and oceans.

2.2.2 Depletion of Resources

Besides decarbonisation reaction by the burning of limestone at high temperatures, CEMBUREAU (1999) addressed the environmental impacts due to the production of cement that includes depletion of raw material.

Naik (2005) observed that for one ton production of cement, 1.6 tons of raw materials are needed including limestone and clay. Therefore the extraction of raw materials from the earth is 20% faster than the earth replenish it, so raw materials consumed in 12 months will take 14.4 months to be filled back. The research conducted; found that limestone is no more a sustainable material. Quarrying of limestone and clay needs energy and also causes destruction of land and vegetation (Wu, 2000).

2.3 WASTE MATERIALS

Many waste materials have been used in concrete and some of the examples are foundry sand (Siddiquea *et al.* 2009), mill scale (steel production) (Mahallati & Saremi 2006), Iron from used tyres, recycled plastic (Siddiquea, *et al.* 2009; Yilmaz & Degirmenci, 2009), glass (Batayneh, *et al.* 2007), Palm oil fuel ash (POFA) (Tangchirapat, *et al.* 2007), blast furnace slag (Barnett, *et al.* 2006), (Yazıcı, *et al.* 2008; Bilim, *et al.* 2009), metakaolin (Sabir, *et al.* 2001), (Rowels & O'Connor, 2003), silica fume (Rao, 1998; Mazloom, *et al.* 2004; Luther, 1990), fly ash (Rangan, 2008; Palomo, *et al.* 2004 & 1999) rice husk ash (Nair, *et al.* 2006) etc.

The best utilization of waste material could be in concrete as a replacement of OPC, because it is the most utilized material after water (Rangan, 2008). The waste materials activated as cementitious materials are classified into two groups depending on the chemical composition of the source material (Khale & Chaudhary, 2007):

- Rich in calcium, producing calcium silicate hydrate gel (CSH) when activated with alkaline solution such as blast furnace slag.

- Low in calcium and rich in SiO_2 and Al_2O_3 , producing alumino-silicate gel when activated with alkaline solution such as metakaolin, fly ash, rice husk ash, silica fume etc.

2.3.1 Disposal Effects on Environment

Waste materials and by-products are undesirable materials for our environment that are the result of continuous expansion of industrialization or agricultural activities such as fly ash and rice husk respectively. These materials eventually disposed of in landfills that are becoming scarce and expensive (Fytianos, *et.al.* 1998) at the same time, leading to a waste disposal crisis. Power plants produce millions of tonnes of fly ash per year, which is mostly wasted in landfills at a cost around \$1 billion. Global production of fly ash is expected to rise by 800 million tons per year in 2010 (Izquierdo, *et al.* 2009). Disposal cost can be saved by proper utilization of fly ash in concrete with actual cost of 11–22 cents/kg (Rohatgi, *et al.* 2006).

Disposal of fly ash causes water and land pollution by contamination of soil which further contaminates ground water resources because fly ash is composed of smaller particle size and contains some toxic elements like arsenic, chromium, boron, vanadium and antimony (Sushil & Batra, 2006).

On the other hand, disposal of rice husk is difficult because of its low nutritional value; long time is required for its decomposition to be used in manure (Zemke & Woods, 2009). Almost 2.2 million tons of rice husk is produced per year from agriculture activity, contributing to 500-600 million metric tons of annual world husks production (Bouman, *et al.* 2007). All the produced husk is disposed of in landfills and cannot be used anywhere i.e. a great threat to our environment (Tashima, *et al.* 2004).

2.4 TYPES OF CEMENT REPLACEMENT WASTE MATERIALS

2.4.1 Fly Ash

Fly ash, also known as pulverized fuel ash, is basically a non-combustible mineral portion of the coal that has been thermally altered as it passes through the combustion process. After the consumption of coal in the power plant, it is first ground to powder. Then blown into a power plant's boiler where the carbon is consumed, leaving behind the molten particles rich in silica, aluminum and calcium. These particles are then solidified as microscopic, glassy spheres that are collected from the power plant's exhaust.

Nowadays fly ash is being dumped into the sea or landfills due to which leaching of metals and organic compounds could occur and contaminates ground water. Only about 25% of fly ash is being recycled worldwide and the rest is dumped into the landfill that is hazardous for our environment (Wang, *et al.* 2004).

ASTM (ASTM C 618) classified pulverized coal ashes by their aggregate alumina, silica, and ferric oxide content into Class F and C (Wang, *et al.* 2004). Class F comprises of at least 70% of these three oxides and Class C contain 50% of the three oxides (Scheetz, 2004). Class F is also known as low-calcium fly ash (LFA) having CaO content less than 10% whereas Class C; high calcium fly ash (HFA) contains more than 10% of CaO (Davidovits, 2008). Average bulk composition of Class F and Class C fly ash is shown in Table 2.1.

Based on X-ray diffraction analysis, Shi & Day (1995) concluded that LFA produced amorphous constituent as compared to HFA which contained quartz in the hydration product. Figure 2.1 shows the result of the X-ray diffraction.

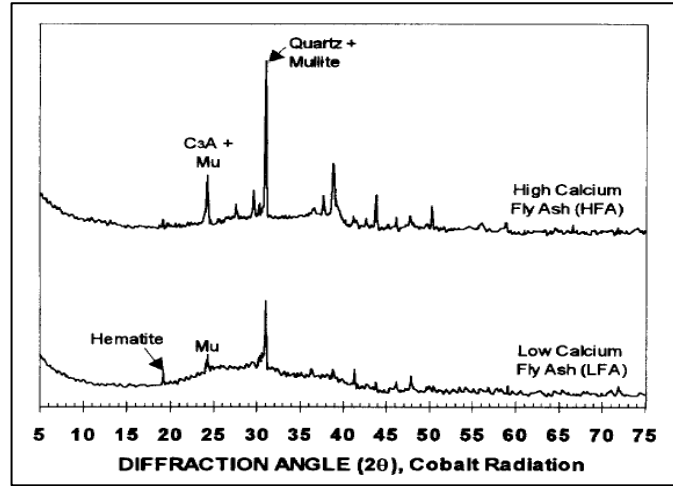


Figure 2.1: The X-ray Diffraction for high calcium fly ash (HFA) and low calcium fly ash (LFA) (Shi & Day, 1995)

Table 2.1: Average Bulk Composition of a Class F and C Fly Ash (Scheetz, 2004).

Oxides	Wt. %	
	Class F	Class C
SiO ₂	52.5±9.6	36.9±4.7
Al ₂ O ₃	22.8±5.4	17.6±2.7
Fe ₂ O ₃	7.5±4.3	6.2±1.1
CaO	4.9±2.9	25.2±2.8
MgO	1.3±0.7	5.1±1.0
Na ₂ O	1.0±1.0	1.7±1.2
K ₂ O	1.3±0.8	0.6±0.6
SO ₃	0.6±0.5	2.9±1.8

Mehta (2004) predicted that, in future primary source of power generation seems to be fossil fuels because of low cost of coal and major coal producing countries will likely to continue with coal-fired power industry such as China, India, and the United States. He also mentioned that according to one of the estimate, approximately 1200 million tonnes of fly ash would be available in 2020. This shows the sustainability of fly ash for the use in concrete.

Malhotra (2006) studied that an estimated 600 million tonnes of FA was produced in the world in 2000. In North America the production was 60 million tons annually and in Canada it was 5.1 million ton in 1999.

2.4.2 Rice Husk Ash

Rice plant absorbs silica from the soil and integrates it into its structure during its growth period. The outer covering of the rice grain is known as ‘husk’ which contains 80-85% of silica which contains 80% of organic and 20% of inorganic substance (Naji Givi, *et al.* 2010). Husk makes 20% of the rice paddy (Tashima, *et al.* 2004). Husk provides rice husk ash after incineration i.e. 20% of its total weight (Anwar, *et al.* 2001) and highly pozzolanic in nature (Tashima, *et al.* 2004).

When this husk is burnt in the microwave incinerator, microwave incinerated rice husk ash (MIRHA) is generated. Recent research showed that pozzolanic activity varies with different burning method used. Based on the research, RHA produced by microwave incinerator burning has the highest value of pozzolanicity as compared to other methods of burning (Nuruddin, *et al.* 2008). It is a fibrous material containing more than 90% silica.

Hwang & Chandra (1996) reported that rice husk that was being incinerated at 800°C, provided the most amorphous constituent. Figure 2.2 shows that crystalline properties emerged by increasing the burning temperature.

Nair *et al.* (2006) investigated that temperatures of 500°C and 700°C and burning time more than 12 hours were favorable conditions to produce reactive rice husk ashes.

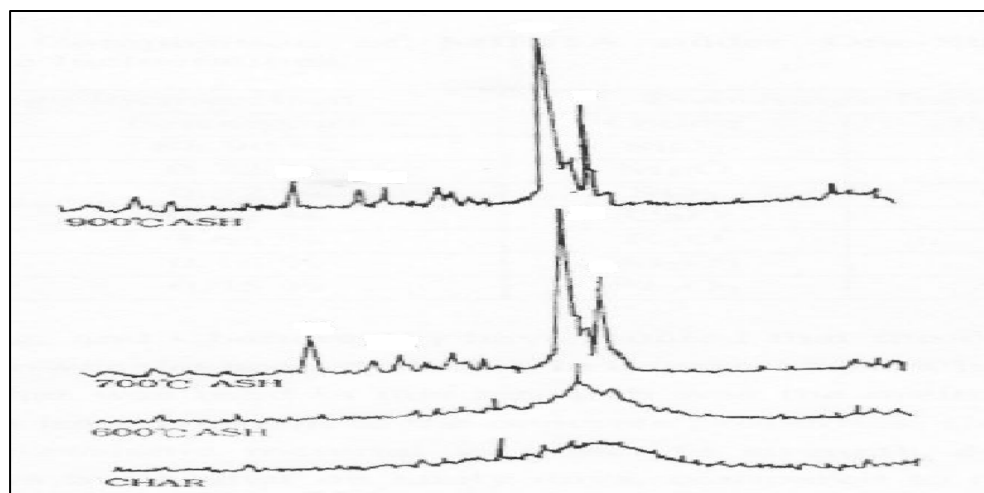


Figure 2.2: The X-Ray Diffraction of RHA under various temperatures burning (Hwang & Chandra, 1996)

Mehta (1992) and James & Subba (1986) also reported the same temperature for incineration process and observed that after 1hr of incineration transforms silica content of the ash into amorphous phase and the reactivity of amorphous silica was directly proportional to the specific surface area of ash.

Research has also been done on the production of most reactive ash (pozzolana) from rice husk. In 2006, Nair *et al.* studied the properties of RHA samples from different types of field ovens and found out that RHA from annular enclosure produced better results as compared to others.

Nair *et al.* (2006) also investigated the pozzolanic activity of RHA and concluded that more reactive RHA was produced after incineration for 12hrs at 500°C and also by quick cooling.

Srivastava *et al.* (2006) presented the study on characterization of low-cost rice husk ash for its various physio-chemical properties and adsorption characteristics of metal ions and concluded that RHA is a mesoporous material.

Comparative test has also been done (Jaubertie, *et al.* 2002) between the specimens stored in dry and wet conditions. Results showed that at high humidity conservation the mortar gained strength with a loss in flexibility and samples stored at 50% relative humidity gained more flexibility with loss in strength.

2.4.3 Silica Fume

Silica fume is a byproduct of the reduction of high-purity quartz with coal in electric furnaces for the production of silicon and ferrosilicon alloys (Federal highway administration) and is also called as microsilica. Silica fume is also collected as a byproduct in the production of other silicon alloys such as ferrochromium and calcium silicon (ACI Comm 226, 1987b).

Diamond & Sahu (2006) studied the particle size distribution of silica fume and found out that it exists in the range of 0.03µm to about 0.16µm for the individual particles but actually they appear as a clusters or chain as shown in Figure 2.3.

Silica fume consists of very fine vitreous particles with particle size approximately 100 times smaller than the average cement particle (Federal highway administration) but the silica fume provided to a customer is densified which shows the particle size in the range of hundreds of μm (Diamond & Sahu, 2006).

2.5 EFFECT OF POZZOLANA ON CONCRETE

According to ASTM 618-94a, pozzolan is a siliceous or siliceous and aluminous material which in itself possesses little or no cementitious value but will, in finely divided form and in the presence of moisture, chemically react with calcium hydroxide at ordinary temperatures to form compounds possessing cementitious properties.

Pozzolana plays an important role in the formation of geopolymer. Added technical benefits were obtained by the utilization of pozzolana in concrete including improvement in durability, reduction in rise of temperature and strength improvement (Khale & Chaudhary, 2007). Although in some cases strength develops slowly (Sabir, *et. al.* 2001). Various researchers studied to develop different methods to make most durable geopolymer cements for which they have used several materials including kaolin, bentonites; rich in Al and fly ash, rice husk ash, silica fume, etc; rich in Si (Khale & Chaudhary, 2007). Some of the pozzolana, used in this study are described as under.

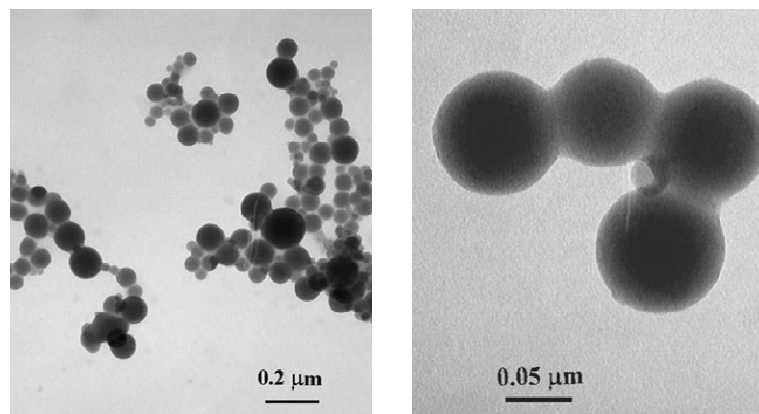


Figure 2.3: TEM of a portion of a silica fume sample, showing characteristic linked clusters of spheres (Diamond & Sahu, 2006)

2.5.1 Fly Ash

Different studies showed that fly ash (FA) could be a terrific replacement of cement if used in certain conditions. Shafiq & Cabrera (2004) presented the experimental study of the influence of two different initial curing conditions, wet and dry. Study showed that FA blended cement concrete requires prolonged wet curing condition to produce lower porosity and higher durability.

Development of chloride resisting fly ash blended cement concrete has also been studied (Dhir & Jones, 1999; Shafiq, 2004) and both studies have shown that fly ash blended cement concrete is more resistant as compared to OPC concrete.

Properties of blended cement concrete also depend upon the composition and source of FA. Shafiq *et al.*(2007) compared the results of coarser and finer FA obtained from Malaysia and UK respectively and found out that coarser FA require more water to achieve the targeted slump of 55 ± 5 mm as compared to the less coarser FA.

2.5.2 Rice Husk Ash

In past years researchers started with the replacement of some percentage of cement and studied the characteristics and properties to find out that RHA benefit the pozzolanic reaction in concrete (Jaubertie, *et al.* 2002). Bouzoubaa & Fournier (2001) replaced 7.5 to 12.5% of the OPC by RHA and found no any significant effect on the compressive strength of concrete so he recommended to increase the percentage of concrete upto 20% or more.

Chin (2007) studied the effects of used engine oil in blended cements with 40% and 50% FA with 20% and 30% RHA on fresh and hardened properties of concrete and she found out more encouraging results as compared to the use of superplasticiser in blended concrete. She also observed that FA has the tendency to increase the slump and RHA demands more water for the required slump.

Also in 2007, Kusbiantoro studied concrete by replacing cement (0%, 5%, 10%, 15%) with microwave incinerated rice husk ash (MIRHA) at three (0.35, 0.4, 0.45) different w/c ratios. He observed that at 0.4 w/c of MIRHA concrete achieved strength 31.73% higher than 0.4 w/c control concrete at 56 days of age. Same results have been found out for 0.45 w/c of MIRHA concrete. 0.35 w/c ratio MIRHA concrete did not perform better as compared to control concrete.

Rodríguez de Sensale (2006) replaced 10%-20% of concrete by RHA with different w/c ratios. Results showed that the concrete with RHA had greater strength as compared to the concrete without RHA at 91 days.

Influence of fineness of RHA on light weight concrete has also been studied (Chindaprasirt, *et al.* 2009). Results showed that RHA has the potential for making light weight aggregate with low bulk density of 0.20–0.40 g/cm³.

2.5.3 Silica Fume

Silica fume is an effective pozzolanic material due to the great fineness and high silica content (Luther, 1990) and pozzolanic action of silica fume was found out to be completed at the early ages but insignificant at later ages (Rao, 1998). Silica fume is used in concrete to enhance its properties such as compressive strength, bond strength, abrasion resistance, permeability and protection of reinforcing steel from corrosion (Federal highway administration).

Silica fume increases water demand when added to the concrete but it was found that less than 10% replacement does not put significant effect on the workability of concrete and high amount of silica decreased flowability which provided dense microstructure and improved mechanical properties (Bagel, 1998; Zhang & Han, 2000).

Mazloom *et al.* (2004) replaced 0-15% cement by silica fume and studied the effect of silica fume on high strength concrete and found out that silica fume decreased the workability so more superplasticizer was needed and compressive strength did not increase after age of 90 days.

Thomas *et al.* (1999) used ternary cementitious blends of ordinary Portland cement, fly ash and silica fume and found out that the combination of silica fume with fly ash is complementary; silica fume enhanced the performance of concrete with the fly ash progressively refining the properties of the hardened concrete.

Atis *et al.* (2005) found out that compressive strength of silica fume concrete cured at 65% relative humidity (RH) was 13% lower than that of silica fume concrete cured at 100% RH and observed the influence of dry curing conditions on silica fume concrete with the increase in silica fume replacement ratio. H found that increase in water-cementitious material ratios makes the concrete more sensitive to dry curing conditions.

Goyal *et al.* (2007) experimented silica fume with Portland cement and observed that with the increase of silica fume in concrete, water demand was increased and slump was decreased which made the addition of superplasticizers necessary for the mix,

2.6 GEOPOLYMERS

2.6.1 Definition

In 1979, Davidovits (2008) created and applied the term geopolymer because polymerization process takes place, in which Si and Al present in the source material such as fly ash, silica fume or rice husk ash, reacts with the alkaline liquid to produce binders. Geopolymers are chains or networks of mineral molecules linked with covalent bonds

Polymerization is a process in which relatively small molecules, called monomers, combine chemically to produce a very large chainlike or network molecule, called a polymer.

Geopolymers are based on silico-aluminates so the chemical name suggested for them was polysialate. Sialate is an abbreviation for silicon-oxo-aluminate.

Polysialates are chain and ring polymers with Si^{4+} and Al^{3+} in IV-fold coordination with oxygen and range from amorphous to semi-crystalline (Figure 2.4) (Davidovits, 2008).

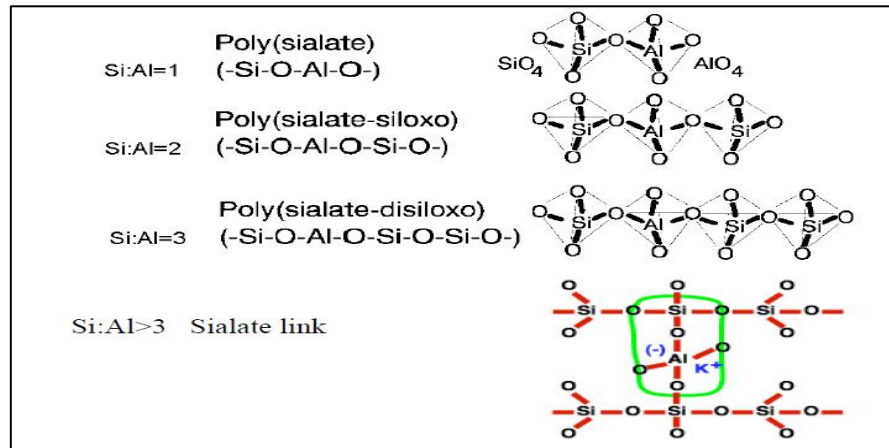


Figure 2.4: Chemical structures of polysialates (Davidovits, 2008)

2.6.2 Microstructure

The chemical composition of geopolymer material is similar to natural zeolitic material (crystalline in nature) but microstructure is amorphous to semi-crystalline (Palomo, *et al.* 1999; Xu and Van Deventer, 2000; Khale & Chaudhary, 2007) because a zeolite forms in closed hydrothermal systems but geopolymer does not (Khale & Chaudhary, 2007).

Most of researchers used fly ash as a source material, containing Si and Al as its main components, that was being activated by alkaline solutions and microstructure of alkali activated fly ash changes with the chemical composition (Rowels & O'Conner, 2003).

Invention of advanced instrumental technologies such as MASNMR, SEM, TEM, etc. made it possible to study the morphology and microstructure of geopolymer concrete. With the help of these technologies, researchers found that prominent reaction product in this material was three dimensional, short range amorphous aluminosilicate gel with a predominance of Q4(3Al) and Q4(2Al) that could be

considered as a zeolite precursor (Palomo, *et al.* 2004; Fernández-Jiménez, *et al.* 2005).

Fernández-Jiménez *et al.* (2005) studied the microstructure of original Class F fly ash (Figure 2.5a) as well as activated fly ash with alkaline solution (8M NaOH) for 5h (Figure 2.5b). They explained that original fly ash morphology showed a series of spherical vitreous particles of different sizes (diameters ranging from 200 to 10 μm), some of them were hollow that contain smaller size particles. They further explained that at first stage of reaction some portion of large spherical particles were dissolved, exposing smaller particles to the alkaline attack. At this stage Si/Al ratio found to be 1.6 (Gel 1 matrix) which showed low mechanical strength in the range of 20 MPa. At later stage of curing the Si/Al ratio became 1.9-2.1 (Gel 2 matrix) which was fully compacted and hardened stage with high strength in the range of 80 MPa. In Figure 2.6a, after 20h at 85°C some small fly ash particles that underwent alkali dissolution appeared to coexist with some undissolved particles and some other particles covered with the reaction product known as sodium aluminosilicate gel.

Figure 2.6b shows small spheres covered with reaction product that is the indication of occurrence of the reaction. The microstructure of fly ash activated with 8M NaOH (7 days of age at 85°C) was also studied with the powerful technology of transmission electron microscopy (TEM). It was found out that inside the bigger particles there were some small particles, shown by arrows in Figure 2.7, that were embedded into sodium aluminosilicate gel (zeolitic precursor) produced during the activation process.

On the basis of previous investigation by Fernández-Jiménez *et al.* 2005, it was believed that reactive silica content, the vitreous phase content and the particle size distribution did not affect the mechanism of activation but affected the potential reactivity of fly ash.

They also studied the effect of soluble silica on the microstructure and found that soluble silica played an important role in the development of microstructure of these types of binding systems (Figure 2.8). It only affected the chemistry and kinetics of material but not the governing mechanisms of the reaction (Palomo, *et al.* 1999).

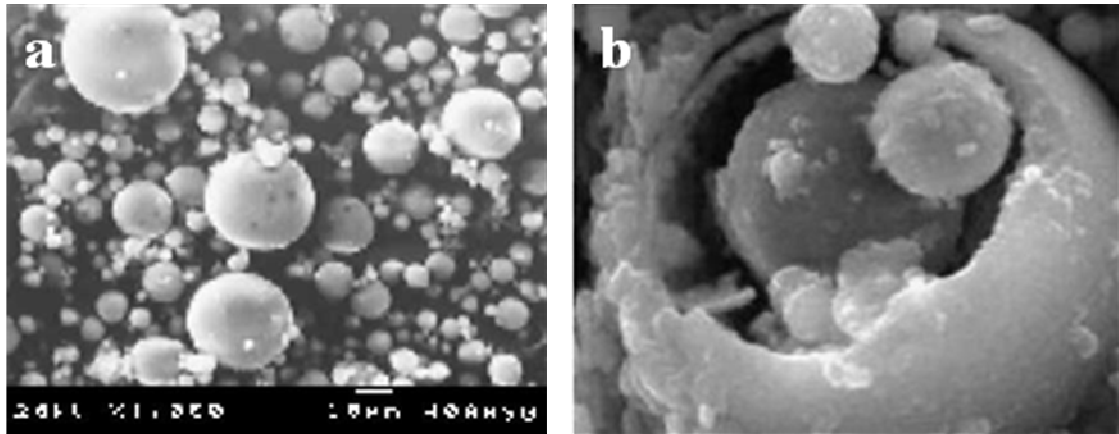


Figure 2.5: SEM images: (a) original fly ash, (b) Fly ash activated with 8 M NaOH for 5 h at 85 °C (Fernández-Jiménez, et al. 2005)

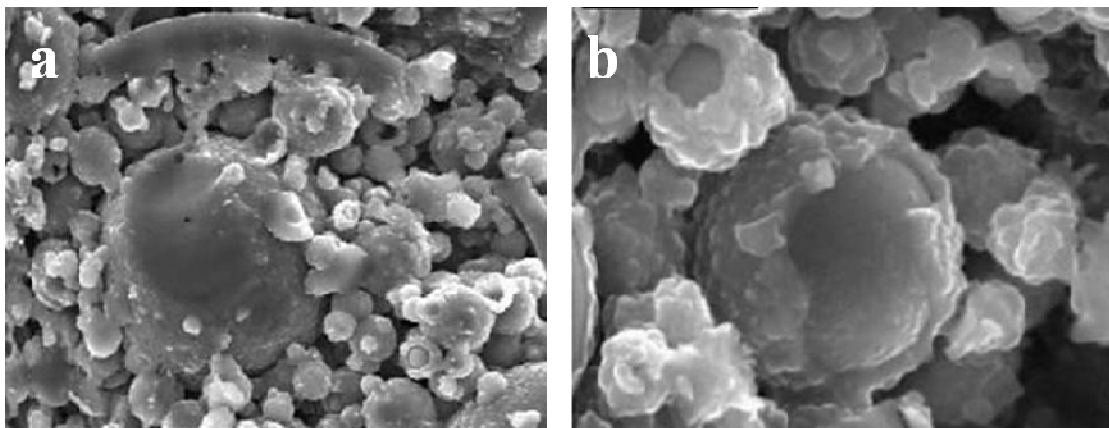


Figure 2.6: SEM images: Fly ash activated with 8 M NaOH for 20 h at 85°C; (a) reaction process of a large sphere, (b) singular details of the reaction of some small spheres (Fernández-Jiménez, *et al.* 2005).

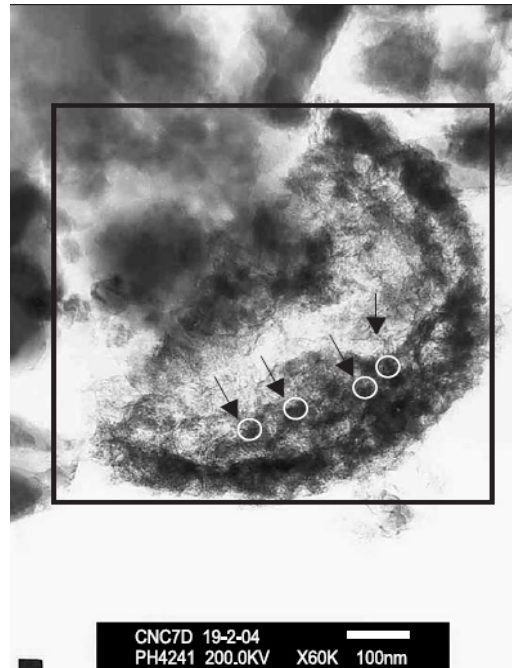


Figure 2.7: TEM picture of an activated fly ash sample. Activator: 8 M NaOH dissolution. Curing conditions: 7 days at 85°C (Fernández-Jiménez, et al. 2005).

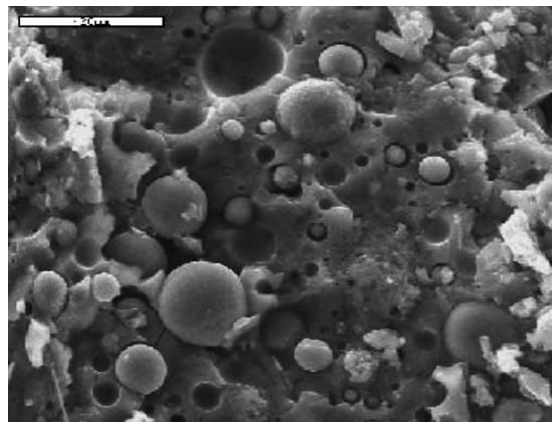
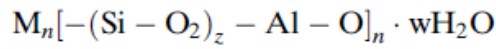


Figure 2.8: Fly ash activated with sodium silicate (Fernández-Jiménez, *et al.* 2005).

2.6.3 Geopolymerization

In geopolymer, polymerization is condensation polymerization in which water is released during chemical reaction and nature of reaction is endothermic. In geopolymerization, the polycondensation of aluminosilicate oxides (Si_2O_5 , Al_2O_2)

with alkali polysilicates (sodium or potassium silicate) takes place producing Si – O – Al bonds (Hardjito & Rangan, 2005).



Where M is the alkaline element, z is 1, 2, or 3 and n is the degree of polycondensation (Hardjito & Rangan, 2005).

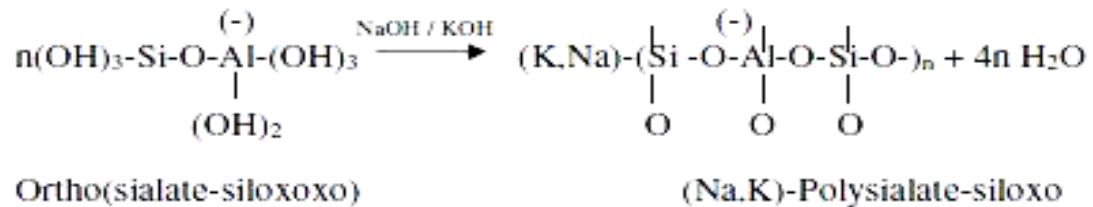
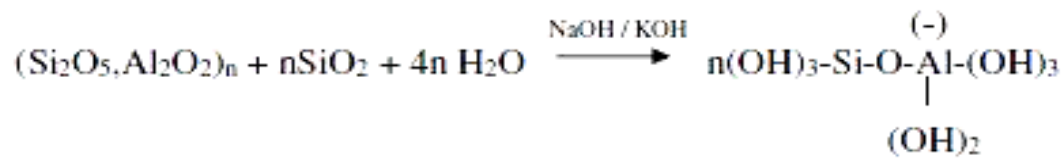
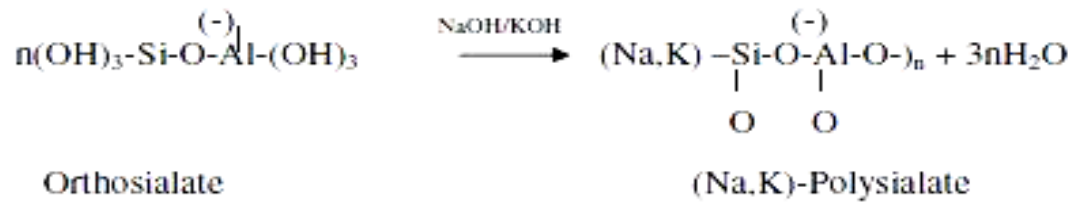
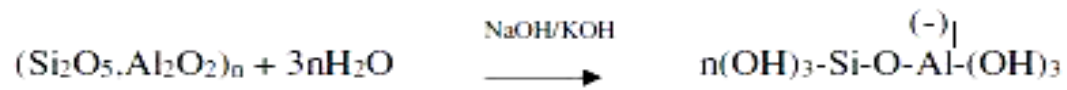
Polycondensation takes place after the constituents get dissolved in an alkaline solution (Sofi, *et al.* 2007). NaOH initiates the reaction to occur and to form a polymer network. This reaction is very important for the formation of dense structure in order to generate material with high strength and other mechanical properties such as strength that is a function of its structure and vary greatly with the variation in structure of molecule (Murray, *et al.* 2007).

Aluminum and silica that are highly soluble in alkaline solutions, tetra-hedrally interlinked, alternately by sharing oxygen atoms. A polymeric structure of Al–O–Si in geopolymeric structure constitutes its main building blocks as shown in Figure 2.9.

Si and Al, randomly placed along the polymeric chain, are cross-linked to provide enough spaces for charge balancing sodium ions (Davidovits, 2008; Krivenko, 1997). Cross-linked polymers are among the strongest that inhibit chain sliding (Murray, *et al.* 2007).

Due to the application of mechanical load, polymer chain disentangles. Disentanglement occurs because of chain sliding and if this chain sliding is easy then the polymer is weak and if this chain sliding is difficult then polymer is strong. Polymer chain possesses intermolecular forces between them that actually give the strength to the polymer and polymer molecules are large enough to inhibit chain sliding (Murray, *et al.* 2007).

Reactions involve in geopolymerization are as follows (Khale & Chaudhary, 2007):



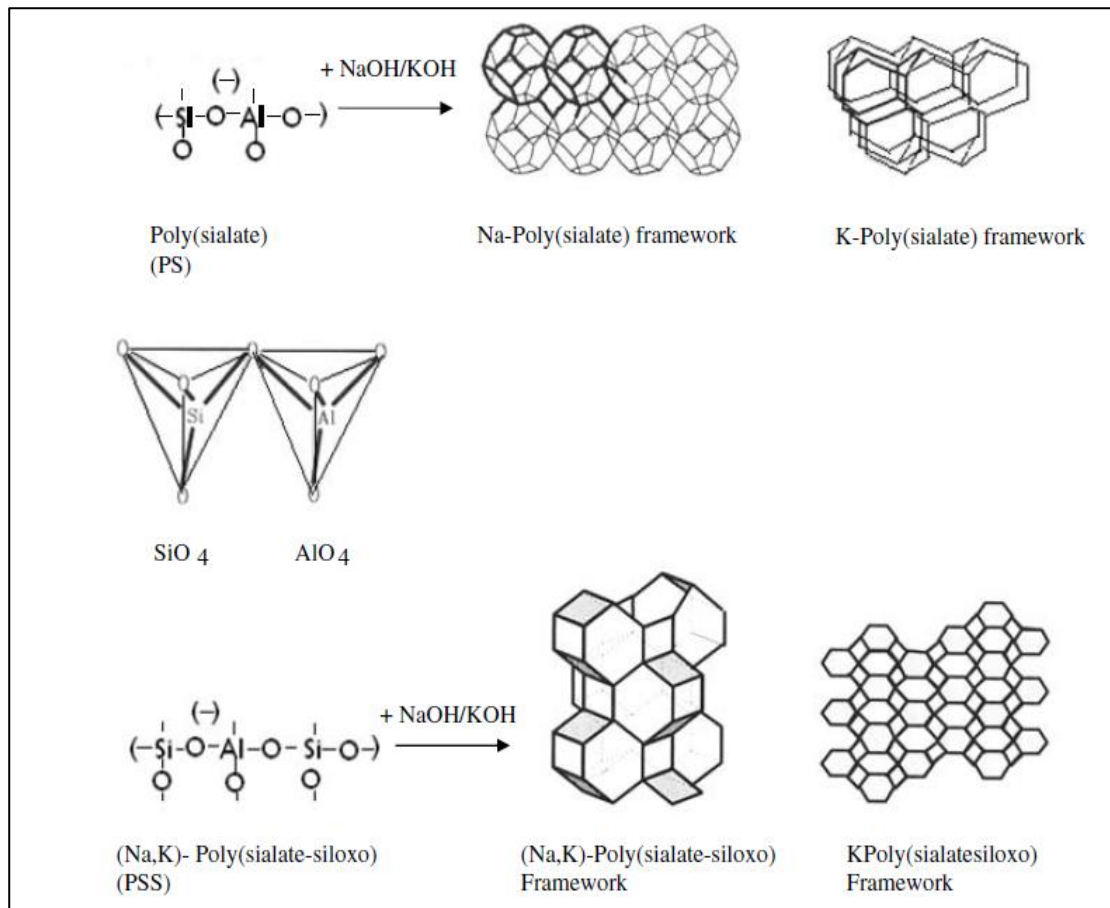


Figure 2.9: Polymeric structure of Al–O–Si (Khale & Chaudhary, 2007)

2.7 POLYMERIC CONCRETE

Till now less work has been done on the concrete purely without cement as a binder. Rangan (2008) presented his study on fly ash-based geopolymer concrete and concluded that low calcium fly ash based geopolymer has excellent compressive strength that is suitable for structural applications. He also concluded that elastic properties, behavior and strength of geopolymer structural members are similar as those observed in the case of Portland cement concrete. Besides that low-calcium fly ash-based geopolymer concrete also have excellent resistance to sulphate attack, good acid resistance, undergoes low creep and suffers very less drying shrinkage.

Alvarez-Ayuso *et al.* (2008) studied the suitability of different class F fly ash to be used in concrete in place of cement and they also studied the process involved in this synthesis. they concluded that strength was increased by increasing curing time

by 24 hours, the optimum curing temperature was 80°C, molarity of alkaline solution that give high strength were 8M and 12M and dissolution of fly ash was an endothermic process.

Komnitsas & Zaharaki (2007) presented a brief history and assessment of geopolymer technology and introduced the most important research finding over the last 25 years. they found that compressive strength of geopolymer concrete depends upon:

- Gel phase strength
- Ratio of gel phase/ undissolved Al-Si particles
- Amorphous nature of geopolymers
- Surface reaction between the gel phase and the undissolved Al-Si particles

Gel phase is highly reactive and formed by the co-polymerization of Al and Si from the source material dissolved by the activators (Khale & Chaudhary, 2007). Co-polymerization is a process resembling polymerization, in which unlike molecules unite in alternate or random sequences in a chain. Therefore activators should be sufficiently provided to the mix for better polymerization.

Xu & Van Deventer (2000) performed X-ray diffractograms (XRD) which revealed that by the action of alkaline solutions, aluminosilicates were partially dissolved as gel and the remaining undissolved Al-Si particles keep bonded behaving as reinforcement in the matrix depending on the extent of surface reaction between gel phase and Al-Si particles. Hardness of the Al-Si minerals played a positive role in compressive strength of concrete. Si concentrations were more than Al which could not only be due to the greater amount of Si content present in the minerals but also by the highly intrinsic extent of dissolution of Si than Al.

Temuujin & Riessen (2009) suggested that amount of activator should be according to the amorphous portion of fly ash (or any other source material) because excess amount of activator caused weakening of the structure and shortage resulted in

insufficient geopolymerization of aluminosilicate material. It shows that the more the amorphous portion in the source material the better will be the polymerization.

Sofi et al. (2007) studied the engineering properties of inorganic polymer concrete with a compressive strength of 50 MPa including modulus of elasticity, Poisson's ratio, compressive strength, and the splitting tensile strength and flexural strength. they used three different types of Class-F fly ash. Results showed that splitting tensile and flexural strength test complied with the models presented by the standards for OPC-based concretes; mechanical properties depend upon the mix design and curing techniques.

In 2006, Wallah and Rangan studied long term properties of low-calcium fly ash-based geopolymer concrete at 60°C for 24hrs. There was no substantial gain in compressive strength with the increase of age. Shrinkage for geopolymer matrix was also very low because water, released after polymerization, occupied the voids resulting in low shrinkage. However at elevated temperatures the situation was vice versa (Temuujin & Riessen, 2009). Therefore temperature should be sufficiently adjusted i.e. suitable for the proper polymerization and removal of water from the matrix.

In 2005, Hardjito and Rangan studied properties of low-calcium fly ash-based concrete and found that higher concentration of sodium hydroxide solution resulted in higher compressive strength and increased curing beyond 24hrs was not significant at elevated temperature in oven curing. More than 2% superplasticiser should not be used because it started decreasing the compressive strength of concrete. Results also showed that by increasing the mixing time up to 16 minutes increased the compressive strength of FA based geopolymer concrete.

Škvára *et al.* (2006) performed experimental study on concrete based on fly ash geopolymer at curing temperature of 60-80°C for 6-12hrs. Geopolymer on the basis of fly ash is a porous material and the porosity was in the region of nano-pores. The ratio of the compressive strength to the tensile strength under bending varies in the range of 10:5.5 that ranged from 10:1.0 to 10:1.5 in OPC concrete which could facilitate the less use of reinforcement in structural elements. Rheological properties of fly ash

based concrete differ from that of OPC such as viscosity which was higher in geopolymer concrete. Due to this longer duration of vibration was being adopted.

Ambiguities over the name 'geopolymer' concrete have been reviewed by many of the researchers in past because according to them not all binders are geopolymers. The name 'alkali-activated' binder was also a confusing term which might be inferred as the generation of alkali-silica reaction by many researchers (Pacheco-Torgal, *et al.* 2008a). To avoid these above mentioned ambiguities, the term 'Polymeric Concrete' has been used throughout the thesis which covered the meanings of all the previous terms.

2.8 INGREDIENTS OF POLYMERIC CONCRETE

Ingredients of polymeric concrete are fine aggregate, coarse aggregate, low calcium FA, MIRHA or SF as a source of Si and Al and sodium hydroxide and sodium silicate solution as alkaline liquids.

Low calcium (ASTM Class F) FA is preferred over high calcium (ASTM Class C) FA because high amounts of calcium may disturb the polymerization process and change the microstructure (Gourley, 2003b; Gourley & Johnson, 2005). CaO and Ca(OH)₂ was used by Temuujin *et al.* (2009) accompanying Class F fly ash in geopolymer concrete, cured at 20°C and 70°C. They found that strength was increased in ambient curing as compared to elevated curing which showed that calcium interrupted the polymerization process in elevated curing which was slow in ambient curing.

The grading curves for the coarse and fine aggregates used in polymeric concrete can be the same as used for OPC concrete (Hardjito & Rangan, 2005; Wallah & Rangan, 2006; Gourley & Johnson, 2005).

2.8.1 Binder

The silicon and aluminum oxides in the source material (FA, MIRHA & SF) reacts with the alkaline liquid to form polymeric paste that binds the loose coarse aggregate and fine aggregates to form the polymeric concrete. Polymeric binder is amorphous three dimensional material that sets quickly without needing high temperatures (Van Deventer, *et al.* 2007).

The mechanical strength of alkali-activated binders depends on the structural conditions of the alumino-silicate materials (Pacheco-Torgal, *et al.* 2008b) and structural integrity was achieved by polycondensation of silica and alumina precursors and high alkali content which formed CaO-free aluminosilicate gel binder (Yunsheng *et al.* 2008).

Pozzolanic cements contain calcium while polymeric concrete does not depend upon calcium-silica-hydrates for strength and matrix formation. This difference gives a benefit in terms of early gain in the strength (Yip, *et al.* 2008).

2.8.2 Alkaline Activators

Si and Al present in source material were being activated by strong alkalis that convert the glassy structure wholly or partially into compact composite, behaving like cement and generated a microporous material (Fernández-Jiménez, *et al.* 2005). Geopolymerization was significantly affected by alkali concentration (Puertas, *et al.* 2000). Accordig to Khale & Chaudhary (2007) commonly used activators were NaOH, Na₂SO₄, waterglass, Na₂CO₃, K₂CO₃, KOH, K₂SO₄ or a little amount of cement clinker. Activators used in this research study are NaOH and sodium silicate (water glass).

2.8.2.1 Sodium Hydroxide (NaOH)

NaOH is produced by oxidation with specific gravity of 2.13 at 25°C, melting point of 318°C and pH (1% aqueous sol) of 12.7. It is easily available in form of pellets, flakes, beads, grains, lumps or powder.

Hydroxide concentration increased the solubility of aluminosilicate (Gasteiger, *et al.* 1992) because as more of the NaOH came in contact with the reactive solid material, the more the silicate and aluminate monomers were released therefore higher the concentration of NaOH, higher will be the strength. Water and NaOH were released during hardening of the gel phase because the alkali metal hydroxide acts as a catalyst and leached out from the hardened alkali activated binder in almost the same amount as that was added during synthesis (Khale & Chaudhary, 2007).

Wang *et al.* (2004) used 2% and 5% NaOH in fly ash and cement kiln dust and found out that 5% NaOH tended to increase the strength of the binder in less than 7 days but decreased the strength at later age, may be because of undesirable morphology and non-uniformity of hydration products in the pastes.

2.8.2.2 Sodium Silicate (water glass)

Sodium silicate is the common name of the compound sodium metasilicate, Na₂SiO₃. Sodium silicate is manufactured by combining soda ash (Na₂CO₃) and sand (SiO₂) as shown by Equation 2.1.



For more than a century sodium silicate has been used for the production of commercial products such as special cements, coatings, molded articles and catalysts (Gourley, 2003a).

Soluble silicate was added to fly ash based geopolymer concrete to promote precipitation of silicates (Khale & Chaudhary, 2007) and to make it water proof as well as acid resistant. Sindhunata *et al.* (2006) found out that with the addition of

soluble silica, spaces in geopolymer matrix were filled resulting in denser microstructure with high degree of polymerization.

2.9 MECHANISM OF REACTION

According to Nugteren (2006), a new binder could be produced by performing the alkaline activation reaction with fly ash in which zeolite crystallization did not occur but only a thin layer of particles was initially dissolved to form an interstitial gel that hardens at low temperature. He further studied that the gel polymerized into a geopolymer that was an inorganic polymeric material having a chemical composition same as zeolite but possessing an amorphous structure and favorable condition for geopolymerization reaction in its amorphous state (Davidovits, 2008).

The chemical reaction may comprise the following steps (Davidovits, 2008; Xu and Van Deventer, 2000):

- Dissolution of Si and Al atoms from the source material through the action of hydroxide ions.
- Transportation or orientation or condensation of precursor ions into monomers.
- Setting or polycondensation/polymerisation of monomers into polymeric structures.

Xu and Van Deventer (2000) found out that the process just after the start of the alkali activation of fly ash was same as that of hydration of Portland cement. A conceptual model was presented by Duxson *et al.* (2006) and shown in Figure 2.10.

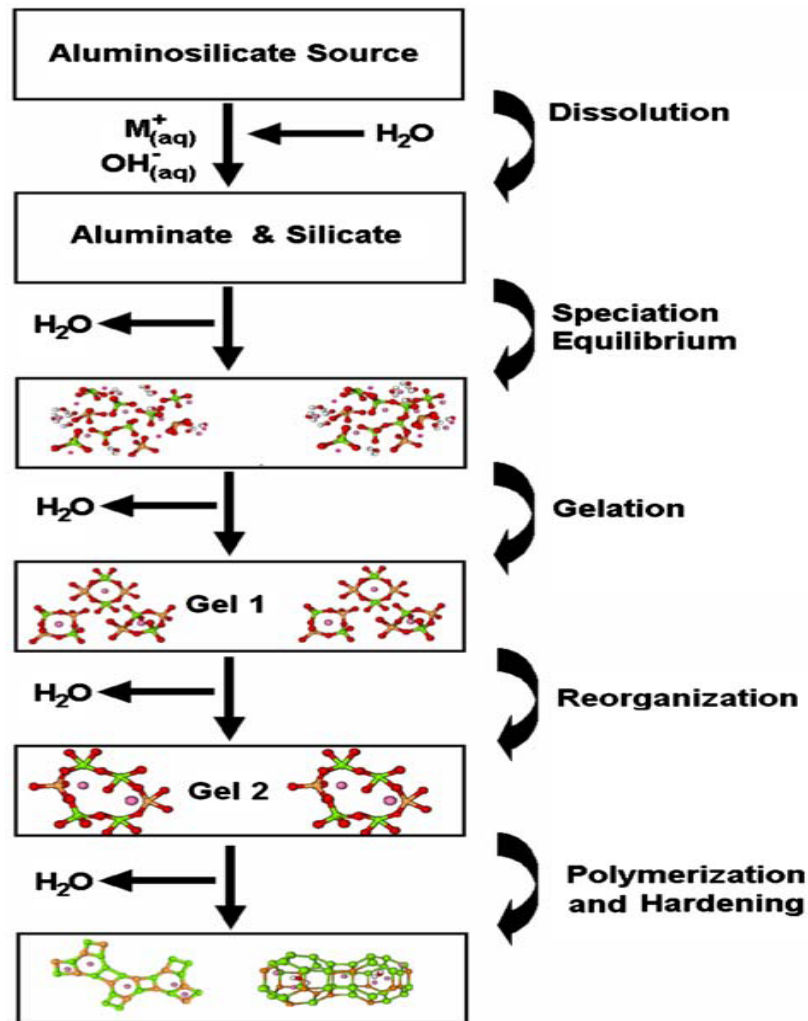


Figure 2.10: Conceptual Model for Geopolymerization (Duxson, *et al.* 2006)

Duxson *et al.* (2006) described the key processes involved in the transformation of solid aluminosilicate material into a synthetic alkali aluminosilicate. The process started with the dissolution of solid aluminosilicate source by consuming alkaline solution and water forming aluminate and silicate species. In next stage division of Si and Al species occurred at equal rate with no any change in concentration of reactant and product with respect to time which was termed as speciation equilibrium. At high pH dissolution of amorphous aluminosilicates was high which rapidly created a supersaturated aluminosilicate solution. This solution further transformed into a gel in which oligomers form large networks. Water was released as a result of this process which only played a role of a reaction medium and accumulated the pores in the gel. This type of gel was named as bi-phasic having aluminosilicate binder and water

forming the two phases. After gelation system continued to reorganize as gel network was increasing resulting in a three dimensional aluminosilicate network known as geopolymers which started hardening by the process of polymerization.

2.9.1 Role of Alkali Metals

Alkali metals played an important role in the development of strength, any alkali earth cation can be used as an alkali element in geopolymerization reaction, theoretically, but most of the researchers emphasized on the use of Na^+ and K^+ ions (Van Jaarsveld, et al. 1999) (Xu & Van Deventer, 2000). According to Khale & Chaudhary (2007), the role of these cations was not understandable that whether they played a charge balancing role or were actively bonded into the matrix.

Morphology was also being affected by the size of cation. Na^+ should be preferably used because of having smaller size than that of K^+ that showed strong pair formation with smaller silicate oligomers (Komnitsas & Zaharaki, 2007).

Alkali hydroxide was necessary for the dissolution of silica and aluminum and on the other hand as a catalyst for condensation reaction. Co-polymerization of individual alumina and silica, dissolved by alkali metals, produced highly reactive gel (Khale & Chaudhary, 2007).

2.9.2 Effect of Curing on Polymeric Concrete

Hardening of concrete depends upon curing temperature (Brooks, 2002) and curing age. Curing for polymeric concrete is different as compared to OPC concrete. For fly ash concrete, setting time was decreased by a factor of six when temperature was increased from 6 °C to 80°C (Brooks, 2002) therefore increased temperature gave rise to pozzolanic reaction (Wang *et al.* 2004). Curing temperature affected the setting time, pore structure and strength development of polymeric concrete (Tempest, *et al.* 2009). At ambient temperature; the reaction of fly ash was very slow (Puertas *et al.* 2000) and delayed the beginning of setting (Kirschner & Harmuth 2004).

Development of the compressive strength was possibly affected by the high temperature curing for more than couple of hours (Papadakis, 2000). At high temperature, the 24 hours developed strength could be compared to one month of developed strength (Bakharev, 2005) but Palomo *et al.* (1999) observed 60 MPa of strength after 5 hours at 85°C and concluded strength did not vary with the age of concrete unlike OPC concrete, which underwent hydration process and gained strength overtime (Harjito, *et al.* 2004). Beyond 48 hours of curing, strength development was not much significant (Palomo, *et al.* 1999) but there was no effect on crystalline part of geopolymer which indicated that, the change responsible for the difference in the strength originated within the amorphous phase of the structure (Van Jaarsveld, *et al.* 2002).

Sindhunata *et al.* (2006) observed that total pore volume and surface area was increased by the elevated curing. Degree of reaction was also increased by the increment in mesopore volume and area. Increased curing temperature gave rise to dissolution of precursors; primary Al and Si which further accelerated polymerization process.

Curing temperature in the range of 30°C - 90°C had a more significant contribution as polymerization proceeds quickly at elevated temperatures (Tempest, *et al.* 2009) but elevated temperature should not be too prolonged as it decreases the compressive strength by breaking the granular structure of geopolymer matrix resulted in dehydration and excessive shrinkage due to the contraction of the gel (Khale & Chaudhary, 2007).

CHAPTER 3

METHODOLOGY

3.1 MATERIALS SELECTION

Materials used in this study were chosen according to the specification set by the British Standards.

3.1.1 Fly Ash

Fly ash was obtained from Manjung power station, Lumut, Perak. Chemical composition of fly ash is shown in Table 3.1, as obtained from XRF. Specific gravity of fly ash was found to be 2.78 at 36°C. Particle size was less than 100µm as shown in Appendix A.

3.1.2 Microwave Incinerated Rice Husk Ash (MIRHA)

Rice husk utilized in this research was obtained from Bernas rice milling plant (Kusbiantoro, 2007). Rice husk was dried in direct sunlight to decrease its moisture so that less amount of smoke is produced during burning process. This dried rice husk was burnt in an automatic microwave incinerator (Figure 3.1) (Appendix B) gradually up to 800°C in four phases (Table 3.2) to produce microwave incinerated rice husk ash (MIRHA) in amorphous form. To produce MIRHA (Figure 3.2) with high reactive silica content, control combustion was done. Flue Gas Filter is equipped to the microwave incinerator and which provides significant positive effect to the environment. It can distil all the dust and ashes that are resulted from rice husk incineration, hence the air pollution from burning process can be reduced.

Table 3.1: Composition of Class F Fly ash using XRF

Oxide content	Percentages (%)
SiO_2	51.19
Al_2O_3	24
Fe_2O_3	6.6
CaO	5.57
MgO	2.40
SO_3	0.88
K_2O	1.14
Na_2O	2.12



Figure 3.1: Automatic microwave incinerator at UTP



Figure 3.2: MIRHA after Burning and Sieving

Table 3.2: Burning Procedure for 800°C Burning Temperature

Phase	Temperature	Duration	Remarks
Phase I	25° C - 150° C	3.5 hours	Remove the carbon and other volatile materials
Phase II	150° C – 800° C	1 hour	Burning Process
Phase III	800° C - 150° C	20 hours	Cooling
Phase IV	150° C - 25° C	1 hour	Cooling in tank until it reached ambient temperature

After burning MIRHA was then ground in the ball mill by 2500 cycles using a Los Angeles abrasion (LA) machine to enhance its fineness (Appendix A). Surface area for MIRHA was 7.81 m²/g with relative density of 2.23. Finally MIRHA was sieved by mechanical siever (Figure 3.3). Chemical composition of MIRHA is given in Table 3.3.



Figure 3.3: Mechanical Siever

Table 3.3: Composition of MIRHA using XRF

Oxide content	Percentages (%)
SiO ₂	86.1
Al ₂ O ₃	0.17
Fe ₂ O ₃	2.87
CaO	1.03
MgO	0.84
SO ₃	0.41
K ₂ O	4.65
Na ₂ O	-
LOI	5.02

3.1.3 Silica Fume

Silica fume was obtained from Elkem materials in dry densified form with Grade 920E with LOI less than 4% and specific surface area (BET) of 15-35 m²/gram confirming to the mandatory requirements of ASTM C1240. Chemical composition of silica fume is given in Table 3.4. Silica fume is densified in order to avoid the difficulties in shipping of submicron-sized particle (dust). Particle size distribution is

shown in Appendix A, where as the graph shows that particle size is for clusters and not for the individual particles.

Table 3.4: Composition of Silica fume using XRF

Oxide content	Percentages (%)
SiO ₂	96.36
Al ₂ O ₃	0.21
Fe ₂ O ₃	0.77
CaO	0.24
MgO	0.52
SO ₃	0.55
K ₂ O	1.02
Na ₂ O	0.12
LOI	< 4%

3.1.4 Aggregates

Coarse aggregate used in this experiment was crushed granite stone with maximum size of 20 mm (BS 812-103.2 1985) while the fine aggregate (Figure 3.4) used was natural Malaysian sand. Fine aggregate was also sieved for size less than 5mm classified in zone 3. Coarse aggregates were washed properly before use. Gradation curves for coarse and fine aggregates are shown in Figure 3.5 (Table 3.5) and Figure 3.6 (Table 3.6) respectively. Gradation curves were with in the gradation limit as proposed by BS code.



Figure 3.4: Coarse Aggregate & Fine Aggregates

Table 3.5: Sieve Analysis Results of Coarse Aggregate

Sieve Size (mm)	Mass Retained(g)	% Mass Retained	$\Sigma\%$ Mass Retained	% Pass
14	1078	10	10	90
10	682	78.58	88.58	11.42
5	224	11.27	99.85	0.15
2.36	1	0.05	99.9	0.1
0	2	0.1	100	0

Table 3.6: Sieve Analysis Results of Fine Aggregate

Seive Size (mm)	Mass Retained(g)	% Mass Retained	$\Sigma\%$ Mass Retained	% Pass
2.36	0	0	0	100
1.18	15	3	3	97
0.6	185	37	40	60
0.3	125	25	65	35
0.15	100	20	85	15
0.08	74	14.8	99.8	0.2
0	1	0.2	100	0

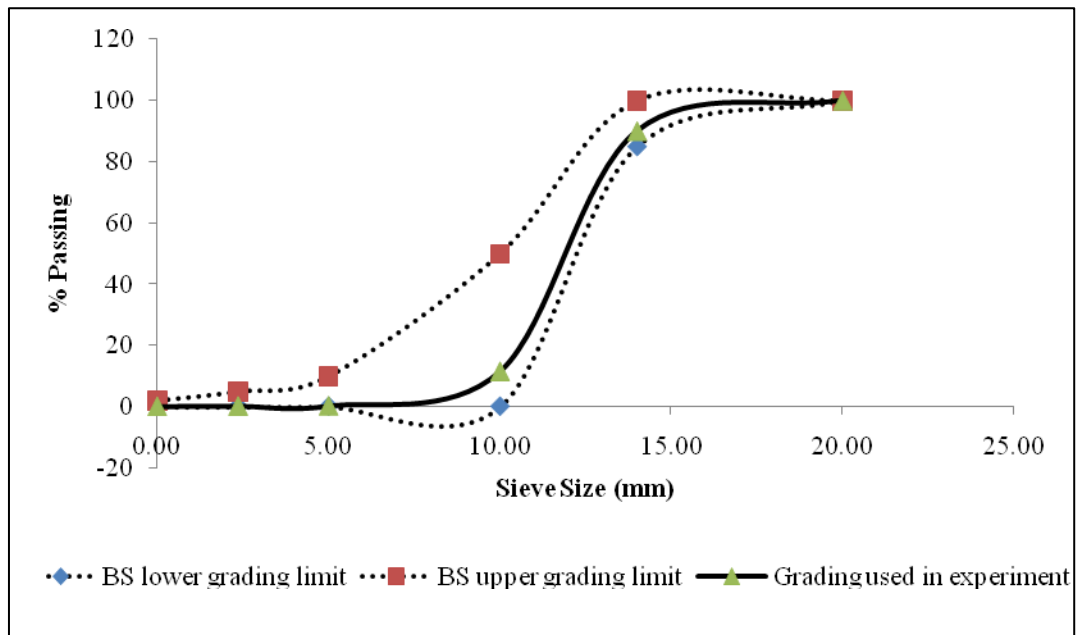


Figure 3.5: Grading Curve for Coarse Aggregate

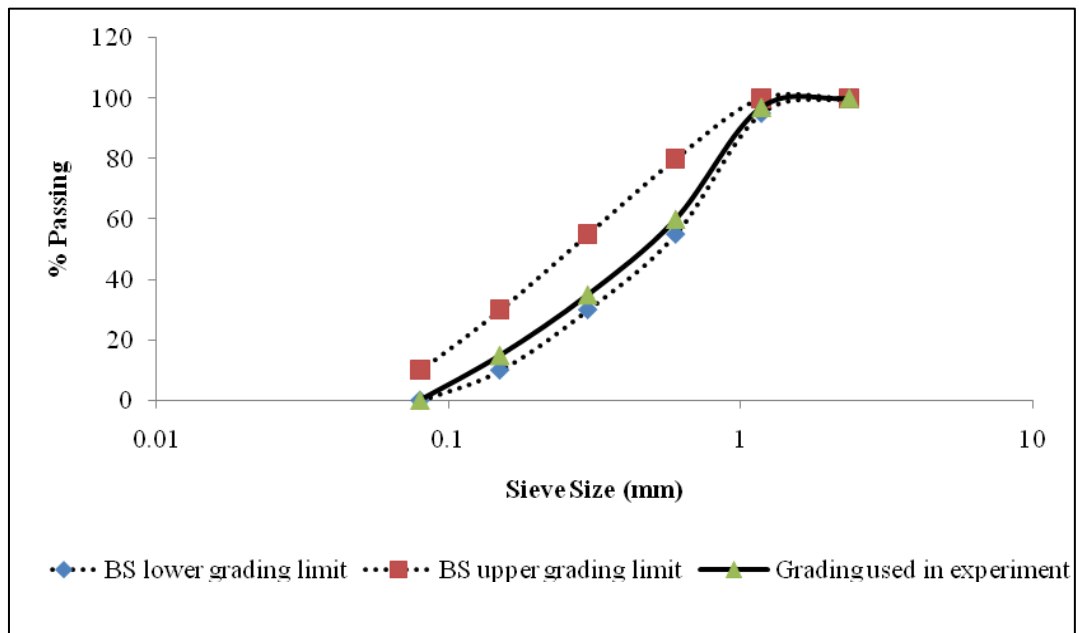


Figure 3.6: Grading Curve for Fine Aggregate

3.1.5 Sodium Silicate (Na_2SiO_3)

Grade A53 solution was used as used by Rangan (2008) with SiO_2 -to- Na_2O ratio by mass of approximately 2. Sodium silicate was used in a solution form mixed with 56.31% of water, 29.43% of SiO_2 and 14.26% of Na_2O .

3.1.6 Sodium Hydroxide (NaOH)

Sodium hydroxide was used in form of pellets i.e. 97-98% pure (Rangan, 2008). Concentration of solution was 8M and in order to make 1 Kg of solution 29.4% of pellets were added to the water. For 8 molar, 320 gm of solid pellets were added per litre of solution.

3.1.7 Table Sugar

Sugar was used to delay the setting time of concrete. Adding plain white sugar in concrete prevented the cement from joining with the water and slowed the hardening of the minerals (McDonell, 2006).

Molecular formula of the sugar, used in this research, is $\text{C}_{12}\text{H}_{22}\text{O}_{11}$ and scientifically, the word sugar is used for any mono- or di-saccharide. Sugar is an organic compound chemically named as sucrose or saccharose. Sugar is obtained universally from fruits, seeds, flowers, and roots of plants. Main two sources of sucrose are sugarcane and sugarbeets; sap of maple tree is also of commercial interest (Sybil, 2002).

Sugar retarded cement hydration at different temperatures and period of retardation shortened as the curing temperature was increased (Garci & Jennings, 2002). Cements high in aluminates required a higher quantity of sugar to obtain the same retardation because sugar adsorbs on aluminates (McDonell, 2006). Sofi *et al.* (2007) found that setting time of polymeric concrete, unlike OPC concrete, was only few minutes which depend on the mix design.

After more than 15 trial mixes using superplasticizers and retarders, it was found out that quick setting time caused difficulty in the placement of concrete in moulds which was increased by the use of sugar (retarder) in this research.

3.1.8 Extra Water

The amount of water added to the mix i.e. besides the water present in the alkaline solutions was referred as extra water which was 10% of the source material. Water used in the mix was tap water free from undesirable organic substances or inorganic constituents in excessive proportions; completely free from all types of harmful chemicals, oil, chloride, silt etc. However there was no detail present in the code regarding quality of mixing water but many project specifications showed that the mixing water should be fit for drinking purpose as it rarely contains dissolved inorganic solids in excess of 2000 parts per million (ppm) (Neville, 1990).

3.2 SAMPLING AND MIXING OF CONCRETE

Class F fly ash was used in the research as a base binder for all mixes. Density of fly ash for control mix was 350 kg/m^3 and was replaced by 3%, 5% and 7% of MIRHA or silica fume. All other material quantities were kept constant in order to see the effect of replacement of fly ash by MIRHA or silica fume on the properties of concrete.

Sodium silicate to sodium hydroxide ratio was 2.5, in which sodium silicate was 103 kg/m^3 and sodium hydroxide was 41 kg/m^3 .

Coarse to fine aggregate ratio was approximately 1.86 as coarse aggregate was 1200 kg/m^3 and fine aggregate was 645 kg/m^3 .

Sugar was used as 3% of the pozzolan and extra water has been added to the mixture equal to 10% of the total binder (Table 3.7)

.All dry materials were first mixed in 100 liter capacity concrete mixer for 3 minutes and then with the continuous mixing of one more minute, water with the

dissolved sugar and alkaline solutions (NaOH and Na_2SiO_3) were added to the dry mixed contents (Figure 3.7). Afterwards casting into the greased moulds, according to the requirements of tests, was done in three layers with the continuous hand mixing. Compaction was done by poker vibrator.

Three types of curing techniques were used namely; hot gunny curing, ambient curing and external exposure curing. In hot gunny curing moulds were covered with white plastic sheet and opened after one day and then covered with the gunny sack (Figure 3.8); dipped in warm water that was renewed the next day and removed from the sample on the third day. In ambient curing with the average temperature of 20-25°C samples were kept under the shade outside the lab (Figure 3.9) and in external exposure curing with the average temperature of 35-40°C samples were placed in plastic coated shelf in the open atmosphere (Figure 3.10).



Figure 3.7: Polymeric Concrete after Mixing



Figure 3.8: Hot Gunny Curing



Figure 3.9: Ambient Curing



Figure 3.10: External Exposure Curing

Table 3.7: Mix design Proportions

Type of Curing	Fly Ash (Kg/m ³)	MIRHA/Silica fume (% of Pozzolan)	MIRHA/ Silica fume (Kg/m ³)	Coarse Agg. (Kg/m ³)	Fine Agg. (Kg/m ³)	NaOH (Kg/m ³)	Na ₂ SiO ₃ (Kg/m ³)	Extra water (10% of Pozzolan) (Kg/m ³)	Sugar (3% of Pozzolan) (Kg/m ³)
Hot gunny Curing/ Ambient Curing/ External exposure Curing	350	0	0	1200	645	41	103	35	10.5
	339.5	3	10.5						
	332.5	5	17.5						
	325.5	7	24.5						

*Water/Solids = 0.3

3.3 CONCRETE TESTING

Concrete was tested in fresh and hardened states. In fresh state its workability has been analyzed through slump test while in hardened state; its tensile, flexural and compressive strength, using both destructive and non destructive methods, were being analyzed.

The non destructive method included Ultrasonic pulse Velocity test (UPV) to analyze the integrity of concrete sample whereas destructive test included the compressive strength test.

3.3.1 Slump Test

Slump test was performed according to BS EN 12350-2:2000. Apparatus consisted of a tamping rod, 600mm long x 16mm diameter; hemispherical at both ends and a truncated cone, 305 mm height, 100mm diameter at the top and 200mm diameter at the bottom.

Polymeric mixes showed high slump after the addition of superplasticizer i.e. higher than 200 mm with different compressive strength value for each mix. Increase amount of extra water resulted in big crystals of geopolymer which decreased the surface area of concrete (Van Jaarsveld, *et al.* 2002), decreasing the strength of geopolymer concrete (Hardjito, *et al.* 2004). However, suitable amount of extra water was necessary to improve the workability of concrete (Rangan, 2008).

Table 3.8: Experimental Details of Tests on Concrete Specimen

Sample Type	Test type	Standard	Equipment	Testing Age	Sample size	Number of sample	Measure-ment Unit
Physical Properties of Source Material Fly Ash MIRHA and Silica Fume	XRF	-	Pioneer X-Ray Spectrometer	28 days	Powdred mortar	-	-
	Particle size analyser	-	Sciocco 2000 dry powder feeder	-	20 gm	-	µm
	Specific Gravity	ASTM D5550 -06	Gas Pycnometer	-	3 gm	-	-
Fresh concrete	Slump test	BS EN 12350-2:2000	Slump cone	Fresh Concrete	-	Each Mix	mm
Hardened Concrete (Non-Destructive Test)	Ultrasonic Pulse Velocity (UPV)	BS EN 12504-4:2004	PUNDIT UPV Tester	3,7,28,56 & 90 days	100 mm ³	3 Readings per cube	Km/s
	Compressive Strength Test	BS EN 12390-3:2002	Compression Testing Machine	3,7,28,56 & 90 days	100 mm ³ cube	3 cubes/mix/age	MPa
Hardened Concrete (Destructive Test)	Split Tensile Test	BS EN 12390-6	2000 KN Digital compressive & flexural Testing Machine	28 days	Cylinder (100 Ø x200)mm	² cylinders/mix/28 days	MPa
	Flexural Strength Test	BS EN 12390-5		28 days	Beam (100x100x500) mm	Beam/mix/28 days	MPa
Microstructure	Scanning Electron Microscopy Analysis	-	LEO1430 VP Inca X-Sight Oxford Inst.	28 days	40mm Ø disc-5mm thickness	All mixes/ 28 days	-

3.3.2 Ultrasonic Pulse Velocity Test

In this experiment ultra pulse velocity test was done according to BS EN 12504-4:2004, utilizing direct transmission method, in which an electro acoustical was placed on the opposite sides of concrete specimen.

UPV was done using portable ultrasonic non destructive digital indicative tester (PUNDIT) as shown in Figure 3.11 and the reading was taken on three concrete cubes per mix at ages 3, 7, 28, 56 and 90 days. Values shown in the Table are average of three values at each age.

ACI Committee 228 (2003) reported that increased moisture content increases the pulse velocity and presence of cracks and voids in concrete increase the path length resulting in a longer travel time.

UPV test requires a little more skill than the resonant frequency test, e.g. in ensuring good acoustic coupling between the transducer and the concrete. On the other hand 100mm cubes could be tested which gives the benefit in testing of smaller and inherently more variable volume of concrete (Non-destructive testing of hardened concrete, 2001).



Figure 3.11: UPV PUNDIT Tester

3.3.3 Compressive Strength Test

Compressive strength test was done according to BS EN 12390-3: 2002 using 2000 kN digital compressive testing machine as shown in Figure 3.12. Three cubes of polymeric concrete, 100x100x100mm were cast, cured and tested for each mix at ages 3, 7, 28, 56 and 90 days. Compressive strength for each mix was obtained by calculating the average of three specimen's strengths. The stress at failure was taken to be the compressive strength of the concrete.



Figure 3.12: Digital Compressive Testing Machine

3.3.4 Split Cylinder Test

Split cylinder test carried out on a standard cylinder specimen by applying a line load along the vertical diameter (BS EN 12390-6). Practically the true line load cannot be applied to the cylinder because of sides which were not smooth enough and high compressive stresses could be induced at the surface. In order to avoid these high



Figure 3.13: Split Tensile Strength Test Apparatus

compressive stresses, a narrow loading strip was used, made up of soft material (Figure 3.13). Two cylinders of each mix with dimension 100x200 mm were casted, cured and tested with pace rate of 0.92 KN/s at the age of 28 days.

3.3.5 Flexural Test

Flexural strength test was done according to BS EN 12390-5 using 2000 KN Digital compressive & flexural Testing Machine. Beam of dimension 100x100x500 mm were cast, cured and tested for each mix at the age of 28 days. Third point flexural testing was executed on the beam with the pace rate of 0.2 KN/s (Figure 3.14). The theoretical maximum tensile stress reached in the bottom fibre fibre of the test beam is known as the modulus of rupture which is calculated as follows on the basis of ordinary elastic theory. Modulus of rupture (MPa) = $PL / (bd^2)$

where

P = maximum total load on the beam

L = span

b = width of beam

d = depth of beam

In Digital compressive & flexural Testing Machine, 'L', 'b' and 'd' were input and load 'P' was applied to get modulus of rupture directly as output.

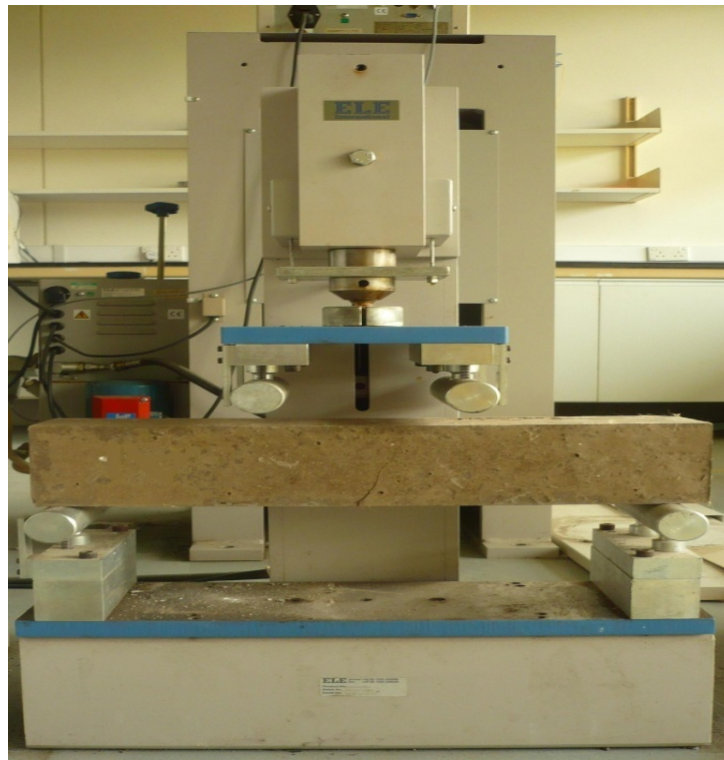


Figure 3.14: Flexural Strength Test Assembly

3.3.6 Scanning Electron Microscopy Analysis

Scanning Electron Microscopy (SEM) analysis was carried out to describe the inner microstructure of samples FA-based concrete and concrete blended with MIRHA and SF. Each of the sample was cured for 28 days with three curing techniques namely:

hot gunny curing, ambient curing and external exposure curing. The analysis was performed with LEO 1430 VP Inca X-Sight Oxford Instrument. Before testing; the samples were cored up to the thickness of 5 mm. The SEM was operated in specific pressure to facilitate the operation of filament and electron inside SEM. Concrete is a non-conductive material which was coated with gold atoms in sputter coater. Coated concrete was then placed in the vaccum chamber inside SEM. The SEM must be operated in specific pressure to facilitate the operation of filament and electron inside SEM. Figure 3.15 shows the SEM instrument used in this research.

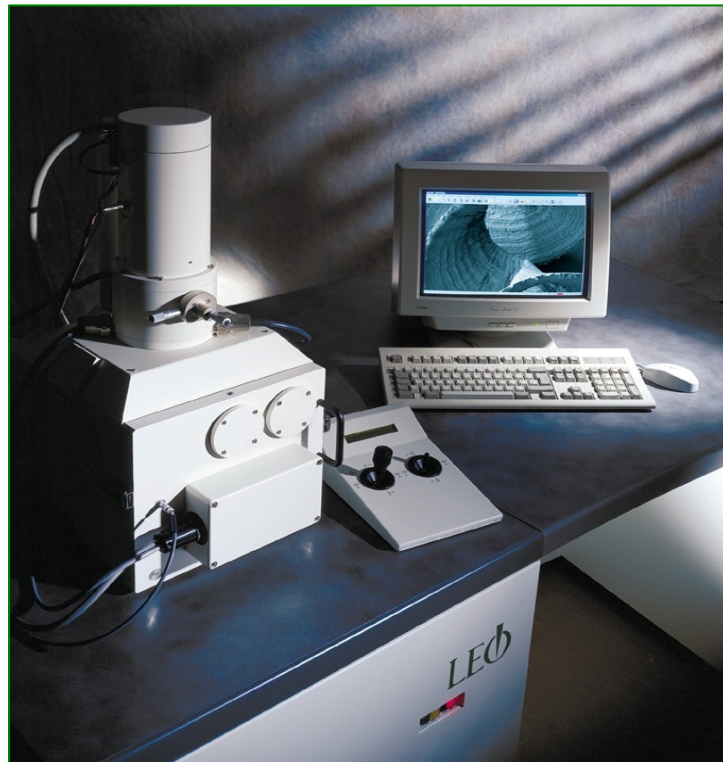


Figure 3.15: LEO 1430 VP Inca X-Sight Oxford SEM Instrument with Sputter Coater

CHAPTER 4

RESULTS & DISCUSSIONS

4.1 POLYMERIC CONCRETE SAMPLE ANALYSIS

This research includes analysis of fresh and hardened states of concrete. The analysed results were used to find out the optimum amount of MIRHA or SF as a replacement of fly ash-based concrete as well as best suited curing regime for the same.

4.1.1 Properties of Fresh Polymeric Concrete

In order to find out the fresh properties of polymeric concrete, its workability was measured through slump test. Extra water (10%) was added to all the mixes, decided as an appropriate amount after several trial mixes. Slump test results are shown in Table 4.1. To improve the workability of polymeric concrete naphthalene based superplasticizer was also being experimented i.e. used by Rangan (2008) but the concrete hardened in short span of time due to the fast setting time of polymeric concrete which made the preparation of samples harder with prolonged vibrations for compaction. However, Rangan (2008) achieved 240mm of slump which was decreased to 210mm when mixing time was increased to sixteen minutes. In this research, sugar was added to delay the setting time of the concrete that provided an ease in making the samples.

Fly ash particles are spherical in shape with smooth surfaces (Figure 4.1) which reduced the water demand in concrete but the addition of MIRHA to fly ash-based polymeric concrete increased the water demand in concrete by reducing the value of slump by 5% and 7% approximately in comparison to SF mix and control mix respectively. With the increase in percentage of MIRHA, slump was decreased which showed that with the increase in MIRHA content (Figure 4.4) water quantity should

also be increased in order to maintain the required consistency of the mix. The decrease in workability was due to the cellular particles (Figure 4.2) of MIRHA that were absorptive in nature. MIRHA is hygroscopic material having specific surface area higher than that of cement due to which it absorbed more water.

On the other hand in case of SF addition to the fly ash-based polymeric concrete, there was no change in the slump value for 3% and 5% replacement but 5% decrease can be seen in 7% replacement of SF (Figure 4.5). This shows that for 7% increment (or more) of SF, water requirement in the concrete increased which was due to the increased amount of silica in the mix. Because of large surface area and smaller particle size (Figure 4.3), silica fume requires more water when increased after a certain amount. In comparison with control mix the slump value of SF mix decreased by 1.8%.

Table 4.1: Slump test results for each mix

Type of Mix	Slump (mm)
FA	230
FA-MIRHA 3%	220
FA-MIRHA 5%	210
FA-MIRHA 7%	200
FA-SF 3%	230
FA-SF 5%	230
FA-SF 7%	220

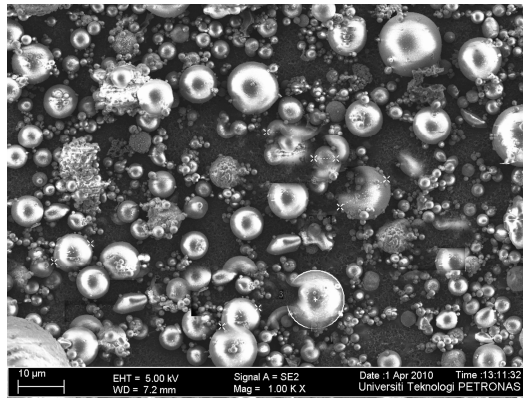


Figure 4.1: FESEM of Fly Ash

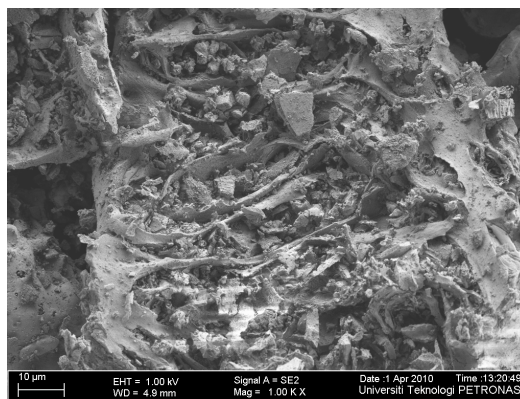


Figure 4.2: FESEM image of MIRHA

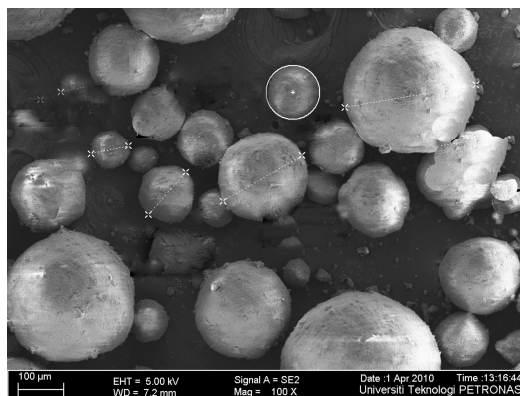


Figure 4.3: FESEM image of Silica Fume

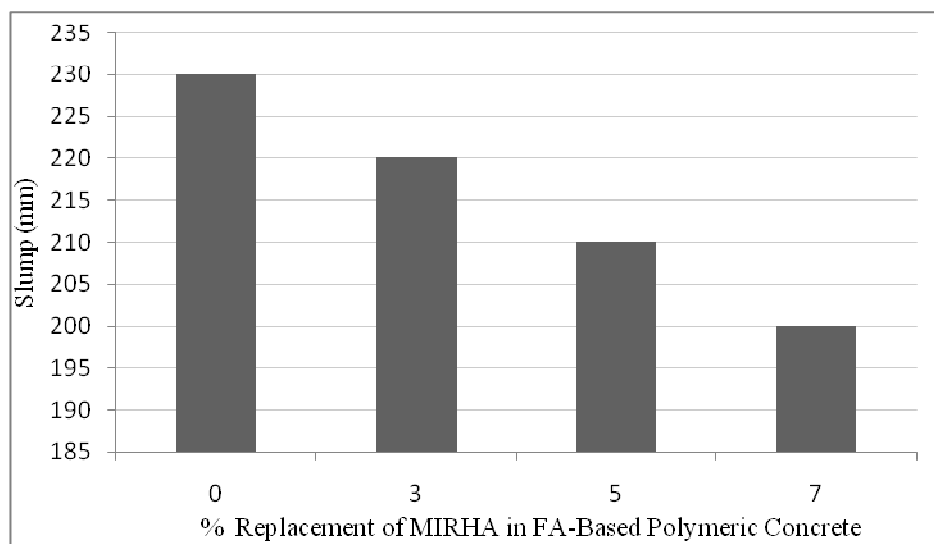


Figure 4.4: Slump test result for FA-Based polymeric concrete with MIRHA

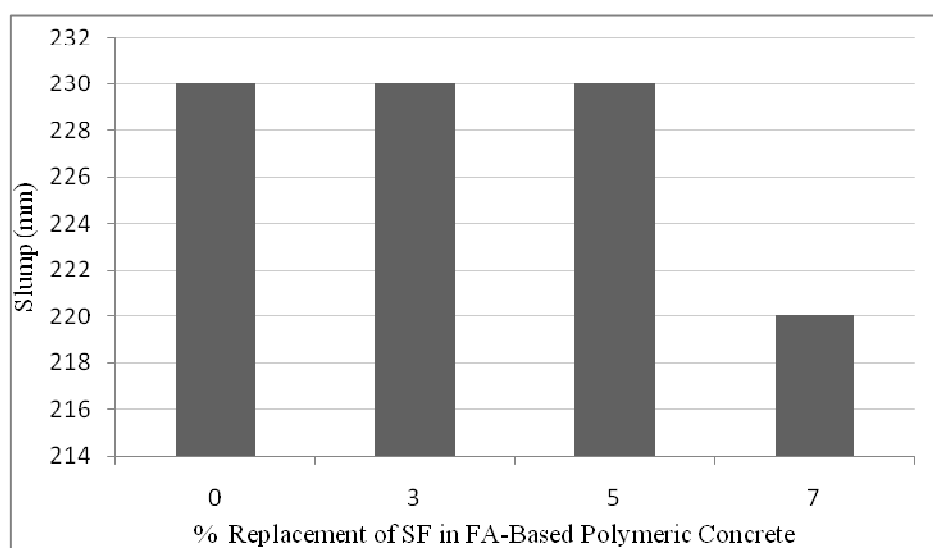


Figure 4.5: Slump test result for FA-Based polymeric concrete with SF

4.1.2 Compressive Strength Test Results

Compressive strength test was conducted to find out the impact of new binder on concrete. Fly ash-based concrete was taken as a control mix which was further blended with MIRHA and SF and their compressive strengths were compared at ages 3, 7, 28, 56 and 90 days. Table 4.2 shows compressive strength results for polymeric concrete replaced by MIRHA and Table 4.3 shows the compressive strength results for polymeric concrete replaced by SF.

Table 4.2: Compressive Strength of FA-Based Polymeric Concrete Replaced by MIRHA

Curing Type	MIRHA (%)	Compressive Strength (MPa)				
		3 days	7 days	28 days	56 days	90 days
Hot Gunny Curing	0	5.0	9.0	15.0	17.0	18.0
	3	3.5	8.3	13.1	15.1	16.1
	5	7.1	11.3	19.0	22.7	23.1
	7	3.2	7.0	11.5	12.8	13.7
Ambient Curing	0	9.5	14.1	19.7	21.9	23.8
	3	9.0	11.9	17.9	19.2	20.4
	5	9.8	15.9	24.1	27.0	28.3
	7	8.6	11.0	16.8	17.0	18.8
External Exposure Curing	0	34.5	42.3	48.7	50.6	51.4
	3	18.5	26.0	33.8	37.3	38.5
	5	15.0	22.1	27.6	29.8	31.0
	7	23.8	31.9	40.7	44.5	46.0

Table 4.3: Compressive Strength of FA-Based Polymeric Concrete Replaced by SF

Curing Type	SF (%)	Compressive Strength (MPa)				
		3 days	7 days	28 days	56 days	90 days
Hot Gunny Curing	0	5.0	9.0	15.0	17.0	18.0
	3	5.3	9.8	16.4	18.9	19.5
	5	8.5	16.3	26.9	31.8	33.2
	7	11.1	19.9	28.8	32.2	34.8
Ambient Curing	0	7.5	14.1	19.7	21.9	23.8
	3	12.1	24.0	30.3	31.8	32.6
	5	5.4	11.0	13.0	15.1	16.5
	7	11.9	18.4	26.5	28.8	30.0
External Exposure Curing	0	34.5	42.3	48.7	50.6	51.4
	3	22.0	28.3	35.0	37.5	38.8
	5	19.1	25.1	30.5	32.0	32.9
	7	31.9	37.0	42.3	45.1	46.5

Table 4.4: Rate of Strength Development of Polymeric Concrete with MIRHA with Respect to 28 Days Strength

Curing Type	MIRHA (%)	Rate of Strength Development with Respect to 28 days Strength (%)				
		3 days	7 days	28 days	56 days	90 days
Hot Gunny Curing	0	33	60	100	113	120
	3	27	63	100	115	123
	5	37	59	100	119	122
	7	28	61	100	111	119
Ambient Curing	0	48	72	100	111	121
	3	50	66	100	107	114
	5	41	66	100	112	117
	7	51	65	100	101	112
External Exposure Curing	0	71	87	100	104	106
	3	55	77	100	110	114
	5	54	80	100	108	112
	7	58	78	100	109	113

Table 4.5: Rate of Strength Development of Polymeric Concrete with SF with Respect to 28 Days Strength

Curing Type	SF (%)	Rate of Strength Development with Respect to 28 days Strength (%)				
		3 days	7 days	28 days	56 days	90 days
Hot Gunny Curing	0	33	60	100	113	120
	3	32	60	100	115	119
	5	32	61	100	118	123
	7	39	69	100	112	121
Ambient Curing	0	38	72	100	111	121
	3	40	79	100	105	108
	5	42	85	100	116	127
	7	45	69	100	109	113
External Exposure Curing	0	71	87	100	104	106
	3	63	81	100	107	111
	5	63	82	100	105	108
	7	75	87	100	107	110

4.1.2.1 Polymeric Concrete Samples with MIRHA in Hot Gunny Curing

Figure 4.6 shows that in FA-based polymeric concrete replaced by MIRHA, 5% replacement showed the highest compressive strength at 90 days i.e. 23.11 MPa which was 46.3% greater than 3% replacement, 68.6% greater than 7% replacement of MIRHA and 28.4% greater than control mix. It showed that 5% inclusion of MIRHA was compatible with the amount of NaOH and Na₂SiO₃ required, promoting polymeric reaction and precipitation of Si from fly ash and MIRHA respectively. MIRHA also absorbed lot of water so beyond 5% inclusion total water was not enough in the mix to dampen all the MIRHA particles which created non-homogeneous mix and led to the 68.6% decrease in strength.

For control mix one of the reasons of low strength was the shortage of water which did not fully dissolve the glassy particles of fly ash which was adjusted by MIRHA in later mixes. Gain of strength at early ages (from 3 days to 7 days) can be seen in all mixes i.e. 80%, 140%, 59% and 120% for control mix, 3%, 5% and 7%

MIRHA mixes respectively between 3 to 7 days. Between 7 to 28 days, 67%, 57%, 68% and 64% strength were gained by control mix, 3%, 5% and 7% MIRHA mixes respectively which is due to the reason that polymeric concrete does not depend on calcium-silicate hydrates to develop the strength, unlike OPC concrete, which privileged in early gain of strength.

Over all hot gunny curing showed the least compressive strength as compared to other two types of curing which is firstly due to the wet curing which restrained the removal of water from the voids; as also explained by UPV results and after 7 days when water started replacement by alumino-silicate gel then the strength development age has already been passed which was crucial in early ages.

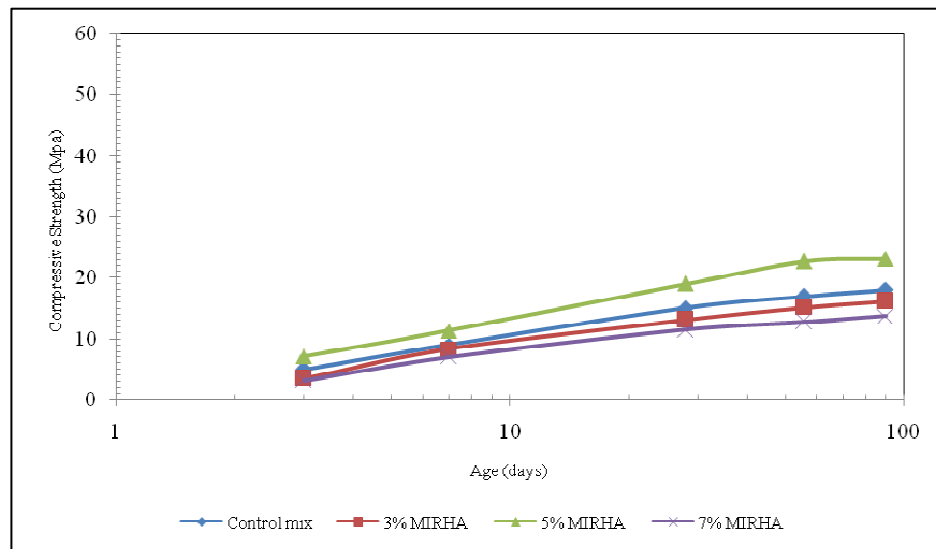


Figure 4.6: Compressive Strength Development for FA-Based Polymeric Concrete with MIRHA in Hot Gunny Curing

4.1.2.2 Polymeric Concrete Samples with MIRHA in Ambient Curing

Figure 4.7 shows that 5% inclusion of MIRHA depicted highest strength in ambient curing i.e. 28.3 MPa at 90 days which was 38.6% greater than 3% inclusion and 50.7% greater than 7% inclusion where as 19% greater than control mix. As regard to that 5% inclusion was found out to be the optimum amount being replaced in FA-based polymeric concrete with MIRHA.

In comparison with hot gunny curing, strength of ambient cured samples was 22.5% higher because of dry curing so that water released, after polymerization, was evaporated and did not accumulate pores. Successful removal of water from the voids allowed the alumino-silicate gel to fill up the pores for better strength development.

In ambient curing, unlike hot gunny curing, strength development is slow but still most of the strength had developed at 28 days. On 56th day average of 8% of 28 days strength was developed (Table 4.4). The reason of this slow strength development is insufficient heat in first 3 days which is higher in case of hot gunny curing. Highest increment in strength can be seen in 5% MIRHA mix i.e. 62.6% from 3 to 7 days.

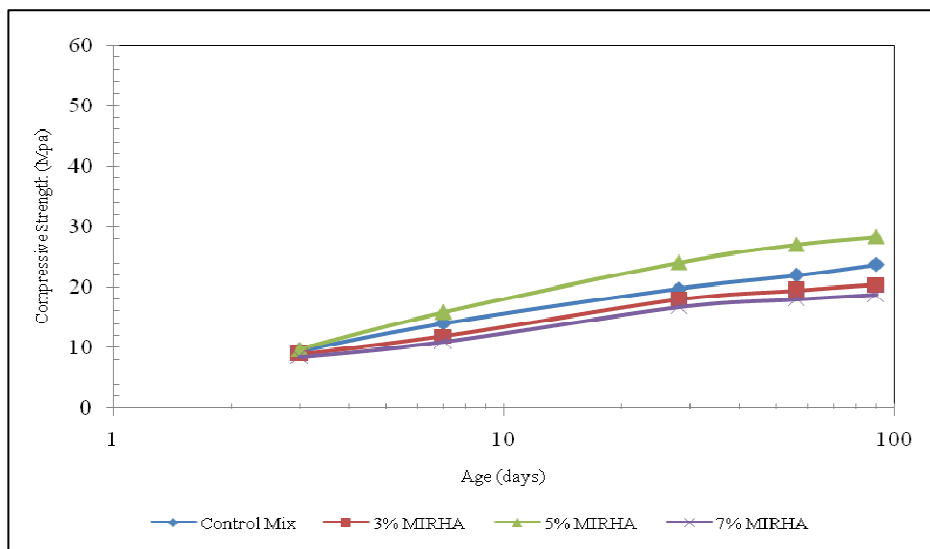


Figure 4.7: Compressive Strength Development for FA-Based Polymeric Concrete with MIRHA in Ambient Curing

4.1.2.3 Polymeric Concrete Samples with MIRHA in External Exposure Curing

External exposure curing resulted in highest compressive strength among all types of curing (Figure 4.8). Among replacements, 7% replacement by MIRHA gave the highest compressive strength i.e. 46 MPa at 90 days which was 48.4% greater than 5% MIRHA mix and 11.7% less than control mix. In control mix 67% of the 90 days strength was developed in first 3 days which then led to 51.36 MPa at 90 days, highest

of all the mixes. Whereas between 7 and 28 days, highest increment was in 3% MIRHA mix i.e. 30%.

These results explained the importance of heat in curing of polymeric concrete which was insufficient in other two curings. Increased temperature gave rise to pozzolanic reaction. In external exposure curing polymeric reaction was benefited by the heat from sunlight which developed the strength in early age. Heat helped in better dissolution of Si and Al atoms from the amorphous portion of source material by the action of hydroxide ions and side by side these precursor ions converted to monomers which further proceeded with the polycondensation process (hardening process) to form a polymeric structure as described by Davidovits (2008).

Performance of MIRHA in polymeric concrete depended upon the proper utilization of its particles from which Al and Si content could easily dissolve to form supersaturated aluminosilicate solution which further transformed into a gel. This gel was a network of oligomers which kept on increasing till the maximum utilization of alkaline liquids. After this the gel started hardening which was better in external exposure curing because of more heat from sunlight.

At 7th day average of 80% of 28 days strength (Table 4.4) was developed which was maximum in external exposure curing as compared to other curing regimes.

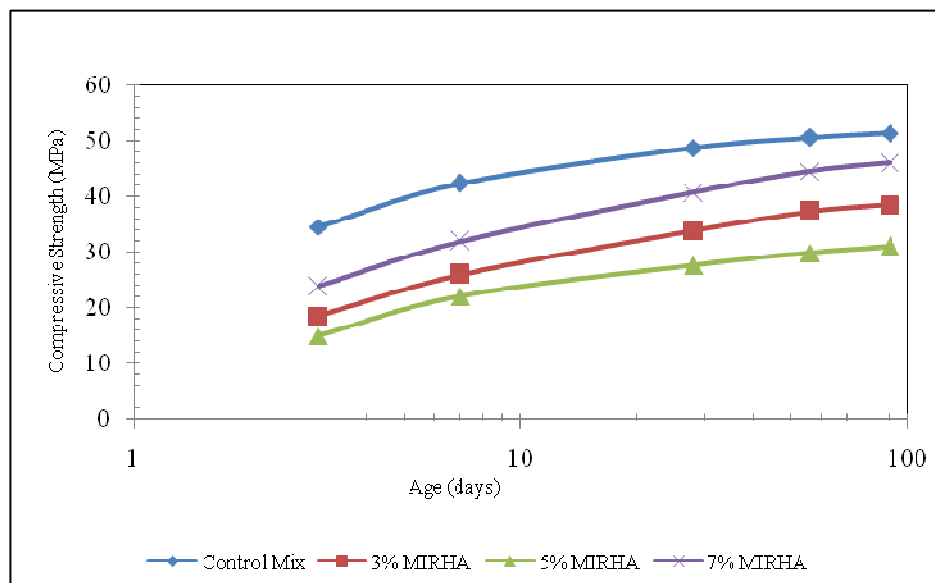


Figure 4.8: Compressive Strength Development for FA-Based Polymeric Concrete with MIRHA in External Exposure Curing

4.1.2.4 Polymeric Concrete Samples with SF in Hot Gunny Curing

Addition of SF to the polymeric concrete resulted in a compressive strength i.e. more than 50% strength of MIRHA mix. Although due to the wet curing water accumulated the voids as in case of MIRHA mixes but still amount of voids was less as compared to MIRHA mix.

7% inclusion of SF showed highest strength (Figure 4.9) among all mixes that was 93.5% greater than control mix and 5% greater than 5% SF mix. Heat was not sufficient in hot gunny curing which hindered the dissolution of Si and Al atoms from SF and FA resulting in an overall lower strength among all other types of curing.

Similar to other mixes age did not have any significant effect on compressive strength of polymeric concrete and most of the strength was developed in early ages. Between 3 to 7 days 5% SF mix showed 92% strength increase whereas 67% increment in strength can be seen in control mix and 3%, SF mix i.e. comparatively higher among all.

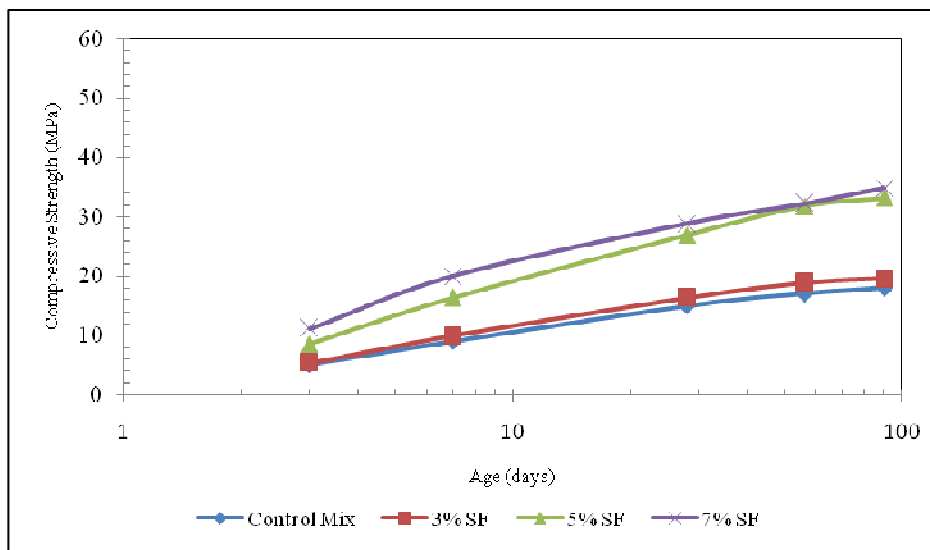


Figure 4.9: Compressive Strength Development for FA-Based Polymeric Concrete with SF in Hot Gunny Curing

4.1.2.5 Polymeric Concrete Samples with SF in Ambient Curing

Figure 4.10 shows that 3% inclusion of SF in FA-based polymeric concrete yielded highest compressive strength as compared to control and other mixes i.e. 32.55 MPa. It was 37% higher than control mix as well as 5% higher than 5% SF sample which showed the lowest strength among all.

This sample also followed the same trend as that of previous mixes and gained most of the strength within 28 days, after which no marked difference can be seen. At 7 days average of 76% of 28 days strength (Table 4.5) was achieved. 106% strength was gained by 5% SF mix respectively from 3 to 7 days.

Unlike MIRHA mixes, hot gunny curing yielded better results as compared to ambient curing which showed that high temperature in early hours of curing helped in more dissolution of Si atoms from SF as compared to MIRHA because of greater surface area of SF.

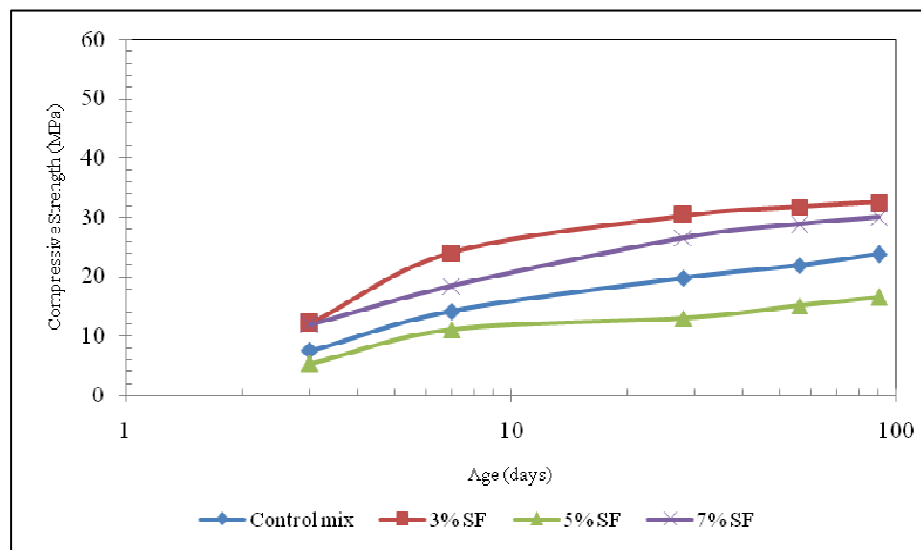


Figure 4.10: Compressive Strength Development for FA-Based Polymeric Concrete with SF in Ambient Curing

4.1.2.6 Polymeric Concrete Samples with SF in External Exposure Curing

Figure 4.11 shows that control mix showed the highest compressive strength results i.e. 32.4% higher than 3% SF mix, 56% higher than 5% SF mix and 10.5% higher than 7% SF mix. Among all replacements, 7% SF replacement provided the highest compressive strength which was comparable with MIRHA mix.

The strength achieved in 90 days of hot gunny curing was achieved in 3 days in external exposure curing and the main difference between them was heat. In external exposure curing heat was gained from sunlight in early hours of curing which helped in better development of strength after good polymeric reaction. 68% of 28 days of strength was gained in 3 days followed by 84% of 28 days strength (Table 4.5) that 7 days which was highest as compared to the MIRHA mix cured with external exposure curing.

SF replacement was slightly better than MIRHA because MIRHA absorbed more water due to its hygroscopic characteristic whereas SF needed water after exceeding 7% in amount which made possible for the precursor ions to fully mobilize and orient themselves into monomers within the provided amount of liquid. These monomers transformed into oligomers to form a network which further moved to gelation process and reorganized themselves to form a three dimensional aluminosilicate network. Polymerization process initiated and improved the better hardening of this aluminosilicate network after utilization of heat from sunlight which resulted in higher compressive strength.

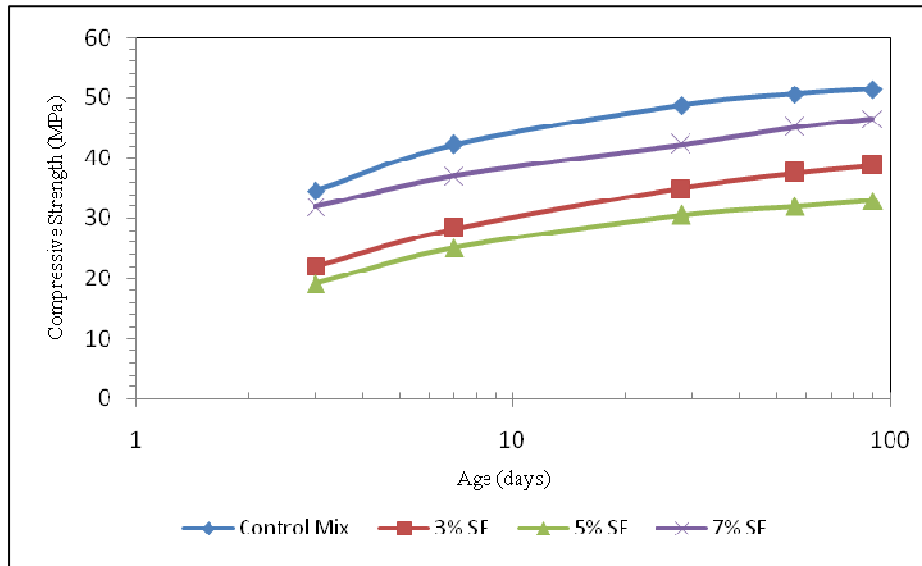


Figure 4.11: Compressive Strength Development for FA-Based Polymeric Concrete with SF in External Exposure Curing

4.1.3 Splitting Tensile Strength Test Results

Splitting tensile strength test was conducted to find out the indirect tensile strength of polymeric concrete at 28 days of curing. Test results are shown in Table 4.6 and Table 4.7 for the mixes replaced partially by MIRHA and SF respectively. Two samples were tested for each mix and their average is shown in the tables.

4.1.3.1 Polymeric Concrete Samples with MIRHA and SF in all Curing Regimes

Figure 4.12 shows that in MIRHA polymeric concrete mixes, control mix showed the highest result for hot gunny and external exposure curing i.e. 1.7 MPa and 2.45 MPa whereas in ambient curing 7% inclusion of MIRHA was better among all with the tensile strength of 1.89 MPa.

In SF polymeric concrete (Figure 4.13), 7% inclusion of SF showed the highest tensile strength value in hot gunny curing i.e. 1.77 MPa while for ambient and external exposure curing results were same as in MIRHA concrete with the strength of 2.17 MPa and 2.22 MPa respectively.

Incase of MIRHA mix, 3% of MIRHA concrete showed tensile-to-compressive strength ratio as 12% in hot gunny curing which is highest among all the mixes but tensile-to-compressive strength ratio also depend upon several other factors other than curing such as type of aggregate, admistures, water to solid ratio etc. In SF mix 5% SF replacement showed the highest tensile-to-compressive strength ratio i.e. 16%. For OPC concrete typical values of tensile strength lie in between 1.0 to 4.0 MPa for f_c of 7.0 to 62.0 MPa respectively. Tensile-to- compressive strength ratio is approximately 10 to 11 percent for low strength, 8 to 9 percent for moderate strength, and 7 percent for high strength concrete (Mehta & Monteiro, 2006). Tensile strength of polymeric concrete was less than OPC concrete which can be improved by the use of fibres or some other appropriate techniques.

Relationship between compressive strength and tensile strength is not linear which is same as in OPC concrete. Correlation of compressive strength with tensile strength of polymeric concrete showed better results for MIRHA mix (Figure 4.14) as compared to SF mix (Figure 4.15). R^2 value is 0.992 for MIRHA mix in ambient curing which is highest among all mixes and the indication of good correlation between compressive and tensile strength.

In SF mix with external exposure curing, tensile strength is increasing with the increase in compressive strength and showing better relationship between compressive strength and tensile strength as compared to other mixes with good R^2 value.

Table 4.6: Splitting Tensile Strength Test Results of FA-Based Polymeric Concrete with MIRHA

Curing Type	MIRHA (%)	28 Days Tensile strength MPa	28 Days Compressive Strength MPa	Ratio of Tensile Strength to Compressive Strength (%)
Hot Gunny Curing	0	1.7	15.0	11.3
	3	1.6	13.1	12.4
	5	1.4	19.0	7.3
	7	1.1	11.5	9.2
Ambient Curing	0	1.0	19.7	4.8
	3	1.5	17.9	8.1
	5	1.9	24.1	7.7
	7	1.9	16.8	11.3
External Exposure Curing	0	2.5	48.7	5.0
	3	1.3	33.8	3.8
	5	2.0	27.6	7.1
	7	2.1	40.7	5.3

Table 4.7: Splitting Tensile Strength Test Results of FA-Based Polymeric Concrete with SF

Curing Type	SF (%)	28 Days Tensile strength MPa	28 Days Compressive Strength MPa	Ratio of Tensile Strength to Compressive Strength (%)
Hot Gunny Curing	0	1.7	15.0	11.3
	3	1.7	16.4	10.5
	5	1.7	26.9	6.3
	7	1.8	28.8	6.1
Ambient Curing	0	1.0	19.7	4.8
	3	1.8	30.3	6.1
	5	2.1	13.0	16.3
	7	2.2	26.5	8.2
External Exposure Curing	0	2.5	48.7	5.0
	3	1.6	35.0	4.5
	5	1.3	30.5	4.3
	7	2.2	42.3	5.3

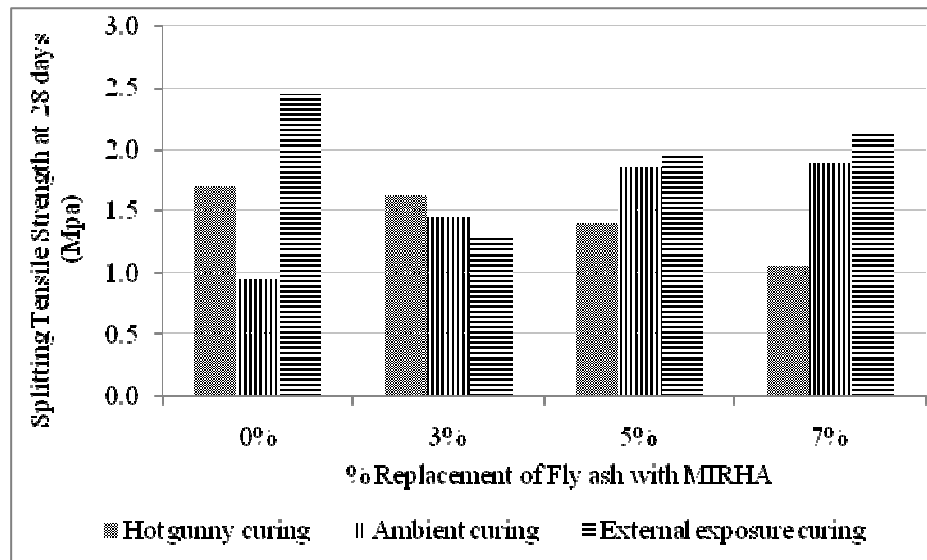


Figure 4.12: 28-Days Splitting Tensile Strength for FA-Based Polymeric Concrete with MIRHA

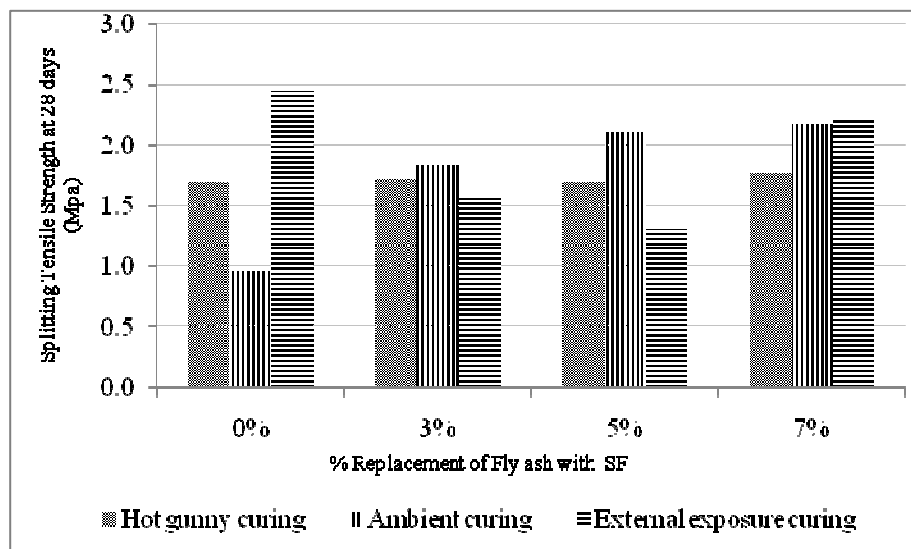


Figure 4.13: 28-Days Splitting Tensile Strength for FA-Based Polymeric Concrete with SF

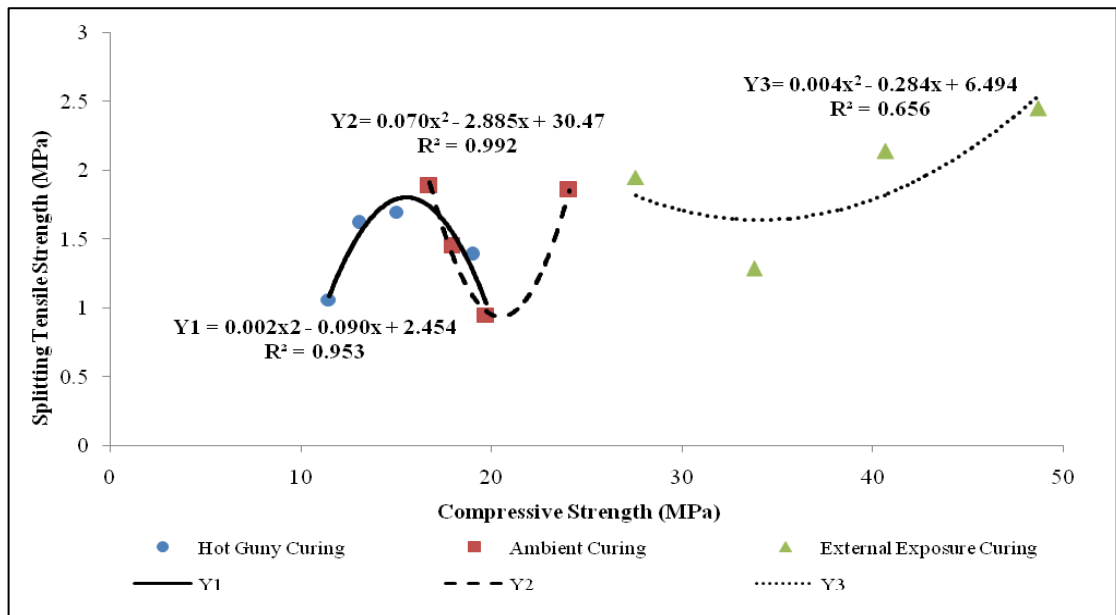


Figure 4.14: Correlation between Compressive Strength & Tensile Strength of Polymeric Concrete with MIRHA

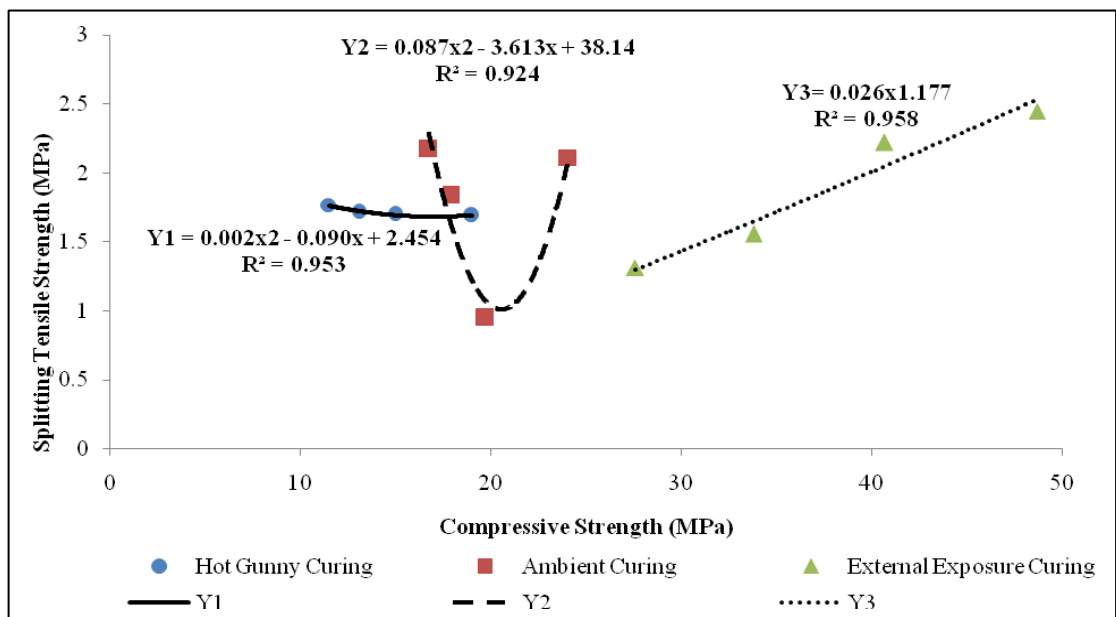


Figure 4.15: Correlation between Compressive Strength & Tensile Strength of Polymeric Concrete with SF

4.1.4 Flexural Strength Test Results

Flexural strength test was conducted on the beams of size 100mm x100mm x500mm that were tested at the age of 28 days under third point loading. Results are shown in Table 4.8 and Table 4.9 for the FA-based polymeric concrete replaced by MIRHA and SF respectively.

4.1.4.1 Polymeric Concrete Samples with MIRHA and SF in all Curing Regimes

Figure 4.16 shows that 7% inclusion of MIRHA depicted the highest flexural strength value for ambient and external exposure curing i.e. 8.38 MPa and 6.52 MPa respectively. For hot gunny curing 3% inclusion of MIRHA showed the highest value i.e. 5.44 MPa. Figure 4.17 shows that in hot gunny and external exposure curing, 7% inclusion of SF showed the highest results i.e. 8.35 MPa and 7.91 MPa respectively. In ambient curing 5% inclusion of SF showed the best strength i.e. 6.58 MPa.

In flexural strength, unlike splitting tensile strength, ambient curing was the best in MIRHA polymeric concrete and in SF polymeric concrete, hot gunny curing was the best. According to ACI commentary, tensile strength in flexure is 10-15% of compressive strength which was slightly better for polymeric concrete. Ratio of flexural strength to compressive strength was found to be more than 10-15% which is the indication of good flexural strength of polymeric concrete as compared to OPC concrete.

Correlation of compressive strength with flexural strength for polymeric concrete showed highest R^2 value for SF mix (Figure 4.18) as compared to MIRHA mix (Figure 4.19). Highest value was found to be 0.953 for hot gunny curing

Table 4.8: Flexural Strength of FA-Based Polymeric Concrete with MIRHA

Curng Type	MIRHA (%)	28 Days Flexural Strength (MPa)	28 Days Compressive Strength (MPa)	Ratio of Flexural Strength to Compressive Strength (%)
Hot Gunny Curing	0	4.9	15.0	32.7
	3	5.4	13.1	41.6
	5	5.0	19.0	26.4
	7	3.3	11.5	28.3
Ambient Curing	0	3.4	19.7	17.1
	3	3.4	17.9	19.0
	5	6.3	24.1	26.3
	7	8.4	16.8	50.0
External Exposure Curing	0	6.3	48.7	13.0
	3	3.9	33.8	11.5
	5	5.2	27.6	18.9
	7	6.5	40.7	16.0

Table 4.9: Flexural Strength of FA-Based Polymeric Concrete with SF

Curng Type	SF (%)	28 Days Flexural Strength (MPa)	28 Days Compressive Strength (MPa)	Ratio of Flexural Strength to Compressive Strength (%)
Hot Gunny Curing	0	4.9	15.0	32.7
	3	6.4	16.4	39.2
	5	5.6	26.9	21.0
	7	8.4	28.8	29.0
Ambient Curing	0	3.4	19.7	17.1
	3	5.2	30.3	17.1
	5	6.6	13.0	50.7
	7	5.9	26.5	22.4
External Exposure Curing	0	6.3	48.7	13.0
	3	6.1	35.0	17.5
	5	4.5	30.5	14.9
	7	7.9	42.3	18.7

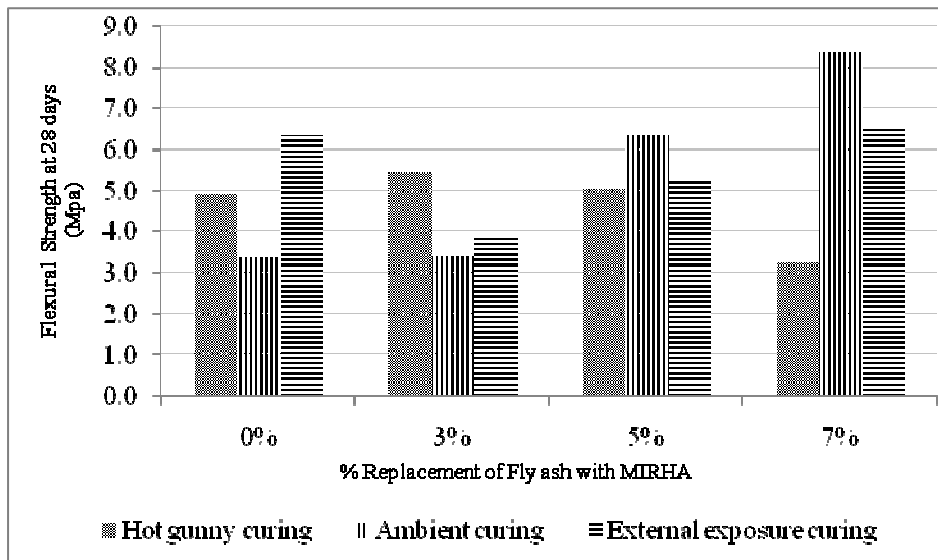


Figure 4.16: 28-Days Flexural Strength for FA-Based Polymeric Concrete with MIRHA

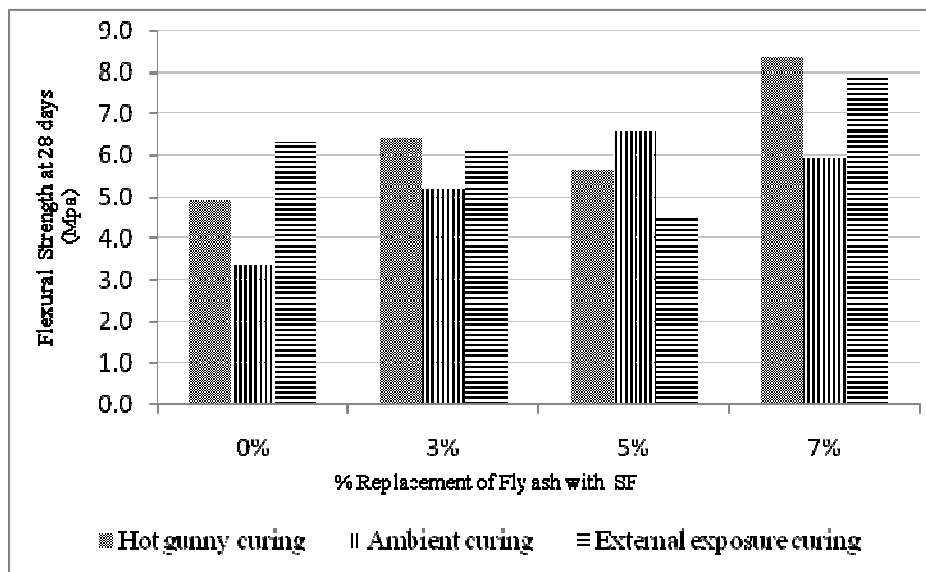


Figure 4.17: 28-Days Flexural Strength for FA-Based Polymeric Concrete with SF

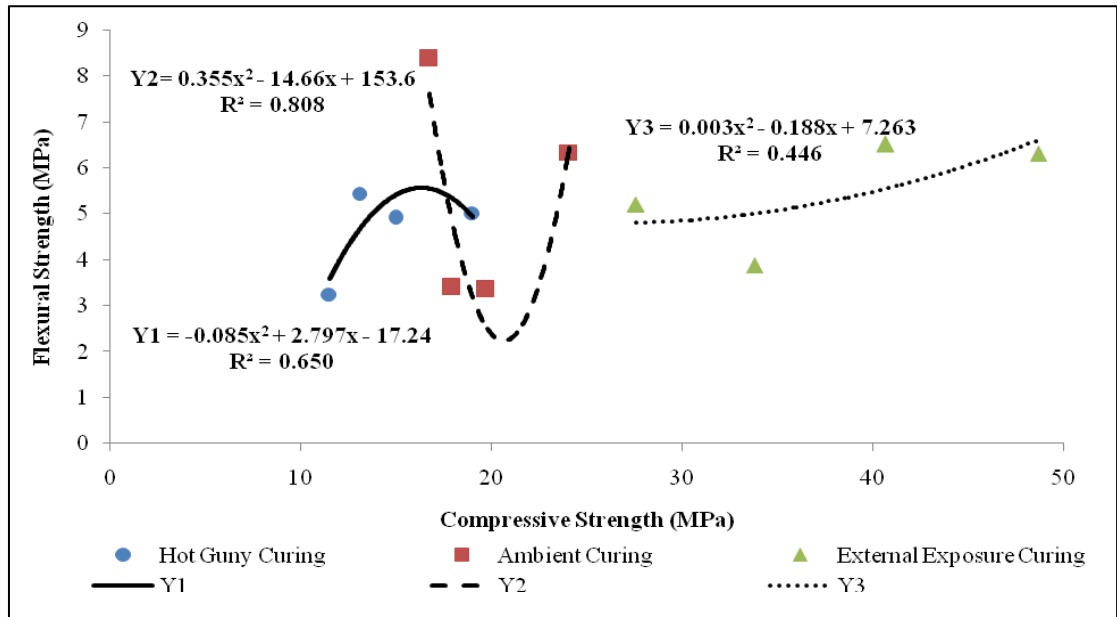


Figure 4.18: Correlation between Compressive Strength & Flexural Strength of Polymeric Concrete with MIRHA

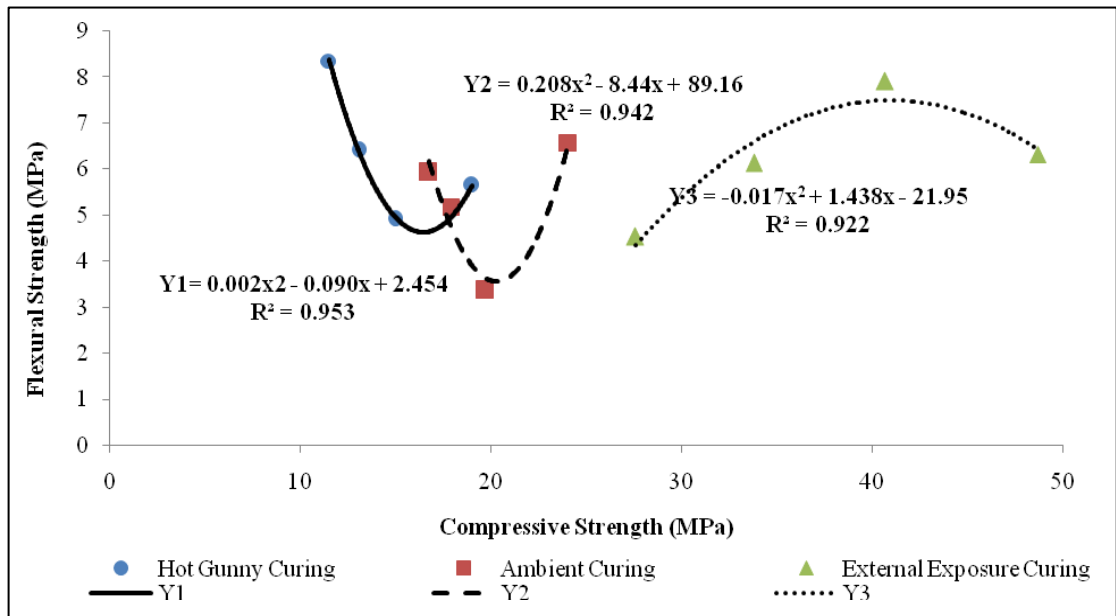


Figure 4.19: Correlation between Compressive Strength & Flexural Strength of Polymeric Concrete with SF

4.1.5 Ultrasonic Pulse Velocity Test Results

UPV test was performed to find out the integrity of concrete samples. Presence of voids can be known by the travelling of pulse from transmitter to receiver through the concrete. UPV results are shown in Table 4.10 and Table 4.11.

Table 4.10: UPV Test Results of FA-Based Polymeric Concrete with MIRHA

Curing Type	MIRHA (%)	Pulse Velocity (km/s)				
		3 days	7 days	28 days	56 days	90 days
Hot Gunny Curing	0	3.6	2.6	3.1	3.5	3.6
	3	3.9	3.1	3.1	3.2	3.2
	5	3.6	3.1	3.1	3.4	3.5
	7	3.6	3.0	3.2	3.2	3.3
Ambient Curing	0	2.7	2.8	3.1	3.5	3.6
	3	3.3	3.2	3.3	3.4	3.5
	5	3.1	3.2	3.3	3.3	3.3
	7	3.0	3.2	3.4	3.5	3.6
External Exposure Curing	0	3.5	3.7	4.1	4.1	4.1
	3	3.4	3.4	3.9	3.9	3.9
	5	3.0	3.4	3.8	3.9	3.9
	7	3.2	3.5	3.9	3.9	3.9

Table 4.11: UPV Test Results of FA-Based Polymeric Concrete with SF

Curing Type	SF (%)	Pulse Velocity (km/s)				
		3 days	7 days	28 days	56 days	90 days
Hot Gunny Curing	0	3.6	2.6	3.1	3.5	3.6
	3	3.4	2.8	2.9	3.3	3.3
	5	3.5	3.2	3.6	3.8	3.8
	7	3.7	3.3	3.4	3.5	3.7
Ambient Curing	0	2.7	2.8	3.1	3.5	3.6
	3	3.3	3.3	3.7	3.8	3.9
	5	2.4	2.9	3.0	3.2	3.4
	7	3.1	3.3	3.5	3.5	3.5
External Exposure Curing	0	3.5	3.7	4.1	4.1	4.1
	3	3.0	3.3	3.9	3.9	3.9
	5	3.0	3.3	3.5	3.6	3.6
	7	3.6	3.8	3.9	4.0	4.0

4.1.5.1 Polymeric Concrete Samples with MIRHA in Hot Gunny Curing

Figure 4.20 shows the trend in UPV among all the mixes. At 3 days UPV was greater as compared to that of 7 days which showed the presence of water in the voids which increased the velocity. While at 7 days UPV lowered down by average difference of 25%, showing the removal of water from the voids. Greater value of UPV at 3 days explained the phenomenon that because of wet curing condition, water released after polycondensation retained in the voids and could not escape the mix. After 7 days UPV kept on increasing till 90 days, showing subsequent reduction of pores in the concrete. This pore development phenomenon is explained in Figure 4.21.

Overall at 90 days, control mix showed the highest value of UPV showing good polymerization reaction which filled up the voids with reaction product i.e. aluminosilicate gel, better as compared to the other mix. Although this UPV result was less than that of 3 days which showed the gradual replacement of water by air and then by aluminosilicate gel in the voids.

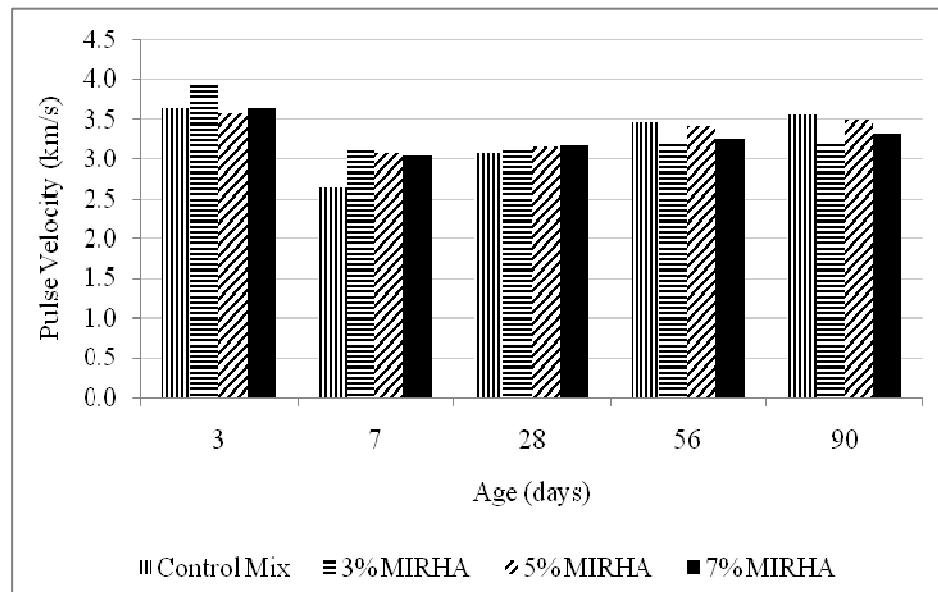


Figure 4.20: UPV Test Results for FA-Based Polymeric Concrete with MIRHA in Hot Gunny Curing

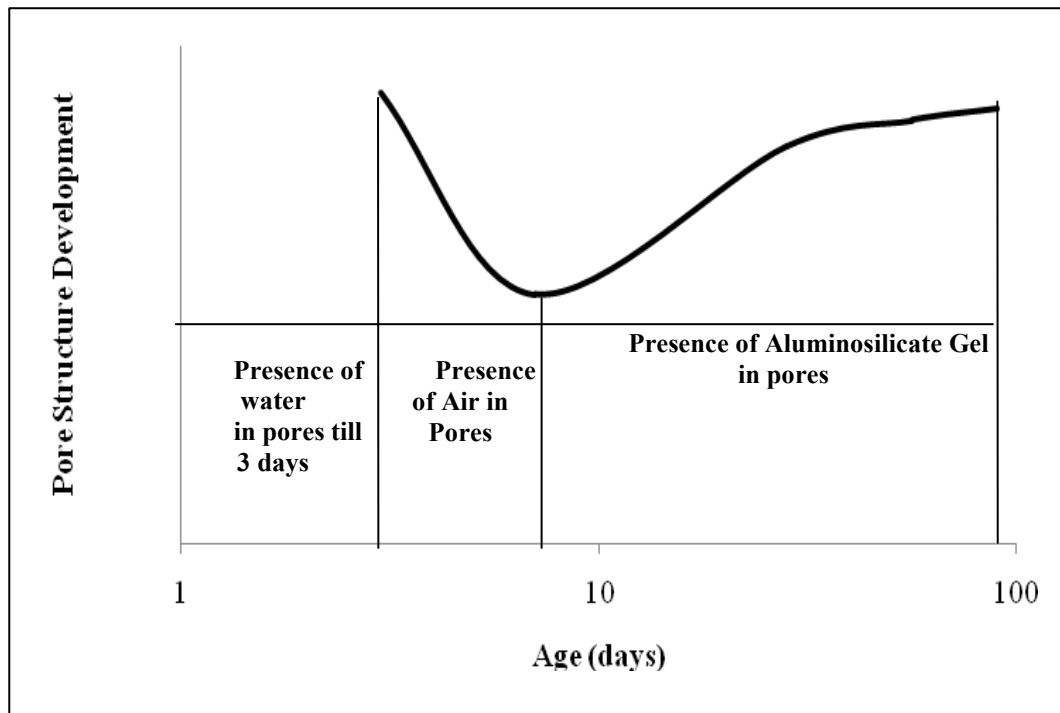


Figure 4.21: Pore Structure Development

4.1.5.2 Polymeric Concrete Samples with MIRHA in Ambient Curing

Figure 4.22 shows the trend in results among control mix, 5% MIRHA sample and 7% MIRHA sample. The continuous gradual increment in UPV can be seen which showed that water released after polymerization successfully channeled out from the concrete and did not accumulate voids which helped in uniform reduction of voids. The removal of water became possible because of dry curing unlike hot gunny curing (wet curing) where external moisture restrained the removal of water. In 3% MIRHA concrete, UPV decreased by 1.6% at 7 days that can be considered as negligible, followed by gradual increment up to 90 days.

Overall both, control mix and 7% MIRHA sample showed the same UPV result in spite of having different rate of reduction of voids in early ages but in control mix void reduction was comparatively faster. Overall 3% SF sample showed the highest value of UPV which means that it contains lowest amount of voids in the concrete as compared to other samples.

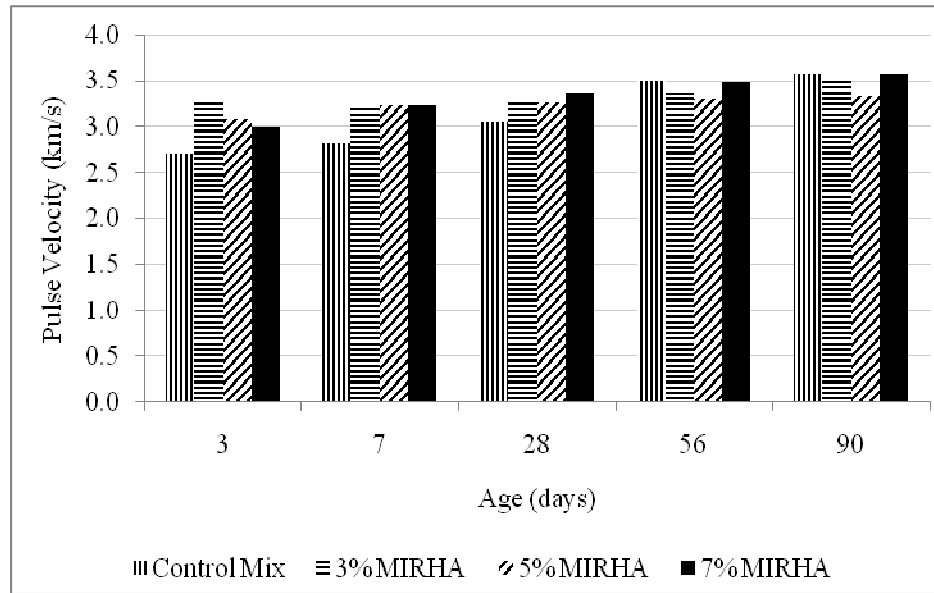


Figure 4.22: UPV Test Results for FA-Based Polymeric Concrete Replaced by MIRHA with Ambient Curing

4.1.5.3 Polymeric Concrete Samples with MIRHA in External Exposure Curing

Figure 4.23 shows that all mixes following the same trend that was gradual increase in UPV till 90 days. This continuous increase was because of greater temperature provided by the sunlight that gradually evaporated all the water from the pores.

Fast void reduction can be seen in 5% MIRHA sample where there is maximum increase in UPV between 3 and 7 days. This showed that polymeric reaction started in early age in 5% MIRHA mix and most of the voids were filled by aluminosilicate gel. In all other samples void reduction was prominent between 7 and 28 days which shows that high temperature helped in early formation of aluminosilicate gel filling the voids.

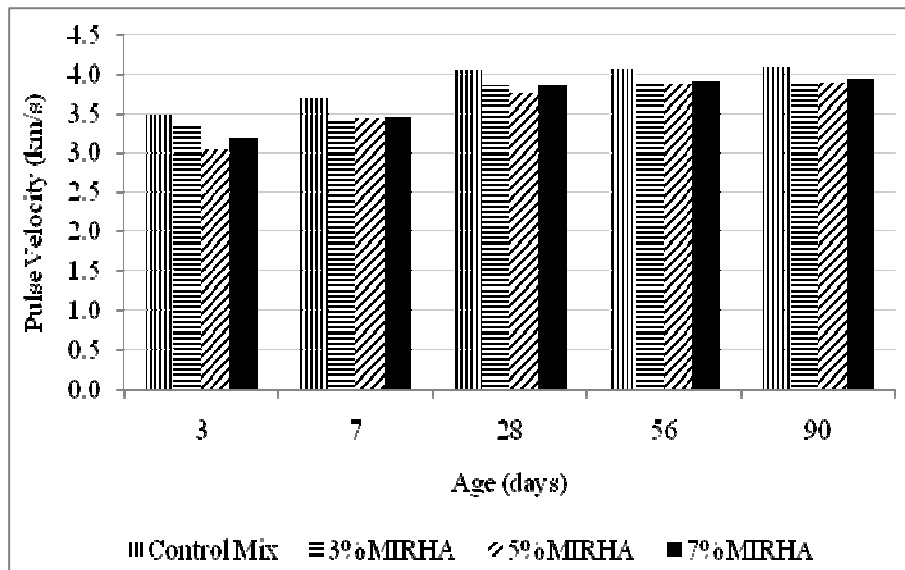


Figure 4.23: UPV Test Results for FA-Based Polymeric Concrete Replaced by MIRHA with External Exposure Curing

4.1.5.4 Polymeric Concrete Samples with SF in Hot Gunny Curing

Figure 4.24 shows that all mixes were following the same trend as that of MIRHA mixes cured by hot gunny. UPV decreased at 7 days, followed by increment in UPV till 90 days (Figure 4.21). This depicted that the water collected in the pores first provided the medium for the pulse to cover the distance without any dispersion which made the UPV value high and after 3 days water was replaced by aluminosilicate gel and removed effectively at later ages.

Overall at 90 days 5% SF sample showed the highest UPV value which showed the minimum amount of voids at this age and maximum pore reduction happened between 28 to 56 days. Fast and continuous reduction of voids can be seen in control mix that is maximized between 7 to 28 days.

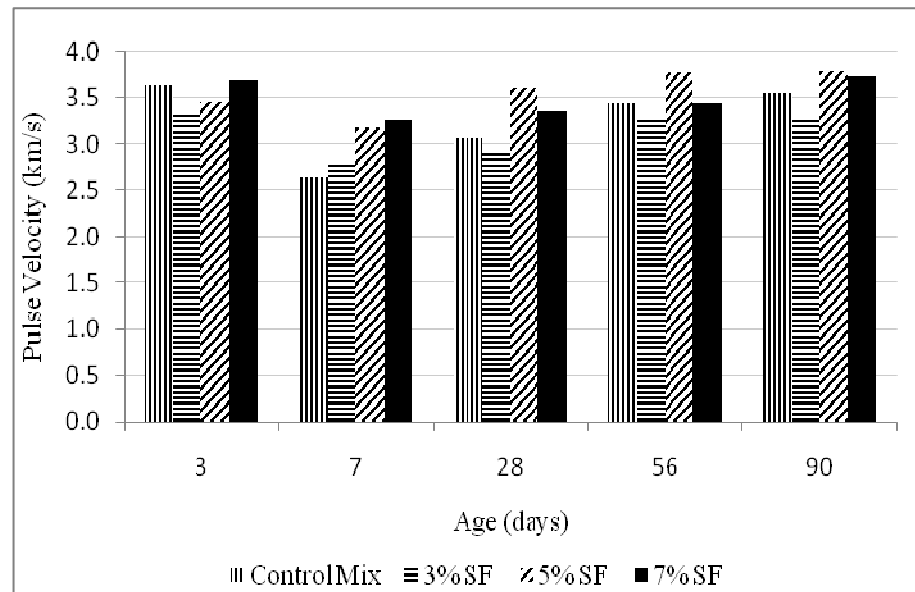


Figure 4.24: UPV Test Results for FA-Based Polymeric Concrete with SF in Hot Gunny Curing

4.1.5.5 Polymeric Concrete Samples with SF in Ambient Curing

Figure 4.25 shows that all polymeric concrete samples showed the same trend as in hot gunny curing. Continuous increment can be seen till 90 days. This may be due to the reason that water was not accumulated in the voids and voids were continuously filled by polymeric gel leaving fewer amounts of voids in the concrete. Void reduction was fast in 5% SF sample as compared to others and most of it was achieved in early ages.

4.1.5.6 Polymeric Concrete Samples with SF in External Exposure Curing

Figure 4.26 shows that there was a continuous increment in UPV in all the mixes which depicts the presence of less voids in the mix due to the small size of silica fume particles which filled up all the voids.

In 5% SF sample void reduction can be seen on early stage as compared to the other samples in which void reduction was prominent after 7 days. This means that amount of silica and the heat were suitable for the polymeric reaction in 5% SF sample. Overall control mix showed the highest UPV value at 90 days which showed the fewer amount of

voids present in the concrete as compared to other mix. When Al and Si from the source material came in contact with the alkaline solution, the polymeric structure started making building blocks of Al-O-Si which further grew up to form aluminosilicate gel. Polymeric chain grew up by utilizing heat from the sunlight and as a result more and more reaction product was formed which filled up all the voids in the concrete. The gel formation depended upon the dissolution of Si and Al contents present in the minerals which kept on increasing by absorbing more heat from the surroundings.

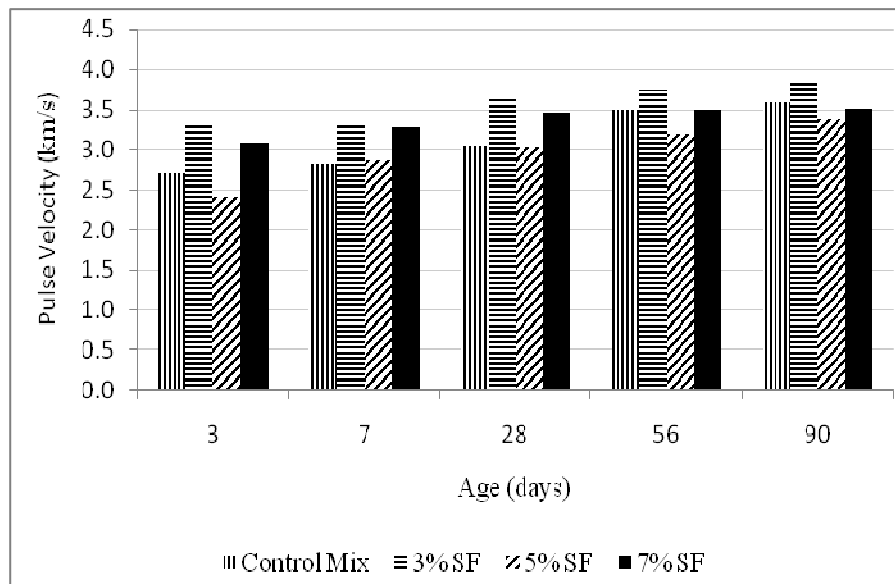


Figure 4.25: UPV Test Results for FA-Based Polymeric Concrete with SF in Ambient Curing

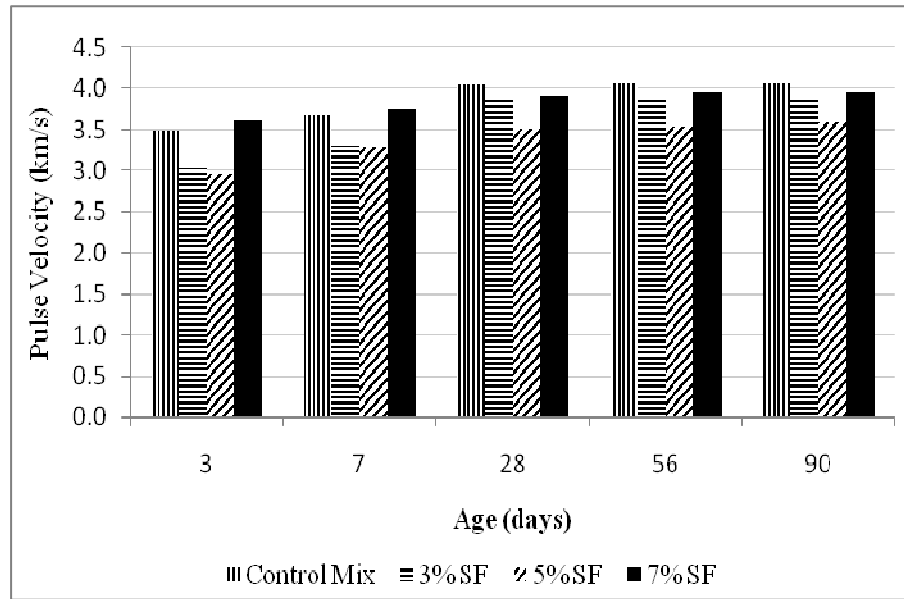


Figure 4.26: UPV Test Results for FA-Based Polymeric Concrete with SF in External Exposure Curing

4.1.6 Microstructure Analysis of Polymeric concrete

4.1.6.1 SEM Analysis of Control Mix in all Curing Regimes

In hot gunny curing, most of the spherical fly ash particles remained unreacted as shown in Figure 4.27a and some of them are covered with reaction product i.e. aluminosilicate gel (Figure 4.28) which showed the lesser degree of reaction. Temperature was one of the reasons for insufficient polymerization. Proper dissolution of Si and Al atoms did not occur due to less amount of heat provided to the concrete. The presence of some gel showed that some polymeric reaction occurred in first two days of hot gunny curing where temperature was somewhat high and after that due to scanty heat further gel did not form and even the existed gel could not hardened properly.

The gel seemed to be wet and not completely hardened even after 28 days of curing. The reason behind dampen microstructure was wet curing by hot gunny in first two days of curing due to which water could not evaporate completely from the concrete which was released due to polycondensation. This overall situation inside the microstructure led to the lowest compressive strength of concrete as compared to all other types of curing.

In Figure 4.27b, under ambient curing, undissolved particles were laid about the microstructure but most of them were embedded in the hardened aluminosilicate gel. As compared to the hot gunny curing, microstructure found to be dry and gel was hardened up to some extent. Overall microstructure was non homogenous due to inadequate heat from the surroundings. Interfacial transition zone (ITZ) was also not strongly developed as it was not completely filled by an aluminosilicate gel that caused the failure at lower stress level being the weakest portion in the concrete. Besides this voids can clearly be observed in ITZ that also reduced the stiffness of concrete. Due to the weak link between aggregates and matrix, the cracks existing in the interfacial zone extended and resulted in the early failure of material.

As compared to all types of curing, external exposure curing (Figure 4.27c) showed better microstructure. Undissolved particles were not present in the matrix and better dissolution of Si and Al atoms took place resulting in more aluminosilicate gel which hardened completely because of high curing temperature. In this curing heat was utilized from sunlight which helped in better polycondensation reaction and due to high temperature, water released after polycondensation, was also evaporated from the matrix. Microstructure was very much compact and homogenous that was the indication of good binding between binder and aggregates leading to higher strength concrete.

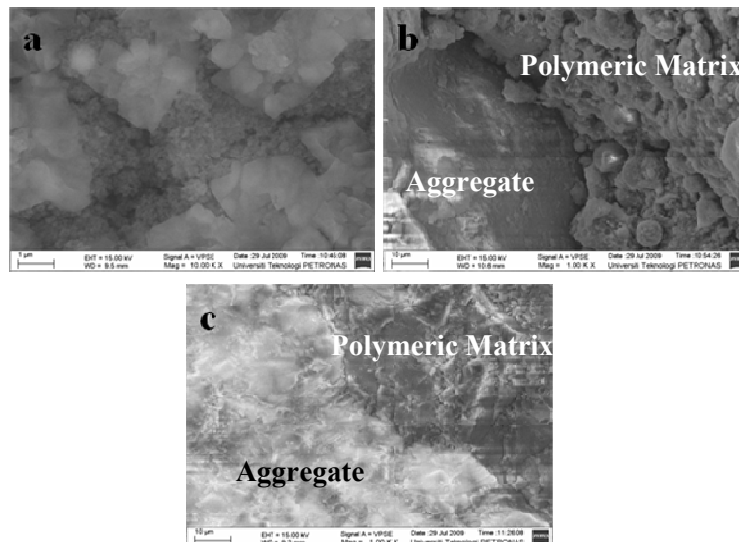


Figure 4.27: SEM images for the Control Polymeric Mixes with a) Hot gunny curing b) Ambient curing and c) External exposure curing



Figure 4.28: FESEM Image of Polymeric Paste Showing Aluminosilicate gel

4.1.6.2 SEM Analysis of Polymeric Concrete with MIRHA & SF in Hot gunny Curing

In 3% and 7% MIRHA (Figure 4.29a) (Figure 4.29c) mix voids can clearly be observed in ITZ which were not filled by aluminosilicate gel. Due to poorly developed ITZ material was not able to take more loads and failed at lower stress value. Un-reacted particles were also in bulk in the microstructure which showed that most of the source material particles did not participate in the polymerization reaction and alkali solution could not effectively activated Si and Al atoms from the source material due to insufficient heat. Although some of the particles were covered with gel that is the indication of polymeric reaction but in less amount.

In 5% MIRHA mix (Figure 4.29b), a broad crack in the matrix was the indication of weak material. May be this was due to the stress induced because of variations in temperature or due to the damage during sample preparation although matrix is better hardened as compared to 3% and 7% MIRHA mix.

Inclusion of SF in polymeric concrete increased the water demand in concrete and added amount of water seemed not to be sufficient because abundant un-reacted particles can be seen mixed with the hardened gel and ITZ was not well developed in 3% SF mix (Figure 4.30a). In 5% SF mix some of the gel was produced and mostly precipitated fly ash and silica fume particles can be seen that was due to inadequate heat (Figure 4.30b). Lots of major and minor cracks were also present in the matrix that may be due to the non-uniform temperature throughout the curing period or due to the damage during sample preparation. In 7% SF mix minor voids can be seen in ITZ. Spherical depressions were due to the hollow dissolved fly ash particles (Figure 4.30c).

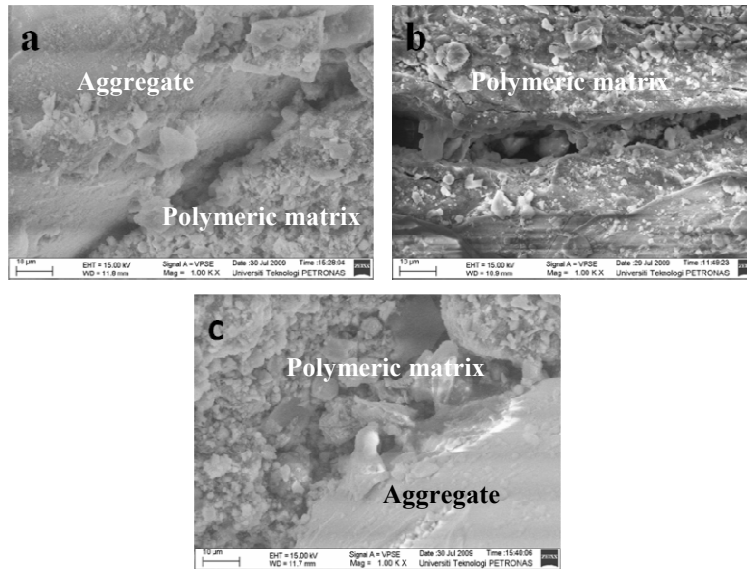


Figure 4.29: SEM images for the FA-based Polymeric Concrete in Hot Gunny Curing with a) 3% MIRHA b) 5% MIRHA and c) 7% MIRHA

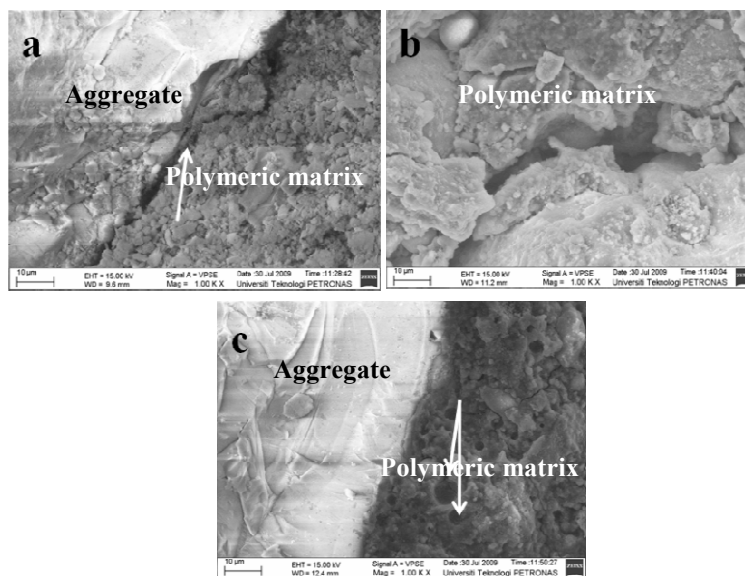


Figure 4.30: SEM images for the FA-based Polymeric Concrete in Hot Gunny Curing with a) 3% SF b) 5% SF and c) 7% SF

4.1.6.3 SEM Analysis of Polymeric Concrete with MIRHA & SF in Ambient Curing

In 3% MIRHA (Figure 4.31a) mix microstructure is better hardened as compared to the control mix (Figure 4.27) which was due to the greater amount of SiO_2 present in MIRHA therefore more Si atoms were expected to dissolve from the source material and participate in polymeric reaction to make polymeric gel. Micro pores were also less in the matrix which was due to the fine MIRHA particles that filled up the spaces. Micro cracks can also be seen in ITZ which may be due to the damage during preparation of the samples.

Microstructure of sample with 5% MIRHA inclusion (Figure 4.31b) was even better than 3% MIRHA mix in terms of hardening of gel because amount of dissolved silica increased with the increase in amount of MIRHA. Although some precipitated particles were present in the matrix; they were not converted to aluminosilicate gel because of low temperature at curing time. In 7% MIRHA mix (Figure 4.31c) undissolved particles were more as compared to 3% & 5% MIRHA mix. It showed that more than 5% inclusion of MIRHA increased the amount of silica in the mix that was not able to fully react with alkaline liquids and due to low heat polymeric reaction was slow and by the time alkaline liquids leached out of the mix before coming in contact thoroughly with reactive solid material. As a result un-reacted particles were more as compared to reactive ones which led to the less compressive strength.

3% SF inclusion (Figure 4.32a) in polymeric concrete was found to be better as compared to 5% and 7% inclusion unlike MIRHA because SF contained more silica content as compared to MIRHA. This showed that beyond 3% SF, alkaline liquids were not sufficient for the mix to dissolve silica from the source material. Un-reacted particles were still there i.e. because of insufficient heat from the surroundings which did not allow precipitated particles to convert to a gel. In 5% and 7% SF mix (Figure 4.32b) (Figure 4.32c), un-reacted particles were abundantly present in the matrix which was also porous because sufficient gel was not formed to fill up these pores.

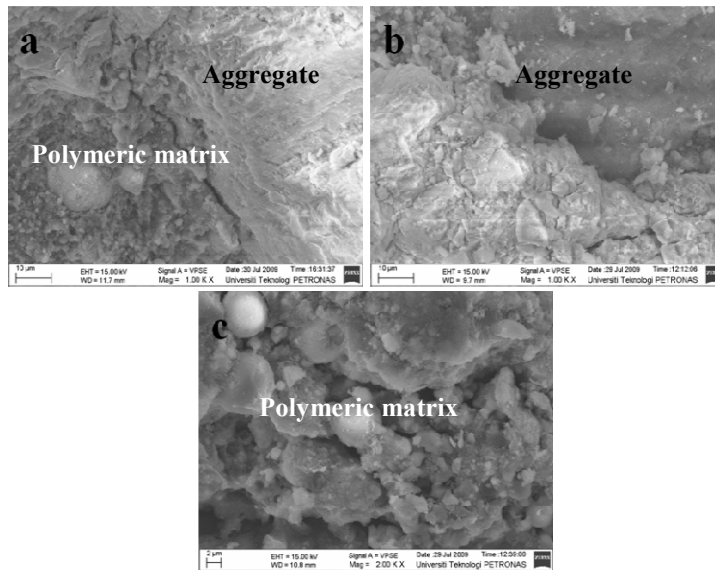


Figure 4.31: SEM images for the FA-based Polymeric Concrete in Ambient Curing with
a) 3% MIRHA b) 5% MIRHA and c) 7% MIRHA

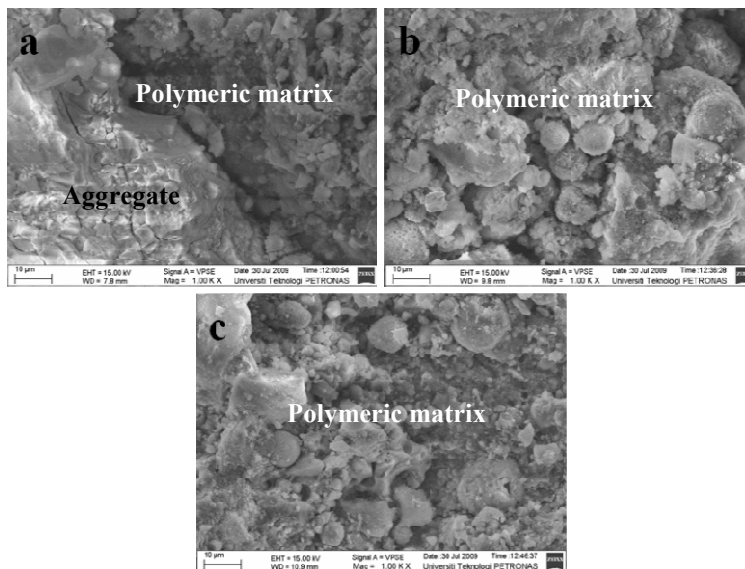


Figure 4.32: SEM images for the FA-based Polymeric Concrete in Ambient Curing with
a) 3% SF b) 5% SF and c) 7% SF

4.1.6.4 SEM Analysis of Polymeric Concrete with MIRHA & SF in External Exposure Curing

In comparison with hot gunny and ambient curing, external exposure curing showed the best microstructure development i.e. due to the sufficient heat provided during curing period. Heat accelerated the polymeric reaction which resulted in the production of aluminosilicate gel that filled up the voids in ITZ and the matrix. Aluminosilicate gel was having a tube like structure unlike CSH gel in OPC concrete (Figure 4.28).

Unlike other types of curing, setting time of polymeric concrete was not delayed and due to the heat from sunlight alkaline liquid easily came in contact with the reactive solid material before leaching out of the mix. All mixes replaced by MIRHA (Figure 4.33) or SF (Figure 4.34) showed a compact microstructure with less number of un-reacted particles which led to the better strength of concrete. ITZ was properly developed as no remarkable border can be seen between aggregates and polymeric matrix. These microstructure properties developed 28 days strength 48.7 MPa which was as good as OPC concrete.

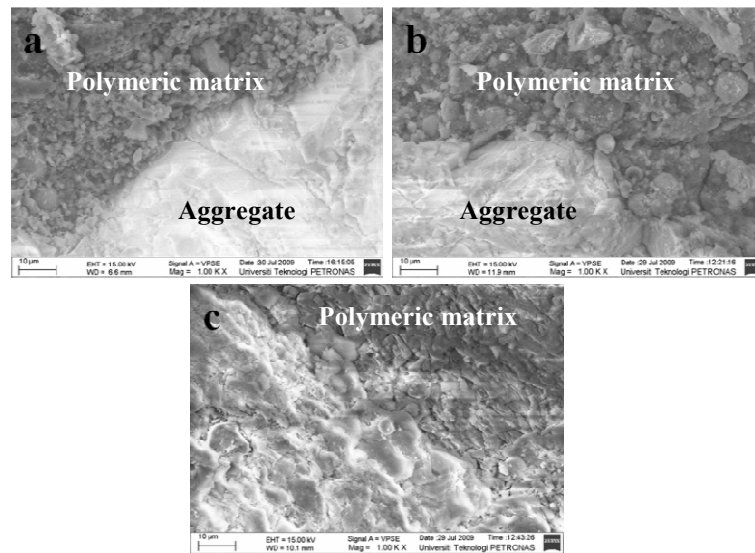


Figure 4.33: SEM images for the FA-based Polymeric Concrete in External Exposure Curing with a) 3% MIRHA b) 5% MIRHA and c) 7% MIRHA

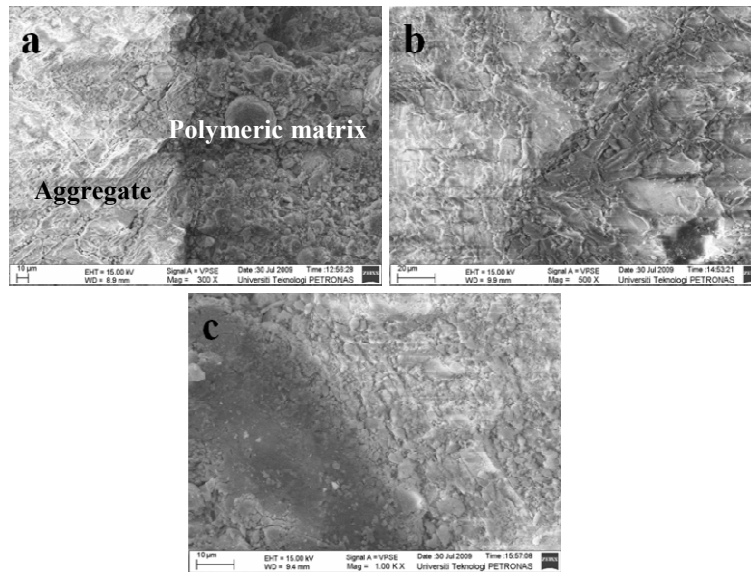


Figure 4.34: SEM images for the FA-based Polymeric Concrete in External Exposure Curing with a) 3% SF b) 5% SF and c) 7% SF

CHAPTER 5

CONCLUSION & RECOMMENDATION

5.1 CONCLUSIONS

The purpose of this research study was to develop a polymeric concrete that fully eliminates the use of OPC in the concrete. It focused on the 28 days target strength of 40-50 MPa, suitable for in-situ construction. To achieve this purpose, a detailed experimental program was designed and the obtained results were discussed for fly ash-based polymeric concrete as well as fly ash based concrete replaced by MIRHA and SF. Based on results and discussions, the following conclusions were drawn.

1. Polymeric concrete was developed which achieved the target compressive strength at 28 days as good as OPC concrete. Microstructure study also verified the cementing potential of polymeric concrete to be used in the real construction industry by showing dense microstructure and well developed ITZ.
2. External exposure curing was found to be the best curing regime which showed the highest value of compressive strength as compared to hot gunny and ambient curing. Compressive strength was developed till 28 days and there was no significant increment in strength beyond 28 days as shown by rate of the strength development tables. 7 days strength of MIRHA mix and SF mix in external exposure curing was average 80% and 84% of 28 days strength respectively. Whereas after 28 days average 9% of strength was gained by mixes cured with external exposure curing.
3. Flexural strength of polymeric concrete was comparable with OPC concrete and tensile strength was found to be less as compared to OPC concrete. In MIRHA mix tensile strength was good for external exposure curing and flexural strength was good in ambient curing as compared to other curing regimes. Whereas for SF

mix tensile strength was also good for external exposure curing but flexural strength was good for hot gunny curing.

4. 5% MIRHA mix found to be the optimum mix for hot gunny and ambient curing. Whereas 3% SF mix showed optimum value in ambient curing only.
5. Best mix that was obtained by this research was based on the compressive strength and microstructure study of fly ash based polymeric concrete without being replaced by MIRHA or SF cured by external exposure curing. It comprises of:

Fly Ash: 350 kg/m^3

NaOH: 41 kg/m^3

Na_2SiO_3 : 103 kg/m^3

Table Sugar: 10.5 kg/m^3 (3% of FA)

Extra Water: 35 kg/m^3 (10% of FA)

Fine aggregate: 645 kg/m^3

Coarse aggregate: 1200 kg/m^3

5.2 RECOMMENDATIONS FOR FUTURE RESEARCH

In this research optimum mix has not been found for the polymeric mix containing MIRHA and SF cured by external exposure as maximum value was 46 MPa and 46.5 MPa for 7% replacement of MIRHA and SF mix respectively. Optimum mix could be achieved beyond 7% replacement which was not included in the scope of this research. Moreover, setting time can be further increased by the adjustments in amount of table sugar and extra water. In order to adopt ambient and hot gunny curing incase of some limitations, self heating material should be introduced in the polymeric concrete to achieve high strength. Limitations in tensile strength can be further studied by making suitable variations in mix proportions of polymeric concrete.

REFERENCES

- ACI Committee 226. (1987b). Silica fume in concrete: Preliminary report. *ACI Materials Journal March-April*, 158-66.
- ACI Committee 228. (2003). In-Place Methods to Estimate Concrete Strength, ACI 228.1R. *American Concrete Institute*, Farmington Hills, MI, 44.
- Alvarez-Ayuso, E., Querol, X., Plana, F., Alastuey, A., Moreno, N., Izquierdo, M., Font, O., Moreno, T., Diez, S., Vazquez, E., & Barra, M. (2008). Environmental, physical and structural characterisation of geopolymer matrixes synthesised from coal (co-)combustion fly ashes. *Journal of Hazardous Materials*, 154(1-3), 175-183.
- Anwar, M., Miyagawa, T., & Gaweesh, M. (2001). Using rice husk ash as a cement replacement material in concrete. *First International Ecological Building Structure Conference*, California, 671- 684.
- ASTM C1240, 05, "Standard Specification for Silica Fume Used in Cementitious Mixtures," ASTM International, West Conshohocken, PA, 2008, DOI: 10.1520/C1240-05
- ASTM D5550, 06, "Standard Test Method for Specific Gravity of Soil Solids by Gas Pycnometer," ASTM International, West Conshohocken, PA, DOI: 10.1520/D5550-06
- ASTM Standard C618, 08a, "Standard Specification for Coal Fly Ash and Raw or Calcined Natural Pozzolan for Use in Concrete," ASTM International, West Conshohocken, PA, 2008, DOI: 10.1520/C0618-08
- ASTM Standard C618-94a, "Standard Specification for Fly Ash and Raw Calcined Natural Pozzolan for Use as a Mineral Admixture in Portland Cement Concrete," ASTM International, West Conshohocken, PA, 1995
- Atiş, C. D., Özcan, F., Kiliç, A., Karahan, O., Bilim, C., & Severcan, M. H. (2005). Influence of dry and wet curing conditions on compressive strength of silica fume concrete. *Building and Environment*, 40(12), 1678-1683.
- Bágel, L. (1998). Strength and pore structure of ternary blended cement mortars containing blast furnace slag and silica fume. *Cement and Concrete Research*, 28(7), 1011-1022.
- Bakharev, T. (2005). Geopolymeric materials prepared using class F fly ash and elevated temperature curing. *Cement and Concrete Research*, 35(6), 1224-1232.

Barnett, S. J., Soutsos, M. N., Millard, S. G., & Bungey, J. H. (2006). Strength development of mortars containing ground granulated blast-furnace slag: Effect of curing temperature and determination of apparent activation energies. *Cement and Concrete Research*, 36(3), 434-440.

Batayneh, M., Marie, I., & Asi, I. (2007). Use of selected waste materials in concrete mixes. *Waste Management*, 27(12), 1870-1876.

Bentech. *Operation & Maintenance Manual for Microwave Incinerator*. 2006

Bilim, C., Atiş, C. D., Tanyildizi, H., & Karahan, O. (2009). Predicting the compressive strength of ground granulated blast furnace slag concrete using artificial neural network. *Advances in Engineering Software*, 40(5), 334-340.

Bouman, B., Barker, R., Humphreys, E., & Tuong, T. P. (2007). Rice: Feeding the billions. In D. Molden (Ed.), *Water for food, water for life: A comprehensive assessment of water management* International Water Management Institute, 515-549.

Bouzoubaa, N., & Fournier, B. (2001). *Concrete incorporating rice-husk ash: Compressive strength and chloride-ion penetrability* (Technical report No. MTL 2001-5 (TR)) Materials technology laboratory.

Brooks, J. J. (2002). Prediction of setting time of fly ash concrete. *ACI Materials Journal*, 99(6), 591-597.

BS 812-103.2. *Testing Aggregates. Method for Determination of Particle Size Distribution. Sedimentation Test*. 1989.

BS EN 12350-2. *Testing Fresh Concrete. Slump Test*. 2000.

BS EN 12390-3. *Testing Hardened Concrete. Compressive Strength of Test Specimen*. 2002.

BS EN 12390-5. *Testing Hardened concrete. Flexural Strength of Test Specimens*. 2000.

BS EN 12390-6. *Testing Hardened concrete. Tensile Splitting Strength of Test*. 2000.

BS EN 12504-4. *Testing Concrete. Determination of Ultrasonic Pulse Velocity*. 2004.

CEMBUREAU - the European Cement Association. (1999). *Environmental benefits of using alternative fuels in cement production*. Brussels, Europe: CEMBUREAU.

Chin Siew Choo. (2007). Performance of used engine oil in fresh & hardened states of normal and blended cement concretes. MSc Thesis, University Teknologi PETRONAS.

- Chindaprasirt, P., Jaturapitakkul, C., & Rattanasak, U. (2009). Influence of fineness of rice husk ash and additives on the properties of lightweight aggregate. *Fuel*, 88(1), 158-162.
- Commodity Research Bureau (2007). In Christopher J. L., Amyl K. (Eds.), *The CRB commodity yearbook 2007*. Hoboken, New Jersey: John Wiley & Sons, Inc.
- Criado, M., Palomo, A., & Fernández-Jiménez, A. (2005). Alkali activation of fly ashes. part 1: Effect of curing conditions on the carbonation of the reaction products. *Fuel*, 84(16).
- Davidovits, J. (2008). In Davidovits J. (Ed.), *Geopolymer chemistry and applications* (2nd ed.). France: Institut Géopolymère.
- Dhir, R. K., & Jones, M. R. (1999). Development of chloride-resisting concrete using fly ash. *Fuel*, 78(2), 137-142.
- Diamond, S., & Sahu, S. (2006). Densified silica fume: Particle sizes and dispersion in concrete. *Materials and Structures*, 39(9), 849-859.
- Dordi, C. M. Be ready for a concrete change. *Project Monitor*, Retrieved on March 12, 2010 from <http://www.projectsmonitor.com/detailnews.asp?newsid=7743>
- Duxson, P., Fernández-Jiménez, A., Provis, J. L., Lukey, G. C., & Palomo, A. (2006). Geopolymer technology: The current state of the art. *Journal of Materials Science*, 42(9), 2917-2933.
- Federal highway administration, U.S. department of transportation, infrastructure; material group (FHWA).
- Fernández-Jiménez, A., & Palomo, A. (2005). Mid-infrared spectroscopic studies of alkali-activated fly ash structure. *Microporous and Mesoporous Materials*, 86(1-3), 207-214.
- Fernandez-Jimenez, A., Palomo, A., & Criado, M. (2005). Microstructure development of alkali-activated fly ash cement: A descriptive model. *Cement and Concrete Research*, 35(6), 1204-1209.
- Fytianos, K., Tsaniklidi, B., & Voudrias, E. (1998). Leachability of heavy metals in greek fly ash from coal combustion. *Environment International*, 24(4), 477-486.
- Garci Juenger, M. C., & Jennings, H. M. (2002). New insights into the effects of sugar on the hydration and microstructure of cement pastes. *Cement and Concrete Research*, 32(3), 393-399.
- Gasteiger, H. A., Frederick, W. J., & Streisel, R. C. (1992). Solubility of aluminosilicates in alkaline solutions and a thermodynamic equilibrium model. *Industrial & Engineering Chemistry Research*, 31(4), 1183-1190.

Global Rural Urban Mapping Project. (2005). The growing urbanization of the world. Message posted to <http://www.earth.columbia.edu/news/2005/story03-07-05.html>

Gourley, J. T. (2003a). Adaptive materials for a modern society. *Materials 2003 Conference*, Centre for Sustainable Resource Processing.

Gourley, J. T. (2003b). Geopolymers; opportunities for environmentally friendly construction materials. *Materials 2003 Conference: Adaptive Materials for a Modern Society*, Sydney.

Gourley, J. T., & Johnson, G. B. (2005). Developments in geopolymer precast concrete. *Paper Presented at the International Workshop on Geopolymers and Geopolymer Concrete*, Perth, Australia.

Goyal, S., Kumar, M., & Bhattacharjee, B. (2007). The influence of flyash addition on fresh properties of silica fume concrete. *NBM Media*, Retrieved from <http://www.nbmcw.com/articles/concrete/575-the-influence-of-flyash-addition-on-fresh-properties-of-silica-fume-concrete.html>

Hardjito, D., & Rangan, B. V. (2005). *Development and properties of low-calcium fly ash-based geopolymer concrete*. Research Report GC 1. Perth, Australia: Faculty of Engineering Curtin University of Technology.

Hardjito, D., Wallah, S. E., Sumajouw, D. M. J., & Rangan, B. V. (2004). On the development of fly ash-based geopolymer concrete. *ACI Materials Journal*, 101(6), 467-472.

Hwang, C. L., & Chandra, S. (1996). The use of rice husk ash in concrete. In S. Chandra (Ed.), *Waste materials used in concrete manufacturing* (pp. 184-234) William Andrew Publishing/Noyes.

Izquierdo, M., Querol, X., Phillipart, C., & Antenucci, D. (2009). Influence of curing conditions on geopolymer leaching. Paper presented at the *World of Coal Ash (WOCA) Conference*, Lexington, Kentucky, USA.

James, J., & Subba Rao, M. (1986). Characterization of silica in rice husk ash. *American Ceramic Society Bulletin*, 65(8), 1177-1180.

Jauberthie, R., Rendell, F., Tamba, S., & Cissé, I. K. (2002). Properties of cement—rice husk mixture. *Construction and Building Materials*, 17(4), 239-243.

Khale, D., & Chaudhary, R. (2007). Mechanism of geopolymerization and factors influencing its development: A review. *Journal of Materials Science*, 42, 729-746.

Kirschner, A. V., & Harmuth, H. (2004). Investigation of geopolymer binders with respect to their application for building materials. *Ceramics - Silikaty*, 48(3), 117-120.

- Komnitsas, K., & Zaharaki, D. (2007). Geopolymerisation: A review and prospects for the minerals industry. *Minerals Engineering*, 20(14), 1261-1277.
- Krivenko, P. V. (1997). Alkaline cements: Terminology, classification, aspects of durability. 4iv046–4iv050.
- Kusbiantoro, A. (2007). The effect of microwave incinerated rice husk ash (MIRHA) on concrete properties. MSC Thesis, University Teknologi PETRONAS.
- Luther, M. D. (1990). High-performance silica fume (microsilica)—Modified cementitious repair materials.
- Mahallati, E., & Saremi, M. (2006). An assessment on the mill scale effects on the electrochemical characteristics of steel bars in concrete under DC-polarization. *Cement and Concrete Research*, 36(7), 1324-1329.
- Malhotra, V. M. (1999). Making concrete "greener" with fly ash. *Concrete International*, 21(5), 61-66.
- Malhotra, V. M. (2002). Introduction: Sustainable development and concrete technology. *Concrete International*, 24(7), 22.
- Malhotra, V. M. (2006). Reducing CO₂ emissions. *Concrete International*, 28(09), 42-45.
- Mazloom, M., Ramezaniapour, A. A., & Brooks, J. J. (2004). Effect of silica fume on mechanical properties of high-strength concrete. *Cement and Concrete Composites*, 26(4), 347-357.
- McCaffrey, R. (2002). Climate change and the cement industry. *Global Cement and Lime Magazine (Environmental Special Issue)*, 15-19.
- McDonell, K. (2006). Is rapid-hardening concrete dangerous? Retrieved on 28 February, 2010 from <http://www.slate.com/id/2141629/>
- Mehta, P. K. (1992). Rice husk ash-A unique supplementary cementing material. *Proceedings of the International Symposium on Advances in Concrete Technology*, Athens, Greece, 407–430.
- Mehta, P. K. (2004). High-performance, high-volume fly ash concrete for sustainable development. *Proceedings of the International Workshop on Sustainable Development and Concrete Technology*, Beijing, China. 3-14.
- Mehta, P. K., & Monteiro, P. J. M. (2006). *Concrete microstructure, properties, and materials* (third ed.) McGraw-Hill Companies, Inc.

Mehta, P. K. Cements and concrete mixtures for sustainability. *NBM Media*, Retrieved on November 25, 2009 from <http://www.nbmcw.com/articles/concrete/579-cements-and-concrete-mixtures-for-sustainability.html>

Murray, G., Charles, V. W., & Weise, W. (2007). *Introduction to engineering materials* (2nd ed.) CRC Press.

Naik, T. R. (2005). Sustainability of cement and concrete industries. *Proceedings of the International Conference Global Construction: Ultimate Concrete Opportunities*, Dundee, Scotland. 141-150.

Nair, D. G., Jagadish, K. S., & Fraaij, A. (2006). Reactive pozzolanas from rice husk ash: An alternative to cement for rural housing. *Cement and Concrete Research*, 36(6), 1062-1071.

Naji Givi, A., Abdul Rashid, S., Nora A. Aziz, F., & Mohd Salleh, M. A. (2010). Contribution of rice husk ash to the properties of mortar and concrete: A review. *Journal of American Science*, 6(3), 157-165.

Nanotechnology and concrete: Small science for big changes (June 5, 2005). . Ottawa, Ontario: Report by National Research council (NRC) Canada.

Neville, A. M. (1990). *Properties of concrete* Longman Singapore Publishers Pte Ltd.

Non-destructive testing of hardened concrete (2001). *Construction materials*, Taylor & Francis. doi:10.4324/9780203478981.ch22.

Nugteren, H. W. (2006). Coal fly ash: From waste to industrial product. *2006 AIChE Spring National Meeting - 5th World Congress on Particle Technology, April 23, 2006 - April 27*, Univ. of Pittsburgh School of Eng.; AICHE.

Nuruddin, M. F., Kusbiantoro, A., & Qazi, S. (2009). Polymeric concrete for sustainable futures. *13th International Conference on Structural and Geotechnical Engineering*, Cairo, Egypt.

Nuruddin, M. F., Kusbiantoro, A., & Shafiq, N. (2008). Microwave incinerated rice husk ash (MIRHA) and its effect on concrete properties. *IMS International Conference*, American University of Sharjah, UAE.

Pacheco-Torgal, F., Castro-Gomes, J., & Jalali, S. (2008a). Alkali-activated binders: A review: Part 1. Historical background, terminology, reaction mechanisms and hydration products. *Construction and Building Materials*, 22(7), 1305-1314.

Pacheco-Torgal, F., Castro-Gomes, J., & Jalali, S. (2008b). Alkali-activated binders: A review. Part 2. About materials and binders manufacture. *Construction and Building Materials*, 22(7), 1315-1322.

- Palomo, A., Alonso, S., Fernández-Jiménez, A., Sobrados, I., & Sanz, J. (2004). Alkaline activation of fly ashes. A NMR study of the reaction products. *Journal of the American Ceramic Society*, 87(6), 1141–1145.
- Palomo, A., Grutzeck, M. W., & Blanco, M. T. (1999). Alkali-activated fly ashes: A cement for the future. *Cement and Concrete Research*, 29(8), 1323-1329.
- Papadakis, V. G. (2000). Effect of fly ash on portland cement systems - Part II. High-calcium fly ash. *Cement and Concrete Research*, 30(10), 1647-1654(8).
- Puertas, F., Martínez-Ramírez, S., Alonso, S., & Vázquez, T. (2000). Alkali-activated fly ash/slag cements: Strength behaviour and hydration products. *Cement and Concrete Research*, 30(10), 1625-1632.
- Rangan, B. V. (2008). *Fly ash-Based Geopolymer concrete*. Research Report GC 4. Perth, Australia: Faculty of Engineering Curtin University of Technology, Australia.
- Rao, G. A. (1998). Influence of silica fume replacement of cement on expansion and drying shrinkage. *Cement and Concrete Research*, 28(10), 1505-1509.
- Rodríguez de Sensale, G. (2006). Strength development of concrete with rice-husk ash. *Cement and Concrete Composites*, 28(2), 158-160.
- Rohatgi, P., Weiss, D., & Gupta, N. (2006). Applications of fly ash in synthesizing low-cost MMCs for automotive and other applications. *JOM Journal of the Minerals, Metals and Materials Society*, 58(11), 71-76.
- Rowles, M., & O'Connor, B. (2003). Chemical optimisation of the compressive strength of aluminosilicate geopolymers synthesised by sodium silicate activation of metakaolinite. *Journal of Materials Chemistry*, 13(5), 1161-1165.
- Sabir, B. B., Wild, S., & Bai, J. (2001). Metakaolin and calcined clays as pozzolans for concrete: A review. *Cement and Concrete Composites*, 23(6), 441-454.
- Scheetz, B. E. (2004). Chemistry and mineralogy of coal fly ash: Basis for beneficial use. *Office of Surface Mining Mid Continent Region* <http://www.Mcrcc.Osmre.gov/PDF/Forums/CCB5/1.4.Pdf>
- Shafiq, N. (2004). Effects of fly ash on chloride migration in concrete and calculation of cover depth required against the corrosion of embedded steel reinforcement. *Structural Concrete*, 5(1), 5-10.
- Shafiq, N., & Cabrera, J. G. (2004). Effects of initial curing condition on the fluid transport properties in OPC and fly ash blended cement concrete. *Cement and Concrete Composites*, 26(4), 381-387.

Shafiq, N., Nuruddin, M. F., & Kamaruddin, I. (2007). Comparison of engineering and durability properties of fly ash blended cement concrete made in UK and Malaysia. *Advances in Applied Ceramics*, 106(6), 314-318.

Shi, C., & Day, R. L. (1995). Acceleration of the reactivity of fly ash by chemical activation. *Cement and Concrete Research*, 25(1), 15-21.

Siddiquea, R., de Schutterb, G., & Noumowec, A. (2009). Effect of used-foundry sand on the mechanical properties of concrete. *Construction and Building Materials*, 23(2), 976-980.

Sindhunata, Van Deventer, J. S. J., Lukey, G. C., & Xu, H. (2006). Effect of curing temperature and silicate concentration on fly-ash-based geopolymerization. *Industrial & Engineering Chemistry Research*, 45(10), 3559-3568.

Škvára, F., Doležal, J., Svoboda, P., Kopecký, L., Pawlasová, S., Lucuk, M., Dvořáček, K., Beksa, M., Myšková, L., & Šulc, R. (2006). Concrete based on fly ash geopolymers. Paper presented at the *Proceedings of 16th Intern. Baustofftagung IBAUSIL 2006*, F.A.Finger Inst. für Baustoffkunde, Weimar, 1.

Sofi, M., Van Deventer, J. S. J., Mendis, P. A., & Lukey, G. C. (2007). Engineering properties of inorganic polymer concretes (IPCs). *Cement and Concrete Research*, 37(2), 251-257.

Srivastava, V. C., Mall, I. D., & Mishra, I. M. (2006). Characterization of mesoporous rice husk ash (RHA) and adsorption kinetics of metal ions from aqueous solution onto RHA. *Journal of Hazardous Materials*, 134(1-3), 257-267.

Sushil, S., & Batra, V. S. (2006). Analysis of fly ash heavy metal content and disposal in three thermal power plants in India. *Fuel*, 85(17-18), 2676-2679.

Sybil, P. P. (Ed.). (2002). *McGraw-hill encyclopedia of science and technology* (5th ed.) The McGraw-Hill Companies, Inc.

Tangchirapat, W., Saeting, T., Jaturapitakkul, C., Kiattikomol, K., & Siripanichgorn, A. (2007). Use of waste ash from palm oil industry in concrete. *Waste Management*, 27(1), 81-88.

Tashima, M. M., Silva, C. A. R., Akasaki, J. L., & Barbosa, M. B. (2004). The possibility of adding the rice husk ash (RHA) to the concrete. *International RILEM Conference on the use of Recycled Materials in Building and Structures*, 778 – 786.

Tempest, B., Sanusi, O., Gergely, J., Ogunro, V., & Weggel, D. (2009). Compressive strength and embodied energy optimization of fly ash based geopolymer cement concrete. Paper presented at the *World of Coal Ash (WOCA) Conference*, Lexington, Kentucky, USA.

Temuujin, J., & Van Riessen, A. (2009). Effect of fly ash preliminary calcination on the properties of geopolymer. *Journal of Hazardous Materials*, 164(2-3), 634-639.

Temuujin, J., Van Riessen, A., & Williams, R. (2009). Influence of calcium compounds on the mechanical properties of fly ash geopolymer pastes. *Journal of Hazardous Materials*, 167(1-3), 82-88.

The Cement Association of Canada. What do you think is holding the pyramids together? *History of Cement*, Retrieved on February 27, 2009 from http://www.cement.ca/index.php/en/Sustainable_Manufacturing/History_of_Cement.html

The McGraw-Hill Companies Inc. (2002). In P. Parker S. (Ed.), *McGraw-hill encyclopedia of science and technology* (5th ed.)

Thomas, M. D. A., Shehata, M. H., Shashiprakash, S. G., Hopkins, D. S., & Cail, K. (1999). Use of ternary cementitious systems containing silica fume and fly ash in concrete. *Cement and Concrete Research*, 29(8), 1207-1214.

Van Deventer, J. S. J., Provis, J. L., Duxson, P., & Lukey, G. C. (2007). Reaction mechanisms in the geopolymeric conversion of inorganic waste to useful products. *Journal of Hazardous Materials*, 139(3), 506-513.

Van Jaarsveld, J. G. S., & Van Deventer, J. S. J. (1999). Effect of the alkali metal activator on the properties of fly ash-based geopolymers. *Industrial & Engineering Chemistry Research*, 38(10), 3932-3941.

Van Jaarsveld, J. G. S., Van Deventer, J. S. J., & Lukey, G. C. (2002). The effect of composition and temperature on the properties of fly ash and kaolinite-based geopolymers. *Chemical Engineering Journal*, 89(1-3), 63-73.

Van Jaarsveld, J. G. S., Van Deventer, J. S. J., & Schwartzman, A. (1999). The potential use of geopolymeric materials to immobilise toxic metals: Part II. Material and leaching characteristics. *Minerals Engineering*, 12(1), 75-91.

Wallah, S. E., & Rangan, B. V. (2006). *Low-calcium fly ash-based geopolymer concrete*. Research Report GC 2). Perth, Australia: Faculty of Engineering Curtin University of Technology.

Wang, K., Shah, S. P., & Mishulovich, A. (2004). Effects of curing temperature and NaOH addition on hydration and strength development of clinker-free CKD-fly ash binders. *Cement and Concrete Research*, 34(2), 299-309.

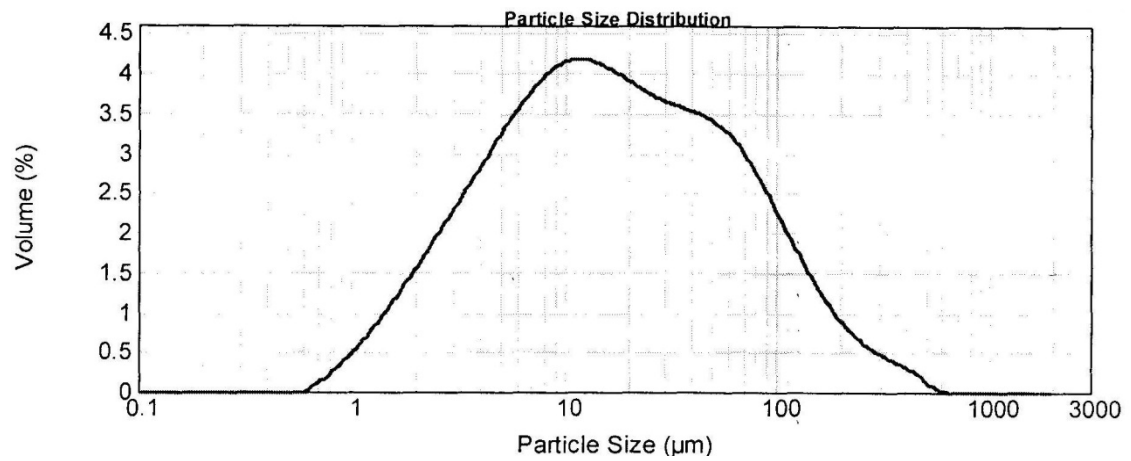
Wang, S. (2008). Application of solid ash based catalysts in heterogeneous catalysis. *Environmental Science & Technology*, 42(19), 7055-7063.

- World Cement Industry (2010). *Global industry forecasts for 2013 & 2018*. The Freedonia Group.
- Wu, Z. (2000). Development of high-performance blended cements. PhD. Thesis, The University of Wisconsin - Milwaukee, 177.
- Xu, H., & Van Deventer, J. S. J. (2000). The geopolymerisation of alumino-silicate minerals. *International Journal of Mineral Processing*, 59(3), 247-266.
- Yazıcı, H., Yiğiter, H., Karabulut, A. Ş., & Baradan, B. (2008). Utilization of fly ash and ground granulated blast furnace slag as an alternative silica source in reactive powder concrete. *Fuel*, 87(12), 2401-2407.
- Yilmaz, A., & Degirmenci, N. (2009). Possibility of using waste tire rubber and fly ash with portland cement as construction materials. *Waste Management*, 29(5), 1541-1546.
- Yip, C. K., Lukey, G. C., Provis, J. L., & Van Deventer, J. S. J. (2008). Effect of calcium silicate sources on geopolymerisation. *Cement and Concrete Research*, 38(4), 554-564.
- Yunsheng, Z., Wei, S., & Zongjin, L. (2008). Synthesis and microstructural characterization of fully-reacted K-PSS geopolymeric cement matrix. *ACI Mater. J.*, 105(2), 156-164.
- Zemke, N., & Woods, E. (2009). *Rice husk ash*. California: California Polytechnic State University. Retrieved from http://cvbt-web.org/uploads/Rice_Husk_Ash/Nick_Emmet_RHA.pdf
- Zhang, X., & Han, J. (2000). The effect of ultra-fine admixture on the rheological property of cement paste. *Cement and Concrete Research*, 30(5), 827-830.

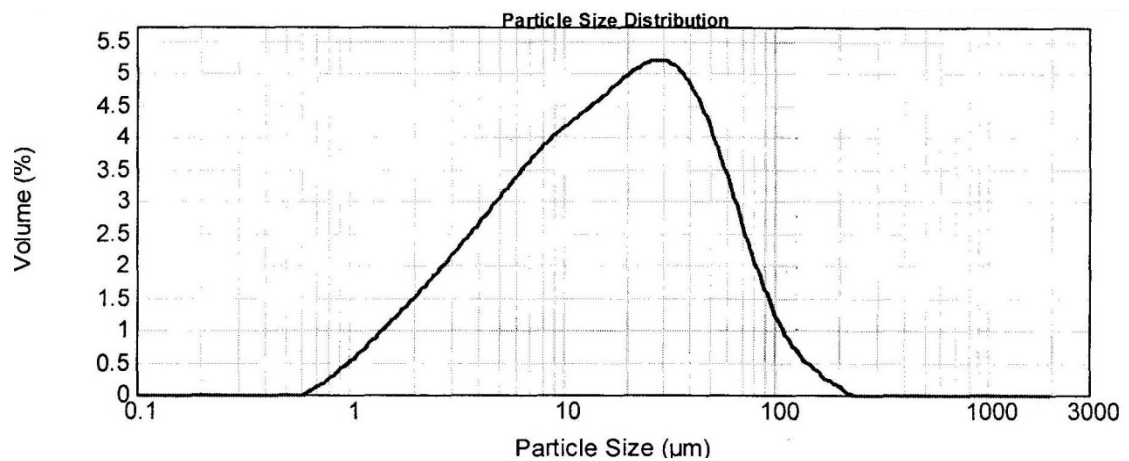
APPENDIX A

PARTICLE SIZE ANALYSIS OF FLY ASH, MIRHA & SILICA FUME

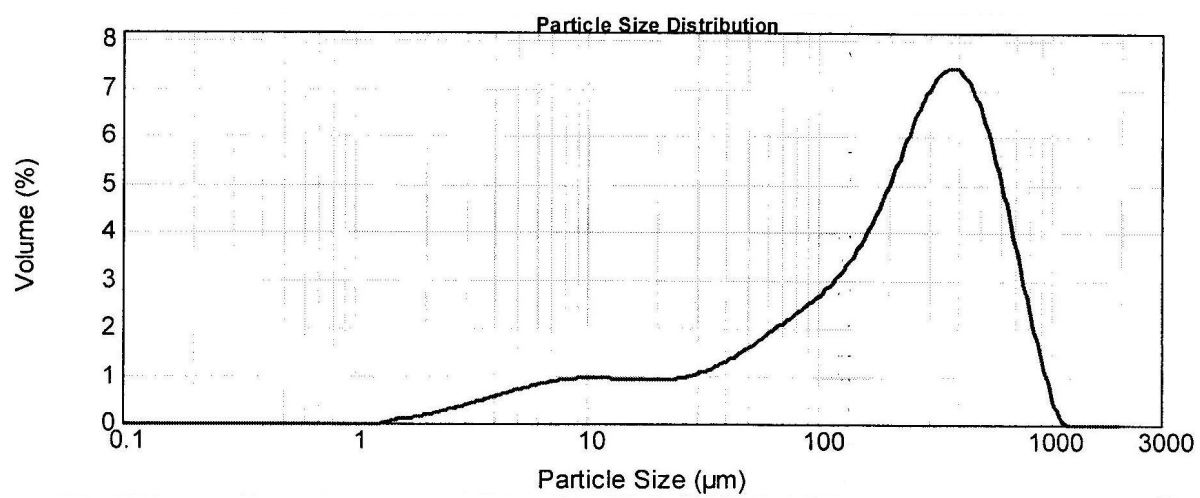
A. Particle size distribution of fly Ash



B. Particle size distribution of MIRHA



C. Particle size distribution of silica fume



APPENDIX B

TECHNICAL SPECIFICATION FOR MICROWAVE INCINERATOR MODEL

BENTECH INC-21 ADAPTED FROM BENTECH (BENTECH)

ITEM		DESCRIPTION
A	GENERAL DESCRIPTION	
	Manufacturer	Pollution Engineering Sdn Bhd
	Model	BENTECH INC-21
	Capacity	1 m ³ Chamber
	Type of Waste	Paddy Husk
	Overall Dimension (m)	2.3 (H) x 4.0 (W) x 4.0 (L)
	Operating Temperature	800°C
	Emission and Ash Control System	Ceramic Filter
	Combustion Control	Temperature Controller
	Mode of Operation	PLC with Manual Overwrite
	Mode of Loading	Manual
	Mode of Waste Ash Removal	Manual
B	KILN CHAMBER	
	Body Casing	
	Material and Thickness	SS 304 Plate Thickness 4.5 mm-5.0 mm
	Support and Thickness	SS 304 Angle Iron 3 inch x 3 inch x t5.0 mm and above
	Charging Door	
	Dimension (mm) Big Door	580 x 455
	Dimension (mm) Small Door	315 x 315
C	MICROWAVE INCINERATOR	
	Type	Air Cooled Magnetron
	Manufacturer/Model	Pollution Engineering Sdn Bhd/ MG-AIR 2450-1100
	Country of Origin	Malaysia
	Power Rating (1/hr)	1100 W
D	THERMOCOUPLE	
	Length	300 450
	Type	In-Connel
	Manufacturer/Brand	IPSH Sdn Bhd
	Country of Origin	Malaysia
	Temperature Range	Up to 1600°C

E	SUPPLY AIR BLOWER		
	Type		TSB 50
	Manufacturer/Brand		Fu-Tsu
	Country of Origin		Taiwan
	Motor Rating		1.5 KW
	Air Capacity (m ³ /min)		Not less than 1.87 m ³ /min
F	CERAMIC FILTER		
	Type		CERAFIL XS-1000
	Manufacturer/Brand		CERAFIL
	Country of Origin		united Kingdom
	Surface Area (m ²)		0.19
G	INDUCED DRAFT FAN		
	Type		HFD 3242 T
	Manufacturer/Brand		Maxis Fan
	Country of Origin		Malaysia
	Motor Rating		4 HP
	Air Capacity (m ³ /min)		Not less than 1.85 m ³ /min
H	AIR COMPRESSOR		
	Type		TS 05 120 H
	Manufacturer/Brand		ELGI
	Country of Origin		India
	Motor Rating		5 HP
	Air Capacity (m ³ /hr)		Not less than 24.6 m ³ /hr at 10 kgf/cm ²
I	CONTROL PANEL		
	Enclosure		IP54
	Model of Operation		Programmable Logic Control (PLC)
	Type of PLC		Omron or equivalent
	Type of Cubicle		MERLIN GERLIN
	Type of Contractor		TELEMECANIQUE
	Type of Starter		TELEMECANIQUE
	Touch Screen		GT21 4.7 Inch Panasonic
J	WIRING WORKS		
	Type of Wiring		PVC
	Type of Conduit/Cable Tray		Galvanized Conduit

APPENDIX C

LIST OF PAPERS & PUBLICATIONS

Nuruddin, M. F., Qazi, S., Kusbiantoro, A., & Shafiq, N. (2009). Mix design of polymeric concrete incorporating fly ash, rice husk ash and silica fume. The 3rd International Conference on Built Environment in Developing Countries, Universiti Sains Malaysia, Penang, Malaysia ,1, 506-516.

Nuruddin, M. F., Kusbiantoro, A., & Qazi, S. (2009). Polymeric concrete for sustainable futures. Thirteenth International Conference on Structural and Geotechnical Engineering, Cairo, Egypt. 1155-1161.

Nuruddin, M. F., Qazi, S., Shafiq, N., & Kusbiantoro, A. (2010). Compressive Strength & microstructure of polymeric concrete incorporating fly ash & silica fume. AM Journal on Civil, Environmental and Construction Engineering, 1(1), 15-19.

Nuruddin, M. F., Qazi, S., Kusbiantoro, A., & Shafiq, N. (2010). Polymeric concrete: Complete elimination of cement for sustainable futures. International Conference on Sustainable Building and Infrastructure (ICSBI2010), Kuala Lumpur, Malaysia.

Nuruddin, M. F., Kusbiantoro, A., Qazi, S., & Shafiq, N. (2010). The effect of retarder on polymeric concrete. International Conference on Sustainable Building and Infrastructure (ICSBI2010), Kuala Lumpur, Malaysia.

Nuruddin, M. F., Qazi, S., Kusbiantoro, A., & Shafiq, N. (2010). Utilization of waste material in polymeric concrete. Institution of Civil Engineers (ICE) and Thomas Telford journals (Accepted).

Nuruddin, M. F., Qazi, S., Kusbiantoro, A., & Shafiq, N. (2010). Application of polymeric concrete for in-situ construction. Journal of the Institution of Engineers, Malaysia (Submitted).